

Response to Referee 1

We thank Referee 1 for the helpful comments. We will address all changes in the revised manuscript as detailed in our responses below. The referee comments are in black and their line numbers refer to the original submitted manuscript. Our responses are in blue text.

We want to note that some of the reviewer's comments may pertain to an original draft of the manuscript which has already been revised. We have tried to address all comments, but in some cases, we do not see what the reviewer is talking about. In our response, we will only be referring to the version that is currently available on the BG website.

We also want to note that we now have submitted a companion paper to this special issue that is specifically about the particulate organic carbon (POC) export using the $^{210}\text{Po}/^{210}\text{Pb}$ technique.

- Specific Comments: One unfortunate aspect of the paper is that it fails to model the data in the context of biogenic carbon flux, the primary strength of the nuclide pair. Perhaps the organic carbon data are missing, or awaiting a more complete synthesis with other nuclides such as ^{234}Th , as done admirably before by the UAB lab group.

We understand the reviewer's concern. In fact, we have submitted two manuscripts to this special issue. In the manuscript reviewed here we discuss the general distribution of ^{210}Po and ^{210}Pb activity along the GEOVIDE transect. The second manuscript entitled "The export flux of particulate organic carbon derived from $^{210}\text{Po}/^{210}\text{Pb}$ disequilibria along the North Atlantic GEOTRACES GA01 (GEOVIDE) transect" addresses the POC export fluxes. In the second paper, we have calculated the POC fluxes using the export flux of ^{210}Po and the $\text{POC}/^{210}\text{Po}$ ratio in total ($> 1 \mu\text{m}$) particles and compared the estimates to those obtained using the $^{234}\text{Th}/^{238}\text{U}$ proxy.

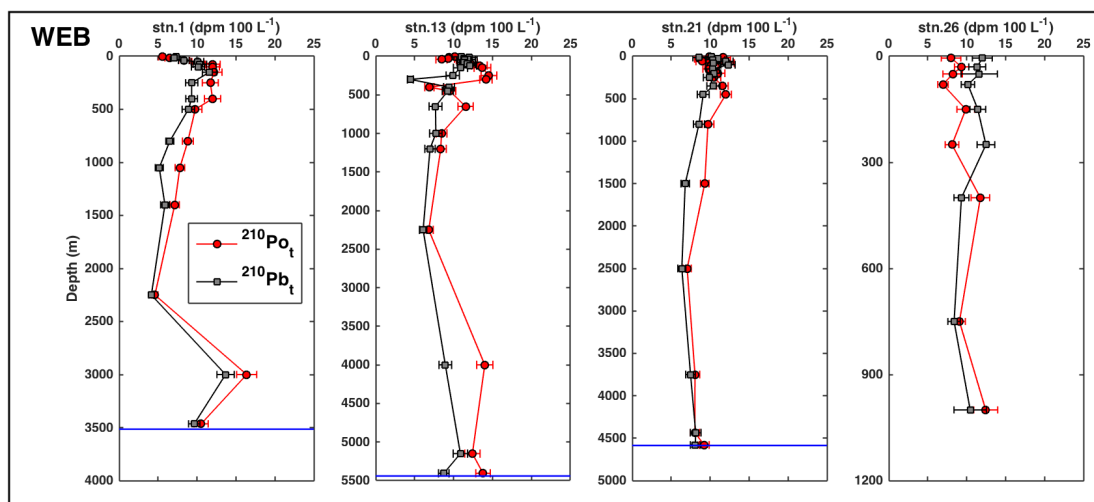
Technical Issues:

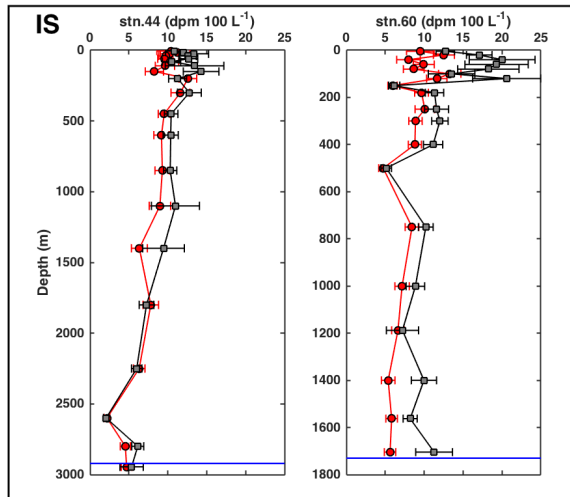
1. Introduction It is noted that there is significant benthic disequilibrium (^{210}Po deficiency) well below the euphotic zone, indeed significantly below the main thermocline at times (e.g. 4000 meters at Station 13; 1400 meters at station 60). This dilemma and benthic consequences has been discussed in the recent literature (Rigaud, et al., 2014). Page 3: As such, maybe the literature citations in the introduction that need to be updated for the current millennium!

We agree that ^{210}Po deficits at depth can be problematic in interpretation, but others have associated them with nepheloid layers or other forms of suspended sediment near the bottom (e.g. Hu et al., 2014; Wei et al., 2014; Rigaud et al., 2015). Mid-depth deficits are more mysterious and have still not really been adequately resolved (Kim, 2001; Church et al., 2012; Rigaud et al., 2015).

We acknowledge that there were deficits in the deep waters at stations 60, and 64. However, we have almost no particle data for those depths so cannot address that in this paper.

In Fig. 2, total ^{210}Po and total ^{210}Pb activity were plotted as red circles and black squares, respectively. There were indeed ^{210}Po deficits below 1400 m at station 60 but at 4000 m at station 13 there was a ^{210}Po excess rather than a deficit. Please see the following profiles for stations 13 and 60.





We agree that the literature citations on Page 3 L55-57 need to be updated. We will add in some recent references (highlighted in bold font) as the following:

“The distribution of ²¹⁰Po and ²¹⁰Pb has been widely measured over the last several decades in the Atlantic (e.g. Bacon et al., 1976; Sarin et al., 1999; **Rigaud et al., 2015**), Pacific (e.g. Nozaki and Tsunogai, 1976; Murray et al., 2005; Verdeny et al., 2008), Indian (e.g. Cochran et al., 1983; Sarin et al., 1994; **Subha Anand et al., 2017**), Arctic (e.g. Moore and Smith, 1986; **He et al., 2015**; **Roca-Martí et al., 2016**) and Southern Oceans (e.g. Shimmield et al., 1995; Friedrich and Rutgers van der Loeff, 2002)”

2. Methods Page 4: What is meant by “Xlarge” station (26), as the number of depths are less than others?

Station naming depended on the number of casts that were conducted: XLarge stations had five casts while Super stations had > 5 casts. Because of the fewer casts, we did indeed sample at fewer depths at Station 26 than at the other stations.

3. Page 5: Is six hours sufficient for equilibration, or were there previous tests performed to verify this? What was the time lag between sample processing on board, and nuclide separation in the lab on shore, unless both were done on board? This can be important as reviewed in Rigaud, et al. 2013. Evidently this is reflected in the data reported in

supplemental tables, although there are not errors assigned to the nuclide ratios in Table 2.

Thank you for this point. Six hours for isotope equilibration was a mistake. In fact we waited for more than 12 hours for isotopic equilibrium between ^{210}Po and ^{209}Po , which is recommended in RiO5 Cookbook (https://cmer.who.edu/wp-content/uploads/2018/01/15-Po-Pb-210-in-sewewater_Co-APDC.pdf) and suggested in Rigaud et al. (2013). We will revise the manuscript accordingly.

We did our best to minimize delays in sample processing. The time elapsed between sampling and nuclide separation (first plating) was 50 and 68 days on average for the seawater samples processed at UAB and QC, respectively, and 58 and 44 days on average for the particulate samples processed at UAB and QC, respectively. This was unavoidable as the cruise was long. However, all this is taken into account into the corrections and calculations, which were performed as described in Rigaud et al. (2013).

The errors for the total particulate $^{210}\text{Po}/^{210}\text{Pb}$ activity ratio ($^{210}\text{Po}_p/^{210}\text{Pb}_p$) are now added in Table 2 as follows:

Table 2. The compilation of total particulate $^{210}\text{Po}/^{210}\text{Pb}$ activity ratios ($^{210}\text{Po}_p/^{210}\text{Pb}_p$) averaged in the upper 200 m, including this study.

Region	Sampling Method	Date	Size (μm)	Depth (m)	$^{210}\text{Po}_p/^{210}\text{Pb}_p$	Reference
Arctic	CESAR	<i>In-situ</i> pump	> 0.45	2-200	1.2 \pm 0.7	(Moore and Smith, 1986)
	Arctic (ARK-XXII/2)	Niskin bottle	> 1	10-200	0.50 \pm 0.20	(Friedrich, 2011)
	Chukchi Shelf	Niskin bottle	> 0.45	0-90	0.37 \pm 0.10	(He et al., 2015)
Atlantic	F.S. Meteor	Niskin bottle	> 0.4	0-200	3.1 \pm 1.4	(Bacon, 1977)
	Cariaco Trench	Niskin bottle	> 0.4	0-200	1.4 \pm 0.6	(Bacon et al., 1980a)
	Labrador (R/V Knorr)	Niskin bottle	> 0.4	0-100	3.9 \pm 1.5	(Bacon et al., 1980b)
	South of New England	Niskin bottle	> 0.45	4-200	1.8 \pm 0.8	(Bacon et al., 1988)
	N. Atlantic (BOFS)	Niskin bottle	> 0.45	0-150	6.0 \pm 4.5	(BODC et al., 2016)
	South-equa. Atlantic	Niskin bottle	> 0.7	10-200	1.3 \pm 1.1	(Sarin et al., 1999)
N. Atlantic (GA03)	BATS	Go-Flo bottle	> 0.45	0-200	3.7 \pm 3.2	(Kim and Church, 2001)
		<i>In-situ</i> pump	> 0.8	30-200	1.5 \pm 0.5	(Rigaud et al., 2015)
		<i>In-situ</i> pump	> 1	8-200	1.4 \pm 0.3	This study
Pacific	North Pacific	Niskin bottle	> 0.4	10-150	8.5 \pm 5.7	(Bacon et al., 1976)
	W. Pacific (FR05/92)	Niskin bottle	> 0.45	0-200	1.3 \pm 1.0	(Towler, 2003)
	Equa. Pacific	Go-Flo bottle	> 0.45 or 0.5	0-200	5.1 \pm 1.2	(Murray et al., 2005)
Pacific	W. Pacific (FR08/93)	Niskin bottle	> 0.45	0-200	16 \pm 4	(Towler, 2013)
	W. Pacific (FR07/97)	Niskin bottle	> 0.45	0-200	7.2 \pm 1.5	(Peck and Smith, 2002)
	Aleutian Basin	Niskin bottle	> 0.2	0-200	1.9 \pm 3.0	(Hu et al., 2014)
Antarctic	E. Pacific (GP16)	<i>In-situ</i> pump	> 1	15-200	2.4 \pm 0.6	unpublished
	S. Ocean (ANT-X/6)	Niskin bottle	> 0.45	20-200	3.0 \pm 1.4	(Smetacek et al., 1997)
	Bellingshausen Sea	Go-Flo bottle	> 0.45	0-100	14 \pm 11	(Shimmiel et al., 1995)

S. Ocean (ANT-XXIV/3)		Niskin bottle	Feb - Apr 08	> 0.45	25-200	1.3 ± 0.9	(Friedrich et al., 2011)
S. China Sea	Go-Flo bottle	Jan-Oct 07, May 08	> 0.45	0-200	1.7 ± 1.1	(Wei et al., 2014)	
W. Taiwan	Go-Flo bottle	Apr 07	> 0.45	8-25	0.85 ± 0.12	(Wei et al., 2012)	
Margin	Niskin bottle	Feb 93	> 0.7	0-100	0.88 ± 0.08	(Hong et al., 1999)	
Sea	Sediment trap	Mar-Jun 03		200	4.5 ± 1.0	(Stewart et al., 2007)	
	Mediterranean Sea						

4. Page 6: Who are the “Planquette group”?

Helene Planquette Group, University of Brest, co-authors in this issue.

5. Results Page 7: As noted above, stations 13 and 60 appear to have total ^{210}Po deficiency at depth (Fig. 2), not excess.

Please see our response to Technical Issue 1.

6. Page 8: Increase in activity with depth for both nuclides is not evident in Figs. 2 and 3, rather decrease.

Figures 2 and 3 are the profiles of total radionuclide activities ($^{210}\text{Po}_t$, $^{210}\text{Pb}_t$) from surface to bottom and from surface to 250 m, respectively.

In the original manuscript Page 8 lines 214-216: “The vertical profiles of $^{210}\text{Pb}_s$ were generally similar to those of $^{210}\text{Po}_s$, with relatively high activity in the surface, lower activity in the subsurface and increasing activity with depth;” $^{210}\text{Pb}_s$ and $^{210}\text{Po}_s$ refer to particulate activity in the small size fraction (not totals as in Figs 2 and 3). This data was shown only in supplementary Table S2, but we realize that it should be included in the paper and have added figures.

We will include the vertical profiles of small and large particulate radionuclide activity as the following:

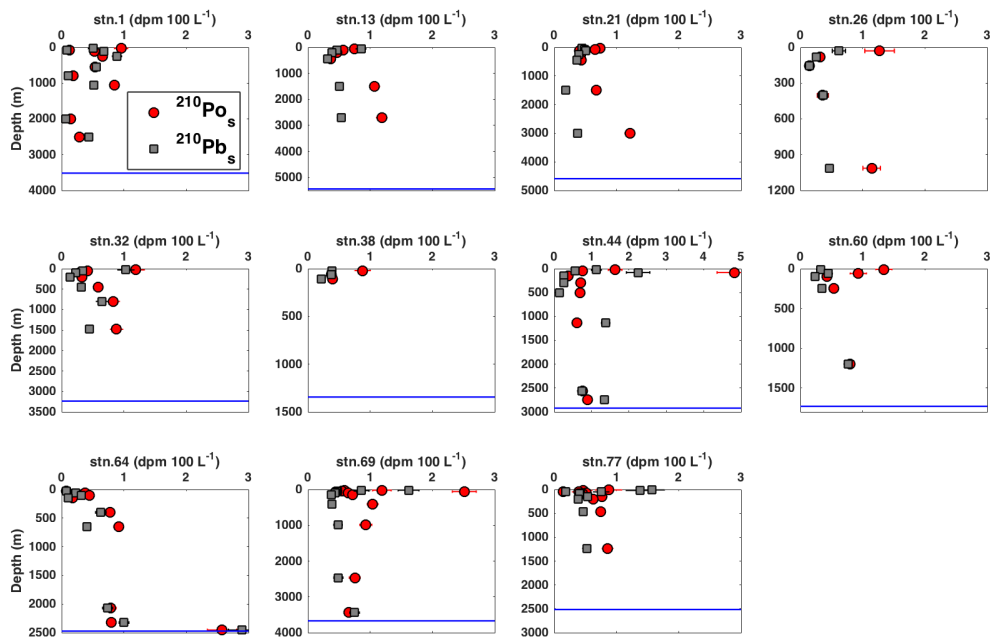


Fig. 4. Vertical profiles of the particulate ^{210}Po and ^{210}Pb activity in the small size fraction (1-53 μm , $^{210}\text{Po}_s$, $^{210}\text{Pb}_s$). Note the different depth scales for the various stations and that the activity scale at Station 44 differs from the scale of all other stations. The horizontal blue line represents the bottom depth at that station.

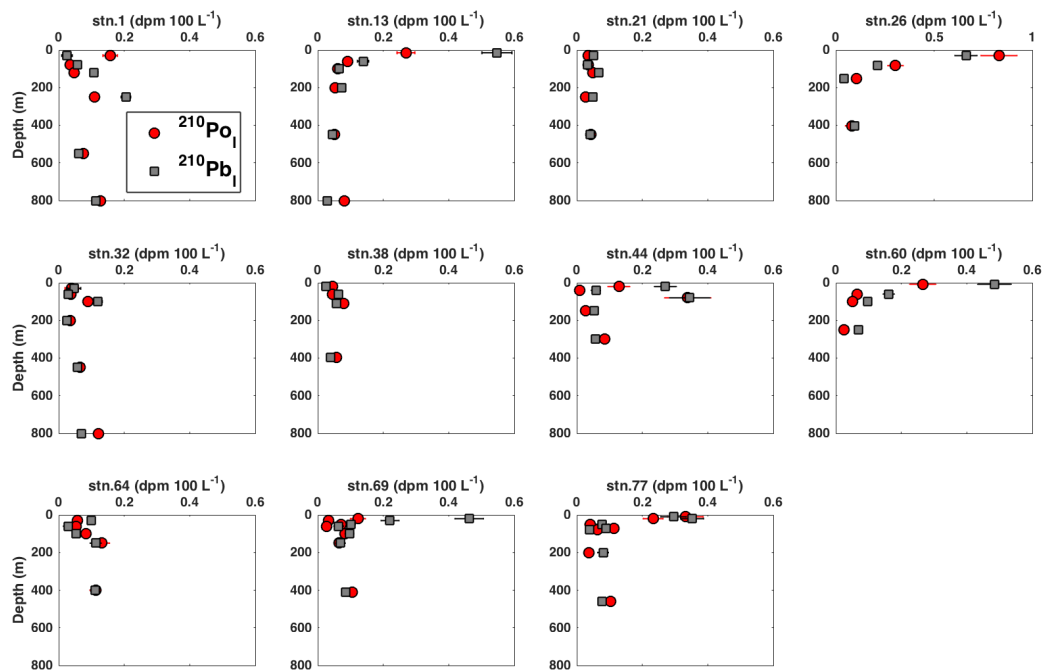


Fig. 5. The vertical profiles of the particulate ^{210}Po and ^{210}Pb activity in the large size fraction ($> 53 \mu\text{m}$, ^{210}Po , ^{210}Pb) in the top 800 m. Note that the activity scale at Station 26 differs from the scale at all other stations.

Discussion Page 10: Usually in the far North Atlantic, ^{210}Pb association with aerosol dust is not as evident in the east, rather alternative fresh water sources (e.g. precipitation) as noted in the west.

We agree. In the submitted manuscript, we acknowledged the possible inputs of ^{210}Pb from freshwater (e.g. sea ice processes and meteoric water) in the high latitude North Atlantic, in particular near the Greenland shelf. Nonetheless, we removed the word “unexpected” from the last sentence of this paragraph on Line 281.

7. Page 11. The lithogenic source of a depleted $^{210}\text{Po}/^{210}\text{Pb}$ ratio should only be evident if the atmospheric scavenging was in the form of precipitation. Alternatively or as with lithogenic particles from the continental margin, the ^{210}Po has been preferentially extracted lately in fecal pellets by organisms.

We find this statement a bit confusing and are not sure how to best address it.

Near the coast, most of the lithogenic particles are terrestrial/riverine particles with a small contribution from aerosols. Aerosols have a very low $^{210}\text{Po}/^{210}\text{Pb}$ AR (< 0.2 , Baskaran, 2011) due to the short residence time of ^{210}Pb in the atmosphere (e.g. Moore et al., 1974; Turekian et al., 1977). For the lithogenic particles sourced from land/river, the particulate ^{210}Po depletion is more related to the nature of those particles that may preferentially adsorb ^{210}Pb vs. ^{210}Po as opposed to the patterns in organic materials (e.g. Fisher et al., 1983; Stewart et al., 2005).

8. Page 12: The alternative scenario is noted here at the end of section 4.2. As such, might there be a corresponding dissolved ratio greater than one?

Yes, we have looked at this relationship and will address it in much greater detail in an upcoming manuscript entirely about this topic (data presented at the Ocean Sciences Meeting, February 2018). In this study, there were a total of 13 depths where the particulate $^{210}\text{Po}/^{210}\text{Pb}$ activity ratio was lower than 1 and 8 of these depths also had a dissolved $^{210}\text{Po}/^{210}\text{Pb}$ activity ratio lower than 1.

9. Page 13: The negative relationship between AOU and $^{210}\text{Po}/^{210}\text{Pb}$ is not very strong. We agree that both negative and positive linear relationships between total particulate $^{210}\text{Po}/^{210}\text{Pb}$ AR and AOU are not very strong, with R^2 as 0.5 and 0.4, respectively. Nonetheless, the p-value for both linear relationships is below the significance threshold of 0.05. It appears that the negative relationship was stronger than the positive relationship in terms of R^2 and p-value. If we had more data available (both particulate ^{210}Po and ^{210}Pb activity and AOU), it would perhaps be possible to observe stronger relationships. This is a topic that will be explored in the future and we thought it was helpful to show the relationships while providing possible mechanisms to explain them.

10. Page 14: Line 387 appears not to be clearly expressed indeed!

We agree and will add the following sentence to make it clearer:

“As claimed previously in Tang et al. (2017), $K_d(\text{Po})$ is complicated because it appears to reflect both the surface adsorption and potential bioaccumulation.”

11. Conclusion Page 15: The impact of a terrestrial origin on the $^{210}\text{Po}/^{210}\text{Pb}$ ratio less than unity might indeed be born out in the Arctic basin during summer seasons of strong biogenic processing. Maybe there is evidence in the recent GEOTRACES cruises on time scales of several months conclusive with that of the grand-daughter/parent nuclide pair?

There are two recent GEOTRACES Arctic cruises (GN01 and GN04) in 2015 which both have sampled for ^{210}Po and ^{210}Pb activity measurements. Unfortunately, the data is not yet available.

12. Figure Captions 4) ...bloom defines the date when the next bloom began.

Corrected.

13. Figure Caption 5) The black and blue colored circles are not well distinguished.

The color code in Figure 5 is now modified. Please see below.

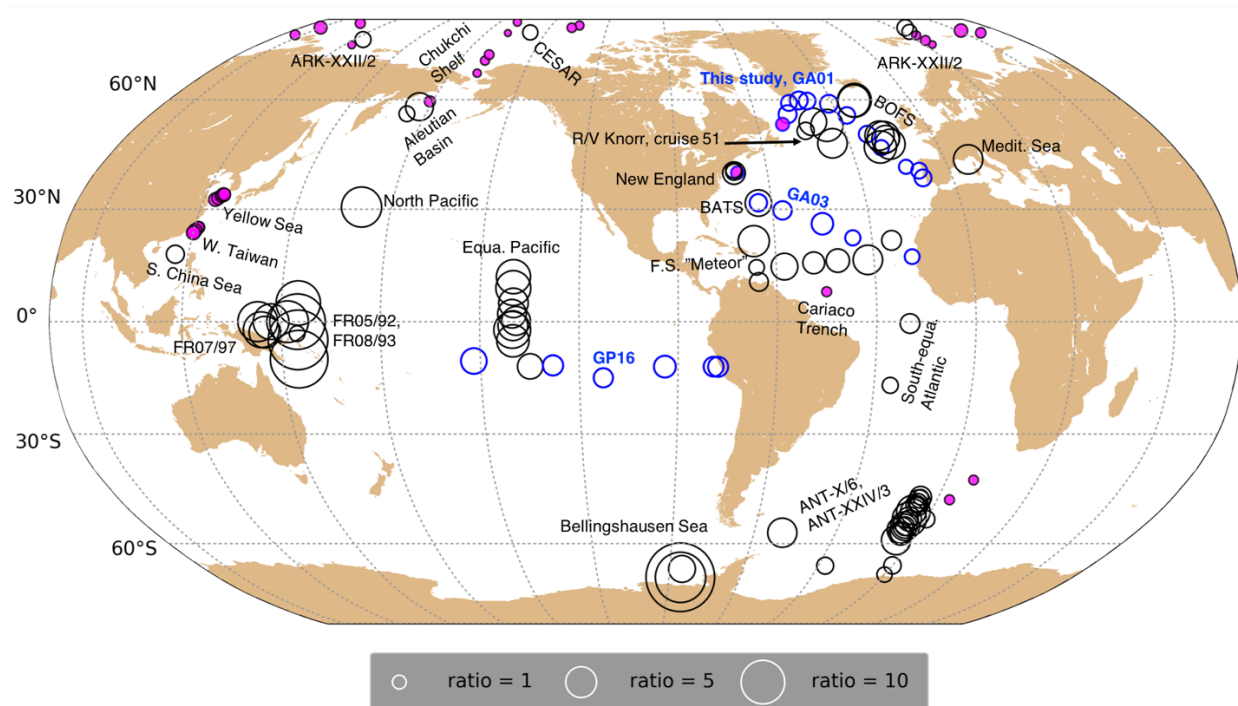


Fig. 8. Comparison of particulate $^{210}\text{Po}/^{210}\text{Pb}$ activity ratios in the upper 200 m from this study and 20 previous studies (references in Table 2). Information about the study site, sampling date, method, and particle size of each study are shown in Table 2. The black circles represent data from previous studies while the blue circles are the results from samples analyzed at QC from three recent GEOTRACES transects (GA03, GP16, and this study, GA01 GEOVIDE). The filled magenta and open circles indicate activity ratios lower and higher than 1, respectively.

References:

Bacon, M. P.: ^{210}Pb and ^{210}Po results from F.S. "Meteor" cruise 32 in the North Atlantic, PANGAEA, 1977.

Bacon, M. P., Belostock, R. A., Tecotzky, M., Turekian, K. K. and Spencer, D. W.: Lead-210 and polonium-210 in ocean water profiles of the continental shelf and slope south of New England, *Continental Shelf Research*, 8, 841-853, 1988.

Bacon, M. P., Brewer, P. G., Spencer, D. W., Murray, J. W. and Goddard, J.: Lead-210, polonium-210, manganese and iron in the Cariaco Trench, *Deep Sea Research Part A. Oceanographic Research Papers*, 27, 119-135, 1980a.

Bacon, M. P., Spencer, D. W. and Brewer, P. G.: $^{210}\text{Pb}/^{226}\text{Ra}$ and $^{210}\text{Po}/^{210}\text{Pb}$ disequilibria in seawater and suspended particulate matter, *Earth and Planetary Science Letters*, 32, 277-296, 1976.

Bacon, M. P., Spencer, D. W. and Brewer, P. G.: Lead-210 and Polonium-210 as Marine Geochemical Tracers: Review and Discussion of Results from the Labrador Sea, *Natural radiation environment III*, T. F. Gesell and W. M. Lowder, 1, 473-501, 1980b.

Baskaran, M.: Po-210 and Pb-210 as atmospheric tracers and global atmospheric Pb-210 fallout: A Review, *International Topical Meeting on Polonium and Radioactive Lead Isotopes*, 102, 500-513, 2011.

BODC, Lowry, R. K., Machin, P. and Cramer, R. N.: Compilation of the results of EU-project BOFS, PANGAEA, 2016.

Church, T., Rigaud, S., Baskaran, M., Kumar, A., Friedrich, J., Masqué, P., Puigcorbé, V., Kim, G., Radakovitch, O., Hong, G., Choi, H. and Stewart, G.: Intercalibration studies of ^{210}Po and ^{210}Pb in dissolved and particulate seawater samples, *Limnology and Oceanography Methods*, 10, 776-789, 2012.

Cochran, J. K., Bacon, M. P., Krishnaswami, S. and Turekian, K. K.: ^{210}Po and ^{210}Pb distributions in the central and eastern Indian Ocean, *Earth and Planetary Science Letters*, 65, 433-452, 1983.

Fisher, N. S., Burns, K. A., Cherry, R. D. and Heyraud, M.: Accumulation and cellular distribution of ^{241}Am , ^{210}Po and ^{210}Pb in two marine algae, *Marine Ecology Progress Series*, 11, 233-237, 1983.

Friedrich, J.: Polonium-210 and Lead-210 activities measured on 17 water bottle profiles and 50 surface water samples during POLARSTERN cruise ARK-XXII/2, PANGAEA, 2011.

Friedrich, J., Robert, M. and Stimac, I.: Polonium-210 and Lead-210 activities measured on 9 water bottle profiles during POLARSTERN cruise ANT-XXIV/3, PANGAEA, 2011.

Friedrich, J. and Rutgers van der Loeff, M. M.: A two-tracer (^{210}Po – ^{234}Th) approach to distinguish organic carbon and biogenic silica export flux in the Antarctic Circumpolar Current, Deep Sea Research Part I: Oceanographic Research Papers, 49, 101-120, 2002.

He, J., Yu, W., Lin, W., Men, W. and Chen, L.: Particulate organic carbon export fluxes on Chukchi Shelf, western Arctic Ocean, derived from $^{210}\text{Po}/^{210}\text{Pb}$ disequilibrium, Chinese Journal of Oceanology and Limnology, 33, 741-747, 2015.

Hong, G.-H., Park, S.-K., Baskaran, M., Kim, S.-H., Chung, C.-S. and Lee, S.-H.: Lead-210 and polonium-210 in the winter well-mixed turbid waters in the mouth of the Yellow Sea, Continental Shelf Research, 19, 1049-1064, 1999.

Hu, W., Chen, M., Yang, W., Zhang, R., Qiu, Y. and Zheng, M.: Enhanced particle scavenging in deep water of the Aleutian Basin revealed by ^{210}Po - ^{210}Pb disequilibria, Journal of Geophysical Research: Oceans, 119, 3235-3248, 2014.

Kim, G.: Large deficiency of polonium in the oligotrophic ocean's interior, Earth and Planetary Science Letters, 192, 15-21, 2001.

Kim, G. and Church, T. M.: Seasonal biogeochemical fluxes of ^{234}Th and ^{210}Po in the Upper Sargasso Sea: Influence from atmospheric iron deposition, Global Biogeochemical Cycles, 15, 651-661, 2001.

Moore, H. E., Poet, S. E., Martell, E. A. and Wilkening, M. H.: Origin of ^{222}Rn and its long-lived daughters in air over Hawaii, Journal of Geophysical Research, 79, 5019-5024, 1974.

Moore, R. M. and Smith, J. N.: Disequilibria between ^{226}Ra , ^{210}Pb and ^{210}Po in the Arctic Ocean and the implications for chemical modification of the Pacific water inflow, Earth and Planetary Science Letters, 77, 285-292, 1986.

Murray, J. W., Paul, B., Dunne, J. P. and Chapin, T.: ^{234}Th , ^{210}Pb , ^{210}Po and stable Pb in the central equatorial Pacific: Tracers for particle cycling, Deep Sea Research Part I: Oceanographic Research Papers, 52, 2109-2139, 2005.

Nozaki, Y. and Tsunogai, S.: ^{226}Ra , ^{210}Pb and ^{210}Po disequilibria in the Western North Pacific, Earth and Planetary Science Letters, 32, 313-321, 1976.

Peck, G. and Smith, J. D.: Uranium decay series radionuclides in the Western Equatorial Pacific Ocean and their use in estimating POC fluxes, J.-M. Fernandez and R. Fichez, Paris, 459-469, 2002.

Rigaud, S., Puigcorbé, V., Camara-Mor, P., Casacuberta, N., Roca-Martí, M., Garcia-Orellana, J., Benitez-Nelson, C. R., Masqué, P. and Church, T.: A methods assessment and recommendations for improving calculations and reducing uncertainties in the determination of ^{210}Po and ^{210}Pb activities in seawater, *Limnology and Oceanography Methods*, 11, 561-571, 2013.

Rigaud, S., Stewart, G., Baskaran, M., Marsan, D. and Church, T.: ^{210}Po and ^{210}Pb distribution, dissolved-particulate exchange rates, and particulate export along the North Atlantic US GEOTRACES GA03 section, *Deep Sea Research Part II*, 116, 60-78, 2015.

Roca-Martí, M., Puigcorbé, V., Rutgers van der Loeff, M. M., Katlein, C., Fernández-Méndez, M., Peeken, I. and Masqué, P.: Carbon export fluxes and export efficiency in the central Arctic during the record sea-ice minimum in 2012: a joint $^{234}\text{Th}/^{238}\text{U}$ and $^{210}\text{Po}/^{210}\text{Pb}$ study, *Journal of Geophysical Research: Oceans*, 121, 5030-5049, 2016.

Sarin, M. M., Kim, G. and Church, T. M.: ^{210}Po and ^{210}Pb in the South-equatorial Atlantic:, *Deep Sea Research Part II*, 46, 907-917, 1999.

Sarin, M. M., Krishnaswami, S., Ramesh, R. and Somayajulu, B. L. K.: ^{238}U decay series nuclides in the northeastern Arabian Sea: Scavenging rates and cycling processes, *Continental Shelf Research*, 14, 251-265, 1994.

Sarthou, G., Lherminier, P., Achterberg, E. P., Alonso-Pérez, F., Bucciarelli, E., Boutorh, J., Bouvier, V., Boyle, E. A., Branellec, P., Carracedo, L. I., Casacuberta, N., Castrillejo, M., Cheize, M., Contreira, P. L., Cossa, D., Daniault, N., De Saint-Léger, E., Dehairs, F., Deng, F., Desprez de Gésincourt, F., Devesa, J., Foliot, L., Fonseca-Batista, D., Gallinari, M., García-Ibáñez, M. I., Gourain, A., Grossteffan, E., Hamon, M., Heimbürger, L. E., Henderson, G. M., Jeandel, C., Kermabon, C., Lacan, F., Le Bot, P., Le Goff, M., Le Roy, E., Lefèbvre, A., Leizour, S., Lemaitre, N., Masqué, P., Ménage, O., Menzel Barraqueta, J. L., Mercier, H., Perault, F., Pérez, F. F., Planquette, H., Planchon, F., Roukaerts, A., Sanial, V., Sauzède, R., Shelley, R. U., Stewart, G., Sutton, J., Tang, Y., Tisnérat-Laborde, N., Tonnard, M., Tréguer, P., van Beek, P., Zurbrick, C. M. and Zunino, P.: Introduction to the French GEOTRACES North Atlantic Transect (GA01): GEOVIDE cruise, *Biogeosciences*, in review.

Shimmield, G. B., Ritchie, G. D. and Fileman, T. W.: The impact of marginal ice zone processes on the distribution of ^{210}Pb , ^{210}Po and ^{234}Th and implications for new production in the Bellingshausen Sea, Antarctica, *Deep Sea Research Part II*, 42, 1313-1335, 1995.

Smetacek, V., de Baar, H. J. W., Bathmann, U., Lochte, K. and Rutgers van der Loeff, M. M.: Export production by ^{234}Th , including ^{210}Po and ^{210}Pb measured on water bottle samples during POLARSTERN cruise ANT-X/6, PANGAEA, 1997.

Stewart, G., Cochran, J. K., Miquel, J. C., Masqué, P., Szlosek, J., Rodriguez y Baena, A. M., Fowler, S. W., Gasser, B. and Hirschberg, D. J.: Comparing POC export from $^{234}\text{Th}/^{238}\text{U}$ and $^{210}\text{Po}/^{210}\text{Pb}$ disequilibria with estimates from sediment traps in the northwest Mediterranean, Deep Sea Research Part I: Oceanographic Research Papers, 54, 1549-1570, 2007.

Stewart, G. M., Fowler, S. W., Teyssié, J. L., Cotret, O., Cochran, J. K. and Fisher, N. S.: Contrasting transfer of polonium-210 and lead-210 across three trophic levels in marine plankton, Marine Ecology Progress Series, 290, 27-33, 2005.

Subha Anand, S., Rengarajan, R., Shenoy, D., Gauns, M. and Naqvi, S. W. A.: POC export fluxes in the Arabian Sea and the Bay of Bengal: A simultaneous $^{234}\text{Th}/^{238}\text{U}$ and $^{210}\text{Po}/^{210}\text{Pb}$ study, Marine Chemistry, 2017.

Tang, Y., Stewart, G., Lam, P. J., Rigaud, S. and Church, T.: The influence of particle concentration and composition on the fractionation of ^{210}Po and ^{210}Pb along the North Atlantic GEOTRACES transect GA03, Deep Sea Research Part I: Oceanographic Research Papers, 128, 42-54, 2017.

Towler, P.: Radionuclides measured on water bottle samples during FRANKLIN cruise FR05/92, PANGAEA, 2003.

Towler, P.: Radionuclides measured on water bottle samples during FRANKLIN cruise FR08/93, PANGAEA, 2013.

Turekian, K. K., Nozaki, Y. and Benninger, L. K.: Geochemistry of Atmospheric Radon and Radon Products, Annual Review of Earth and Planetary Sciences, 5, 227-255, 1977.

Verdeny, E., Masqué, P., Maiti, K., Garcia-Orellana, J., Bruach, J. M., Mahaffey, C. and Benitez-Nelson, C. R.: Particle export within cyclonic Hawaiian lee eddies derived from ^{210}Pb – ^{210}Po disequilibrium, Deep Sea Research Part II: Topical Studies in Oceanography, 55, 1461-1472, 2008.

Wei, C., Lin, S., Wen, L. and Sheu, D. D. D.: Geochemical behavior of ^{210}Pb and ^{210}Po in the nearshore waters off western Taiwan, Marine Pollution Bulletin, 64, 214-220, 2012.

Wei, C. L., Yi, M. C., Lin, S. Y., Wen, L. S. and Lee, W. H.: Seasonal distributions and fluxes of ^{210}Pb and ^{210}Po in the northern South China Sea, Biogeosciences, 11, 6813-6826, 2014.

Response to Referee 2

We thank Referee 2 for the helpful comments. We will address all changes in the revised manuscript as detailed in our responses below. The referee comments are in black and their line numbers refer to the original submitted manuscript. Our responses are in blue text.

We want to note that some of the reviewer's comments may pertain to an original draft of the manuscript which has already been revised. We have tried to address all comments, but in some cases, we do not see what the reviewer is talking about. In our response, we will only be referring to the version that is currently available on the BG website.

We also want to note that we now have submitted a companion paper to this special issue that is specifically about the particulate organic carbon (POC) export using the $^{210}\text{Po}/^{210}\text{Pb}$ technique.

Reviewer Recommendation and Comments for Manuscript BG-2018-210

General comments

The manuscript reports on total, small particles and large particles activity of ^{210}Po and ^{210}Pb nuclides along the North Atlantic GEOTRACES GA01 (GEOVIDE) cruise. The paper is well written, well structured and I believe that such measurements in this areas are essential for the scientific understanding of TEI's and biogenic elements in the global ocean. The approach is very good and the compilation of many other joined data (AOU, PP, SPM, chlorophyll, ...) is essential to reach this goal. In addition there is a huge effort to include this new dataset with previous ones in order to get a better view of the processes controlling the behaviors of ^{210}Po and ^{210}Pb at a larger scale. Finally I found very interesting news findings that emerge from a new way to confront this ^{210}Po and ^{210}Pb dataset to other variables (comparison with chlorophyll-a from satellite-based data, AOU, ...) that merit to be published.

However I found some questioning points that need to be addressed:

1. the splitting of the samples between two different labs with two methods that differ in some points is very surprising. Some practical reasons can certainly explain this

procedure but they are not mentioned. The reader need to be sure that the results can be compared. Especially since there are distinct features that can be seen between the samples from the two labs and that a part of the discussion relies on such differences.

Thank you for your suggestion. We agree that there are some differences in the procedure between the two labs. We will add explanation in the text. Please see our responses to Specific comments 13 and 14.

2. the last section of the discussion about the sorption, distribution coefficient and implication for particles and POC export very speculative. This is embarrassing as this appears in the abstract and the conclusion as the most important finding of the study while there are other findings much more robust that are not presented in that way.

There may be a misunderstanding, but we don't see POC export in the current abstract. We have submitted a companion paper to this special issue that is specifically about POC export, unlike this paper. We will remove the reference to POC export and rephrase the last section of the discussion to support our observations of ^{210}Po and ^{210}Pb distributions. Please see our response to Specific comment 47.

3. the presentation of the context in the introduction and the state of the art about ^{210}Po and ^{210}Pb isotopes in the ocean is a little bit weak and I think the importance of such measurement in this area should be specifically strengthened.

Thank you for your suggestion. We will edit the Introduction section by adding more rationale for the GEOVIDE section and strengthening the objective section. Please see our responses to the Specific comments 4 and 5.

Consequently, I believe this paper must be published when these points will be addressed.

Thank you for your positive evaluation. Please see our responses to the specific comments below.

Specific comments:

Title:

1. The part of the title "partitioning between the dissolved and particles phase" is maybe not really appropriate as the most important discussions in the paper is about the processes explaining the variations in the $^{210}\text{Po}/^{210}\text{Pb}$ activity ratio within each phase (i.e., total and small/large particles).

We agree and will change the title to “Distributions of total and size-fractionated particulate ^{210}Po and ^{210}Pb activities along the North Atlantic GEOTRACES GA01 (GEOVIDE) transect”.

Abstract

2. P2, L22-23: this was not shown in the manuscript

We agree that we didn't mention it in the original manuscript.

We will add the sentence of “The average values of $K_d(\text{Po})$ was 1.6 times of those of $K_d(\text{Pb})$ in both small and total particulate phases, suggesting a higher affinity with particles for ^{210}Po with respect to ^{210}Pb , which is commonly observed in the global ocean (Bacon et al., 1988; Hong et al., 1999; Masqué et al., 2002; Wei et al., 2014; Tang et al., 2017).” on L399. We will keep this in the Abstract after the addition.

Introduction

3. P3, L42: "seventh repetition of the OVIDE section": please precise what is the OVIDE section/program?

OVIDE is an acronym of “Observatoire de la variabilité interannuelle et décennale en Atlantique Nord,” and this section covers Portugal to Greenland. This will be clearly explained in the summary paper of this special issue (Sarhou et al., in review).

4. P3, L44-46: please give a short summary on the hydrological properties on the area.
P3, L47-49: you should illustrate what is this expected "mixture of complex ..." and why this section may present a special opportunity.

We agree that we did not provide detailed information on the hydrological properties of the study area nor the rationale for the cruise track. There will be multiple papers in this special issue and in other journals specifically describing the hydrographic and physical characteristics, justification of the GEOVIDE cruise track, and the sampling strategies (e.g. García-Ibáñez et al., 2015; Benetti et al., 2017; García-Ibáñez et al., 2018; Zunino et al., 2018; Sarthou et al., in review). We therefore will only add some information about the section as the following:

“The major goal of the international GEOTRACES program is to characterize the distributions of trace elements and isotopes (TEIs) in the ocean on a global scale, and to identify and quantify processes that control these distributions (GEOTRACES Planning Group, 2006). The GEOVIDE section was a contribution of the French GEOTRACES program to this global program in the subpolar North Atlantic. The GEOVIDE GA01 cruise was carried out in 2014 in the North Atlantic and consisted of two sections: a section along the OVIDE (Observatoire de la variabilité interannuelle et décennale en Atlantique Nord) line between Lisbon (Portugal) and Cape Farewell (southern tip of Greenland), and a Cape Farewell to St. John’s (Canada) section across the Labrador Sea (Fig. 1). Since 2002, the OVIDE section has been occupied biennially to collect physical and biogeochemical data (Mercier et al., 2015). The knowledge of the currents, water masses, and biogeochemical provinces gained from the previous OVIDE campaigns enabled the optimal strategy for TEIs sampling and provided help for the interpretation of the distribution of TEIs in the subpolar North Atlantic (García-Ibáñez et al., 2015). In addition to the OVIDE line, the Labrador Sea section provided a unique opportunity to study TEIs distributions along the boundary current of the western North Atlantic subpolar gyre (Sarthou et al., in review).”

5. P4, L72-78: I found this objectives section disappointing and clearly not ambitious enough with respect to the dataset compiled and presented in this paper. I suggest the authors to strengthen this part.

We agree with the reviewer’s comments and will rewrite the objectives section as:

“In this work, we describe the distributions of total and size-fractionated particulate ^{210}Po and ^{210}Pb activity along the GEOVIDE cruise in the North Atlantic. These data are a significant

contribution to the high-latitude North Atlantic ^{210}Po and ^{210}Pb activity data set. We present a compilation of particulate $^{210}\text{Po}/^{210}\text{Pb}$ activity ratios (AR) from previous studies in the global ocean and the results are discussed in regards to the aging of water and biochemical processes. We also describe the relationship among small particles, adsorption, and scavenging of radionuclides. These results lead to recommendations for the estimation of particulate organic carbon export flux based on the $^{210}\text{Po}/^{210}\text{Pb}$ disequilibrium, a topic that is covered in a companion paper (Tang et al., submitted)."

Methods

6. P5, L104: Please correct the sentence to avoid confusion: what was transferred into a clean bottle? The filters? The filtrate?

The filter was placed into a clean falcon tube. We will rephrase the sentence as: "Samples were filtered through a 0.45 μm membrane filter and the filters with the precipitate were placed into falcon tubes, sealed with parafilm, and stored in double-bags."

7. P5, L107: is the "Stewart laboratory" the official name of the laboratory?

The lab doesn't have an official name. Because G. Stewart is the investigator of this lab at Queens College (QC), we used "Stewart Laboratory" in the text. We now will use QC in the revised manuscript.

8. P5, L107-108: why this splitting procedure of the sample? The reader need to know why this splitting procedure allow to "ensure higher counting statistic in the samples". Did the laboratory performed intercalibration experiments?

We will answer the question in the text as follows: "As the delay between sample collection and first Po plating increases, the uncertainty of the calculated ^{210}Po activity also increases. In addition, it is necessary to balance counting periods with the number of samples as the uncertainty due to alpha spectrometry counting decreases by increasing the counting time. To limit the delay between sampling and processing and to ensure higher counting statistics by having more alpha spectrometers devoted to this project, sample processing and analyses were

split between Universitat Autònoma de Barcelona (UAB) (samples from stations 1, 13, and 21) and Queens College (QC) (stations 26, 32, 38, 44, 60, 69, and 77)."

Unfortunately, there wasn't enough material to perform an intercalibration experiment.

9. P5, L110: Please correct the sentence to avoid confusion: the filter was not evaporated to dryness.

We will change the sentence to "Briefly, the filters were digested into a solution of concentrated HNO₃ and HCl, and after the solution was evaporated to dryness, the samples were recovered in 1M and 0.5 M HCl solution at UAB and QC, respectively (a 0.5-2 M HCl solution is recommended, Rigaud et al., 2013)."

10. P5, L110: Remove "eventually"

Done. Please see the previous response.

11. P5, L112: what weak acid solution?

We now write this as "1 M/ 0.5 M HCl solution".

12. P5, L120: write "to determine Pb recovery" instead of "to determine sample recovery".

Done.

13. P5, L125-127: why this difference between the two labs?

The higher uncertainties for the samples processed at QC were due to additional corrections on the 1st stable Pb recovery. We will explain this in the text as:

"The activities of ²¹⁰Po and ²¹⁰Pb at the time of collection were determined by a series of corrections, including nuclide decay, ingrowth, chemical recoveries, detector backgrounds, and blank contamination following the methods in Rigaud et al. (2013). The activity uncertainties from UAB were on average 8% for both ²¹⁰Po and ²¹⁰Pb activity, while the QC uncertainties were on average 13% for ²¹⁰Po activity and 16% for ²¹⁰Pb activity. The greater uncertainties of

^{210}Po and ^{210}Pb activities in the samples processed at QC were due to the longer delay between sampling and first plating (68 vs. 50 d) and higher uncertainties in the determination of the recovery of lead.”

14. P6, L137: These two different digestion procedures may give different results? Please explain if tests were carried out. Are the data from the two groups comparables?

We agree that there were different digestion procedures (with or without HF), and we didn't run comparisons and need to rely on both labs working well.

15. P6, L144: what is the Planquette group?

Helene Planquette Group, University of Brest, co-authors in the special issue.

16. P6, L144: is this sentence correct: "the material on the balance of the screens and filters"?

The sentence will be rephrased as “The Helene Planquette group (University of Brest) collected subsamples from the same screens and filters that were sampled previously for radionuclides to determine major phase composition (particulate organic matter (POM), lithogenic material, calcium carbonate (CaCO_3), opal, $\text{Fe}(\text{OH})_3$, and MnO_2) (references therein Lam et al., 2015).”

17. P6, L148-149: if the method is the same as described by Lam et al. 2015, I suggest to remove the Lemaitre et al. in prep. reference if it is not published at the time of the publication of this paper. Same comment for other reference in prep. in the manuscript.

Thank you for your suggestion. We will remove the references in prep. from the manuscript but keep the references submitted or in review as the journal suggests.

18. P6, L158: what is the Dehairs group?

Frank Dehairs group, Vrije Universiteit Brussel, co-authors in this special issue.

19. P6, L157-164: a little bit more details is needed here: how the photometric conditions was applied on deck? I guess that ^{13}C was spike before the incubation? ...

Yes, the sample was spiked with $\text{NaH}^{13}\text{CO}_3$ before the incubation. More details on the experimental procedure were added in the text as: “The seawater was then spiked with 3 mL of a $\text{NaH}^{13}\text{CO}_3$ solution (200 mmol L^{-1} , 99%, Euriotop), and incubated on deck for 24 h in the circulating incubators wrapped with neutral density screens to simulate *in-situ* irradiance conditions.”

20. P7, L173-174: Before to compare the AOU data from the GEOVIDE program, you should explain how you get it. In facts, the section 2.7 is disturbing. There are two things here: the AOU and the comparison with historical data but there is no link between them. I suggest to split this section in two (even short) sections.

As suggested, we have split the original section 2.7 into two sections: section 2.7 Historical values and section 2.8 Apparent oxygen utilization as the following:

“2.7 Historical values

The historical data of the particulate ^{210}Po and ^{210}Pb activity, and the hydrological parameters (pressure, temperature, salinity, and dissolved oxygen) were obtained from databases and publications. The location, date, database address or publication name, and type of data (particulate ^{210}Po and ^{210}Pb activity or hydrological parameters) from all other studies is listed in supplemental Table S1.

2.8 Apparent oxygen utilization

Apparent oxygen utilization ($\text{AOU} = \text{O}_2_{\text{ saturated}} - \text{O}_2_{\text{ measured}}$) is defined as the difference between the saturated oxygen at a given temperature and salinity and the measured in-situ oxygen concentration (Ito et al., 2004; Duteil et al., 2013). A positive AOU indicates either water mass aging and outgassing of oxygen or biological activity, namely respiration (e.g. Keeling et al., 1998; Boyer et al., 1999). Negative AOU, indicating that the water is oversaturated with

dissolved oxygen, can appear under the conditions of an intense bloom (e.g. Coppola et al., 2017).

The dissolved oxygen concentration was measured by Winkler titration and the saturated oxygen concentration was calculated as a function of in-situ temperature and salinity, and one atmosphere of total pressure based on the built-in function in Ocean Data View (<https://odv.awi.de>).”

21. P2, L182-187: SPM, PP, chlorophyll were not considered to try to explain the ^{210}Po - ^{210}Pb activities and activity ratios distribution?

The time-series chlorophyll-a data was considered to explain the distribution of total particulate $^{210}\text{Po}/^{210}\text{Pb}$ ratios < 1 at variable depths on L299-309 in the original manuscript.

The SPM and PP data, were indeed not used to try to explain the distribution of the radionuclide activities nor activity ratios. Instead, SPM were used to calculate the partitioning coefficient (K_d) while the in-situ PP and in-situ pigment data were considered to investigate the role of small particles in primary production and phytoplankton composition.

Results

22. p7, L195-202: there are a clear difference between station 1, 13, 21 and the other ones. These differences also correspond to the two samples groups that were processed by two labs. This is embarrassing if there is nothing that certify that labs results can be compared.

We agree there is a clear difference between stations 1, 13, 21 and the others along the transect. We acknowledge that the greater uncertainties of ^{210}Po and ^{210}Pb activities in the samples processed at QC were due to the longer delay between sampling and first plating (68 vs. 50 d) and higher uncertainties in the determination of the recovery of lead. It is unfortunate that we could not collect additional material to perform intercalibration between the two labs.

23. p7, L200-202: please rewrite this sentence which is very confusing.

We will change the sentence to: “ $^{210}\text{Po}_t$ excesses relative to $^{210}\text{Pb}_t$, which were larger than $^{210}\text{Po}_t$ surface depletions at the same stations, were observed below the surface at some depths at stations 1, 13, and 21 in the Western European Basin (Fig. 2).”

24. p7, L195-207: this paragraph is confusing. Please describe firstly the surface water then the depth (or in the other way) but not a mixing description.

We concur. We will rewrite section 3.1 by describing first the activity range of all samples, then the surface samples, and last the deep samples. Section 3.1 will be changed to the following:

“Total ^{210}Po activities ($^{210}\text{Po}_t$) in all samples ranged from 2.2 to 16.4 dpm 100 L⁻¹ and the mean $^{210}\text{Po}_t$ was 8.8 ± 2.4 dpm 100 L⁻¹ (n = 198, Fig. 2). $^{210}\text{Po}_t$ activities were generally low within the mixed layer and euphotic zone (15 – 47 m), slightly increased or remained relatively constant in the depth range between the mixed layer and 250 m, and then decreased with water depth at most of the stations except station 26. Near the seafloor, stations 1, 13 and 44 had a slight increase of $^{210}\text{Po}_t$ activity.

Total ^{210}Pb activities ($^{210}\text{Pb}_t$) were between 2.1 and 20.6 dpm 100L⁻¹ with a mean value of 10.0 ± 3.0 dpm 100 L⁻¹ (n = 198, Fig. 2). $^{210}\text{Pb}_t$ activities were low in the surface, slightly increased in the subsurface and decreased with water depth. Stations 1, 13, 44, and 60 exhibited an increase near the seafloor.

The mean $^{210}\text{Po}_t/^{210}\text{Pb}_t$ activity ratio (AR) of all samples was 0.92 ± 0.28 (n = 198, Fig. 2). When considering different basins separately, there is a tendency of decreasing $^{210}\text{Po}_t/^{210}\text{Pb}_t$ AR from the Western European Basin (1.10 ± 0.35) westwards to the Iceland Basin (0.90 ± 0.19) and the Irminger Sea and the Labrador Sea (0.80 ± 0.18 and 0.83 ± 0.21 , respectively).

For all regions, significant deficits of $^{210}\text{Po}_t$ (0.80 ± 0.20 , n = 40) were observed within the mixed layer and euphotic zone (Fig. 3). Secular equilibrium was also observed at some shallow depths (i.e. 80 m at station 44) and even in surface waters (i.e. 15 m at station 38). $^{210}\text{Po}_t$ excesses relative to $^{210}\text{Pb}_t$, which were larger than $^{210}\text{Po}_t$ surface depletions at the same stations, were observed below the surface at some depths at stations 1, 13, and 21 in the Western European Basin (Fig. 2). At depths below the surface to ~ 1500 m in the Iceland Basin, the

Irminger Sea, and the Labrador Sea, the water samples still indicated a ^{210}Po deficiency (AR: 0.84 ± 0.17 , $n = 27$). Secular equilibrium was generally reached near the bottom depths in all basins except at stations 13 and 60 where the water samples were either enriched in $^{210}\text{Po}_t$ ($^{210}\text{Po}_t/^{210}\text{Pb}_t$ AR = 1.58 ± 0.16) or depleted in $^{210}\text{Po}_t$ ($^{210}\text{Po}_t/^{210}\text{Pb}_t$ AR = 0.50 ± 0.12), respectively.”

25. p8, L214-216: why the figure is not shown? The particulate profiles should be plotted (at least in the appendix material).

Thank you for the suggestion. The profiles of the particulate activity in the small and large size fractions will be shown as the following:

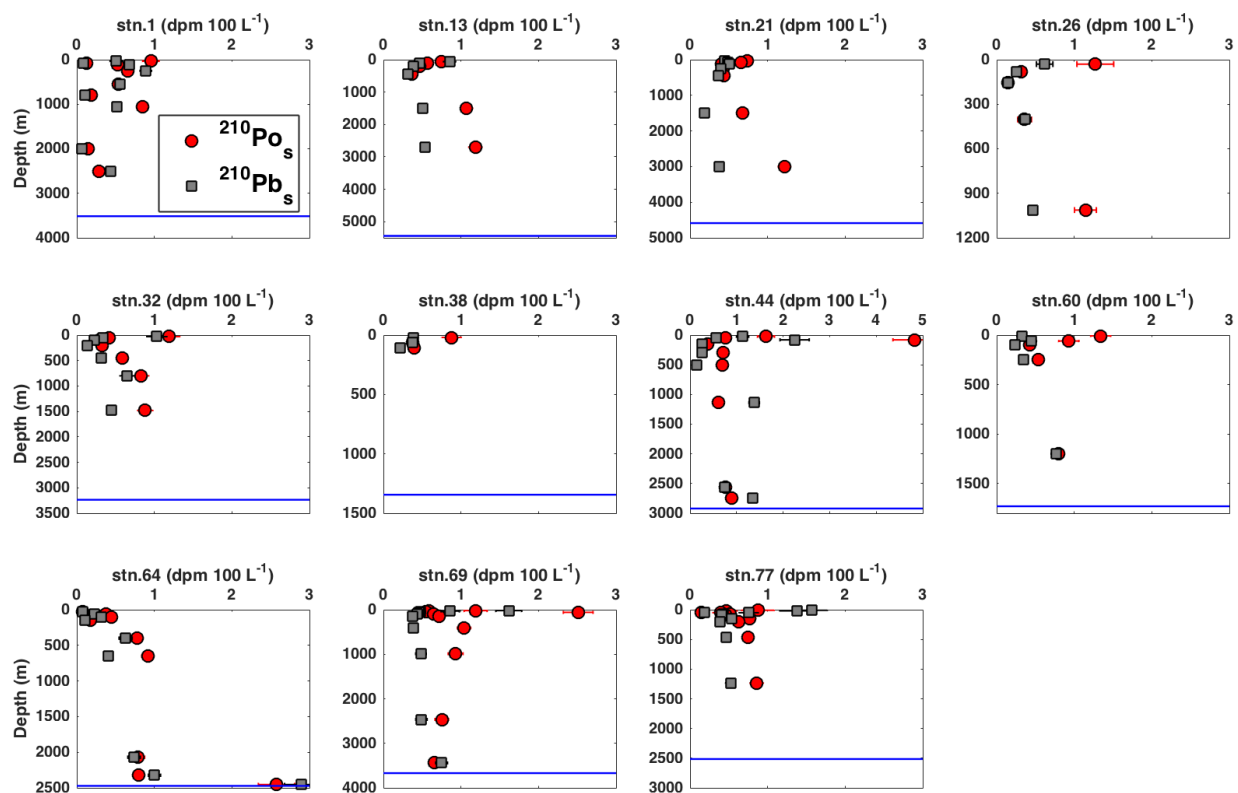


Fig. 4. Vertical profiles of particulate ^{210}Po and ^{210}Pb activity in the small size fraction (1-53 μm , $^{210}\text{Po}_s$, $^{210}\text{Pb}_s$). Note the different depth scales for the various stations and that the activity scale at Station 44 differs from the scale of all other stations. The horizontal blue line represents the bottom depth at that station.

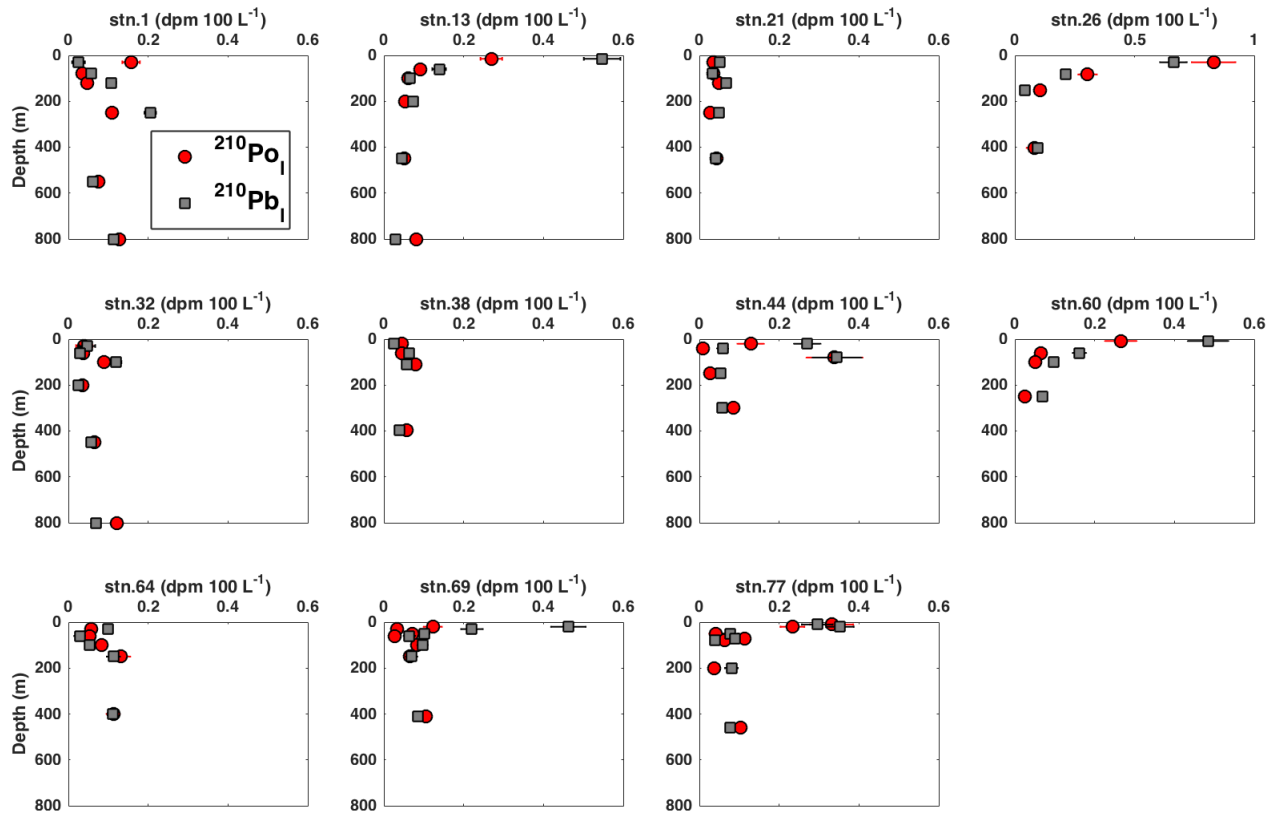


Fig. 5. The vertical profiles of the particulate ^{210}Po and ^{210}Pb activity in the large size fraction ($> 53 \mu\text{m}$, $^{210}\text{Po}_i$, $^{210}\text{Pb}_i$) in the top 800 m. Note that the activity scale at Station 26 differs from the scale at all other stations.

26. p9, L242-244: yes, this is not surprising as the small particle are the main particulate reservoir.

Yes, we agree. No change.

27. p9, L245-246: which particulate samples are depleted? Where they are located? In surface? Subsurface? Variable depths?

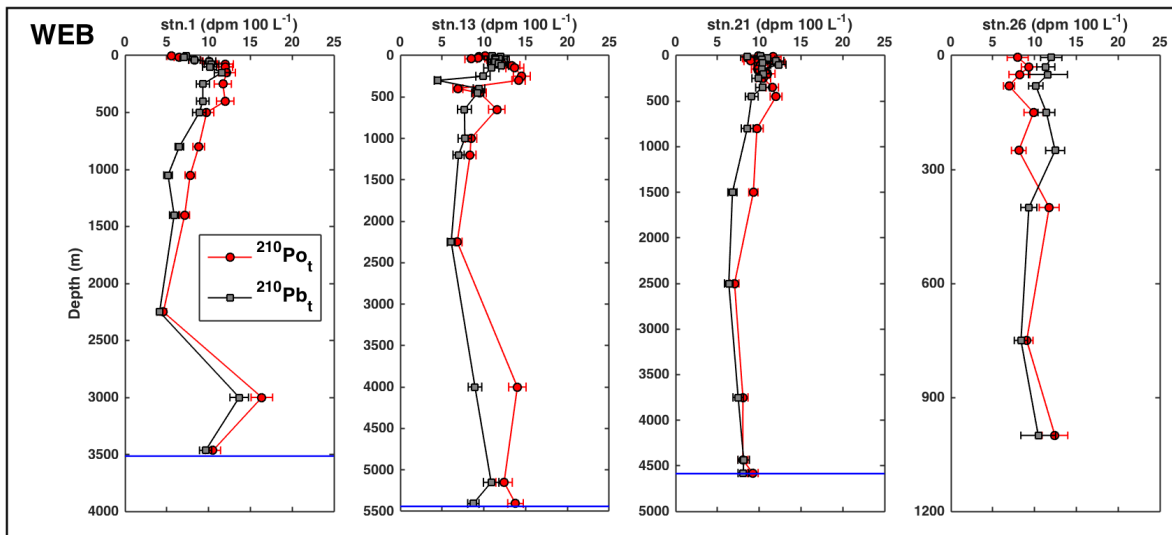
The information about those particulate samples with $^{210}\text{Po}/^{210}\text{Pb}$ AR < 1 was given in Table 1 and on Line 303-304. We will add the information here as: “While the majority of particulate

matter was enriched in ^{210}Po ($^{210}\text{Po}_p/^{210}\text{Pb}_p \text{ AR} > 1$), there were 13 out of 56 total samples from various depths that were depleted in ^{210}Po relative to ^{210}Pb .”

Discussion

28. p10, L264-265: large excess is not seen at depth.

In the most recent submitted draft, we don't use the word “large”, but we do see ^{210}Po activity excess at stations 1, 13 and 21 at depth. Please see the vertical profiles below (Fig. 2). In fact, the average $^{210}\text{Po}/^{210}\text{Pb}$ AR from 100 m down to the bottom depth was 1.2 ± 0.1 , 1.4 ± 0.6 , and 1.1 ± 0.1 at stations 1, 13, and 21, respectively.



29. p10, L260-267: I don't understand how an upwelling along the Iberian coast can bring excess ^{210}Po all over the water column in the 3 station from the WEB.

We now rephrase the sentences on L260-267 as following:

“One possible source of these sub-surface ^{210}Po activity excesses below 200 m at stations 1 and 13 could be the North-East Atlantic Deep Water, lower (NEADW_L) which was the dominant water mass in the Iberian Basin from 2000 m to the bottom, and had a concentration of silicate up to $48 \mu\text{mol kg}^{-1}$ (García-Ibáñez et al., 2015). High activity of ^{210}Po in deep samples could be due to the dissolution of diatoms or herbivore feces (Cooper, 1952). As these particles sink and dissolve, ^{210}Po activity may have been preferentially released to the dissolved phase compared

to ^{210}Pb activity (Bacon et al., 1976), leading to ^{210}Po excess observed in the deep waters at stations 1 and 13. For the sub-surface ^{210}Po activity excesses at station 1 between 400 and 1000 m where lateral inputs of particulate Fe from the margin was observed (Gourain et al., 2018), the likely process is diffusion of ^{210}Po from those particles originated from the margin and such excess could be transported westwards to station 13 by lateral advection. An alternative source of ^{210}Po activity excess between 50 and 250 m at stations 1 and 13 (Fig. 3) could be the eastern boundary upwelling along the coast of the Iberian Peninsula (García-Ibáñez et al., 2015). Even though no strong upwelling events were revealed from temperature and density profiles during the cruise, northerly winds favoring upwelling were recorded 2 – 3 months before the sampling (Shelley et al., 2017). The deep water may have excess ^{210}Po activity due to the remineralization of sinking particles. The upwelling of this water mass prior to the sampling date could maintain such sub-surface excess ^{210}Po activity. Similar findings have been reported in the Cariaco Trench for the upper 300 m of the water column by Bacon et al. (1980).”

30. p11, L295-298: what do you mean by significant? Are they significantly different than this other station? Statistically tested? Is this confirmed from the data on the geochemical composition of SPM?

They are different from the other stations, but no statistical test was performed. Therefore, we will rephrase this sentence in the text as “In addition, the $\text{AR} < 1$ observed at station 1 (120, 250, and 550 m) could be associated with lithogenic particles from the Iberian Margin where 100% of the particulate Fe (PFe) had a lithogenic origin while the lithogenic contribution to PFe at other stations was smaller (Gourain et al., 2018).”

31. p11, L304-308: this is an interesting point. Is there a figure (or a way) to illustrate this? For example a plot showing the AR in surface or subsurface as a function of the time since the last bloom?

We appreciate the suggestions. We have plotted the depths at which total particulate $^{210}\text{Po}/^{210}\text{Pb}$ AR was found to be lower than unity as a function of the time since the last bloom in the following figure:

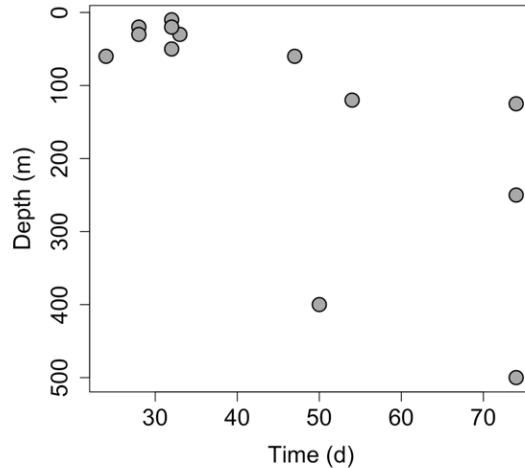


Fig. 7. Depths at which the total particulate ($> 1 \mu\text{m}$) $^{210}\text{Po}/^{210}\text{Pb}$ activity ratio was lower than unity vs. the time since the last bloom (data is presented in Table 1).

32. p12, L321: Is this particulate ^{210}Po depletion in the coastal sea related to the $^{210}\text{Po}/^{210}\text{Pb}$ AR in these the terrestrial/riverine particles or is this due to the nature of those particles that present a lower scavenging efficiency of dissolved ^{210}Po with respect to ^{210}Pb ?

Near the coast, most of the lithogenic particles are terrestrial/riverine particles with a small contribution from aerosols. Aerosols have a very low $^{210}\text{Po}/^{210}\text{Pb}$ AR (< 0.2 , Baskaran, 2011) due to the short residence time of ^{210}Pb in the atmosphere (e.g. Moore et al., 1974; Turekian et al., 1977). For the lithogenic particles sourced from land/river, the particulate ^{210}Po depletion is more related to the nature of those particles that may preferentially adsorb ^{210}Pb vs. ^{210}Po as opposed to the patterns in organic materials (e.g. Fisher et al., 1983; Stewart et al., 2005).

33. p12, L331: AOU must be defined in the method section. What a negative AOU value means?

Thank you for your suggestion. AOU is now defined in the method section 2.8 where the meaning of positive and negative AOU values are explained. Please see our response to specific comment 20.

34. p12, L332: remineralization + respiration + oxidation reactions.

We have corrected it. Please see that in the following response.

35. p12, L333-334: I do not see why water mass aging may change the OAU if there is no mineralization. To my opinion, only biogeochemical processes may change OAU values while the time can only change the intensity of O₂ consumption by those biogeochemical processes. I think this should be better specified in this part to avoid confusion.

We agree that this sentence is not clear and will rephrase it as the following:

“AOU is a time-integrated measure of the amount of oxygen removed during the biogeochemical processes (e.g. respiration, remineralization, oxidation) in the ocean interior. Therefore, AOU is a product of apparent oxygen utilization rate (AOUR) and the age of water mass (e.g. Stanley et al., 2012), i.e. high AOU could be due to either intense biogeochemical processes that have occurred in a short period of time (young water mass) or weaker processes over a longer period of time (old water mass). Consequently, the rate of these biogeochemical processes and time (water mass age) would have different/similar impacts on the $^{210}\text{Po}_p/^{210}\text{Pb}_p$ AR value depending on the initial AR in the particles and the nature of the particles.”

36. p12, L336: what is an old particle? Weeks? Months? Years?

It would be months to years as after 5 half-lives of ^{210}Po (~ 700 days), activity of ^{210}Po would be 95% of the activity of ^{210}Pb if there is no additional removal or addition of either isotopes.

37. p12, L336-338: time will induce an AR approaching 1: decreasing AR if the initial AR is >1 and increasing if the initial AR is < 1. Here you hypothesize that the initial AR in particle is <1 but both cases are possible. Please correct.

We agree and will change this sentence to “For example, the $^{210}\text{Po}_p/^{210}\text{Pb}_p$ AR would tend to increase with time if the initial AR is < 1 because particulate ^{210}Po activity would increase from the decay of ^{210}Pb and trend towards secular equilibrium ($^{210}\text{Po}_p/^{210}\text{Pb}_p$ AR = 1), and to decrease

with time if the initial AR is > 1 as the original excess of particulate ^{210}Po activity would disappear after 7 half-lives of ^{210}Po .”

38. p12, L343-357: very interesting results and interpretation! However, I have two main questions:

Thank you for your comment. Please see our responses to the two main questions below.

39. Why the increase of AR from negative value to value close to 1 for $\text{OAU} > 25 \mu\text{mol}/\text{kg}$? Higher the OAU, higher the mineralization. So intuitively, the AR should be maintained more and more negative with increasing OAU?

We will rephrase the sentences on L350-355 as follows:

“The two contradictory linear trends likely reflect the nature of the particles. For example, the observation of $^{210}\text{Po}_p/^{210}\text{Pb}_p$ AR > 1 with $\text{AOU} < 25 \mu\text{mol kg}^{-1}$ may suggest relatively fresh/organic particles in the young water mass. When AOI increases either due to water mass aging or higher AOI, the $^{210}\text{Po}_p/^{210}\text{Pb}_p$ AR decreases with a slope of -0.17 ± 0.04 . On the other hand, refractory/lithogenic particles may be suggested by the observation of $^{210}\text{Po}_p/^{210}\text{Pb}_p$ AR < 1 with $\text{AOU} > 25 \mu\text{mol kg}^{-1}$. For those particles, increasing in AOI either due to water mass aging or higher AOI would change the $^{210}\text{Po}_p/^{210}\text{Pb}_p$ AR to a much lesser degree than that for organic particles with a slope of 0.008 ± 0.003 .”

Increasing AOI doesn't necessarily cause the AR to decrease if the particles are lithogenic or refractory.

40. I do not understand why it is said that this observation stands only for high latitude in the northern hemisphere. Other campaigns from high latitude in the Northern hemisphere are also reported on figure 5 but are not considered. In addition, GA-03 campaign are not from high latitude. What gives this relationship for other campaigns? Why this 4 campaigns was selected?

We found a general trend of lower particulate $^{210}\text{Po}/^{210}\text{Pb}$ AR in samples from relatively high latitude stations in the Northern Hemisphere. We wanted to specifically study the relationship between AR and AOI for those stations. However, we couldn't obtain the hydro-data

(temperature, salinity, dissolved oxygen) from the other campaigns at the high latitude in the Northern Hemisphere, therefore AOU could not be derived as it is a function of these parameters. That is why the other campaigns from the high latitude in the Northern Hemisphere reported on Figure 5 were not considered in the AR and AOU relationship on Figure 6.

We agree that GA03 is not from high latitude. But in the original manuscript when we included GA03 into the 4 campaigns, we obtained the two-phase correlation between AR and AOU on Figure 6 (AR < 1 & AOU > 25, AR > 1 & AOU < 25). It needs to be mentioned that the two-phase correlation still exists without GA03 data but R^2 will decrease to ~ 0.3 for both relationships with less data points. We investigated the ANT-X/6 in the Southern Ocean (AOU data only available at 13 stations) as it also seemed to have relatively low AR but the similar two-phase correlation between AR and AOU did not exist.

41. p13, L370: What do you mean by investigation of pigments? There is nothing about it in the material and methods section.

Yes, we indeed didn't include pigments in the methods section because the data has not been published yet.

We now removed the pigment data from the manuscript.

42. p14, L377-378: what do you mean by "as the above cited papers have seen elsewhere"?
Please Precise

We now removed pigment and primary production from the manuscript. Please see our response to specific comment 47.

43. p14, L378-380: this is expected for the eastern part of the transect only?

Yes, it is. But it has been removed now. Please see our response to specific comment 41.

44. p14, L391-392: how did you calculate the dissolved activity? This is not indicated. When you consider the K_d for the small particles you normalize with the SPM for the small particles also? Same question for the total particulate. Please precise.

We calculated the dissolved activity by subtracting particulate activity from the total activity.

Yes, we used Eq. (1) to calculate K_d for both small and total particulate fractions, and K_d for small and total particulate fractions was normalized by the SPM in the small and particulate fractions, respectively.

We will clarify this as following:

“In this study, the size-fractionated data of radionuclide activity and SPM allowed us to calculate the partitioning coefficients for both radionuclides on small and total particles by using Eq. (1). The dissolved radionuclide activity was calculated as the difference between total and particulate activity. The coefficients for the small and total particulate phases were normalized by the SPM in the small and total particulate phases, respectively.”

45. p14, L399-401: How this is possible as the small particulate activity is necessary lower than the total particulate activity? Is it associated to the SPM normalization?

Yes, it is indeed associated to the SPM normalization. Please see our previous response.

46. p14, L401-403: here you affirm that the scavenging and export is mostly driven by small particles. But there is nothing to confirm this. Although this can be plausible, this is just an hypothesis.

We agree that we don't have direct evidence of small particles sinking nor that export was driven by the small particles. We therefore removed this topic from this manuscript and will discuss it further in the companion paper. However, the comparison of K_d for both radionuclides in the small size fraction vs. total size fraction suggests that the adsorption/scavenging of radionuclides were driven by the small particles.

47. p12-14, L362-404: this section is very surprising. From the title of the section I expected to find POC export calculation. In facts, there is no data really discussed or even showed

(pigment, primary production, ...) and most of the discussion is based on hypothesis without real solid basis to support them. I suggest to rewrite this section around concrete data only and to change the title of this section.

In fact, we have submitted two manuscripts to this special issue. In the manuscript reviewed here we discuss the general distribution of ^{210}Po and ^{210}Pb activity along the GEOVIDE transect. The second manuscript entitled “The export flux of particulate organic carbon derived from $^{210}\text{Po}/^{210}\text{Pb}$ disequilibria along the North Atlantic GEOTRACES GA01 (GEOVIDE) transect” addresses the POC export fluxes. In the second paper, we have calculated the POC fluxes using the export flux of ^{210}Po and the $\text{POC}/^{210}\text{Po}$ ratio in total ($> 1 \mu\text{m}$) particles and compared the estimates to those obtained using the $^{234}\text{Th}/^{238}\text{U}$ proxy.

We agree that the title of this section is not appropriate. We will change it to “Relationship among small particles, adsorption, and scavenging”.

We now removed the statements about the pigment and primary production from this section and will rewrite it as follows:

“4.4 Relationship among small particles, adsorption, and scavenging

The partitioning coefficient, K_d (L kg^{-1}), has been used to describe the particle adsorption behavior of radionuclides. It is defined as the ratio of the adsorbed radionuclide activity (A_p , $\text{dpm } 100\text{L}^{-1}$) to the dissolved radionuclide activity (A_d , $\text{dpm } 100\text{L}^{-1}$), normalized by the suspended particulate matter concentration (SPM , $\mu\text{g L}^{-1}$):

$$K_d = \frac{A_p}{A_d} \times \frac{1}{SPM} 10^9 \quad (1)$$

Owing to the different biological and chemical behaviors of ^{210}Po and ^{210}Pb , the interpretation of measured K_d for ^{210}Po ($K_d(\text{Po})$) may not be as clear as that for ^{210}Pb ($K_d(\text{Pb})$). As claimed previously in Tang et al. (2017), $K_d(\text{Po})$ is complicated because it appears to reflect both the surface adsorption and potential bioaccumulation.

In this study, the size-fractionated data of both radionuclide activity and SPM allowed us to calculate the partitioning coefficients for both radionuclides on small and total particles. The dissolved radionuclide activity was calculated as the difference between total and particulate activity. The coefficients for the small particulate and the total particulate phases were

normalized by the SPM in the small and total particulate phases, respectively. We present only the coefficients for the small particulate phases ($K_d(\text{Po})_s$, $K_d(\text{Pb})_s$) and the total particulate phases ($K_d(\text{Po})_p$, $K_d(\text{Pb})_p$) because most of the particulate activity (> 80%) was associated with the small particles along the GEOVIDE transect, and most conceptualized scavenging models consider either the two-box model (dissolved – total particulate phases, i.e. $K_d(\text{Po})_p$) or the three-box model (dissolved – small – large, i.e. $K_d(\text{Po})_s$) (Clegg and Whitfield, 1990; 1991; Rigaud et al., 2015) and thus activity is concentrated from the dissolved phase to the total or small particles.

The average values of $K_d(\text{Po})$ was 1.6 times of those of $K_d(\text{Pb})$ in both small and total particulate phases, suggesting a higher affinity with particles for ^{210}Po with respect to ^{210}Pb , which is commonly observed in the global ocean (Bacon et al., 1988; Hong et al., 1999; Masqué et al., 2002; Wei et al., 2014; Tang et al., 2017). The K_d values for the small particulate phase were slightly higher than those for the total particulate phase but overall these values were very similar for both radionuclides (Fig. 7), suggesting that adsorption/scavenging of radionuclides was driven by small particles along the transect. In addition, there are increasing studies which argue that small particles can form aggregates that sink, and their contribution to carbon export could be larger than previously thought (e.g. Richardson and Jackson, 2007; Lomas and Moran, 2011; Amacher et al., 2013; Puigcorbé et al., 2015). We, therefore, recommend combining the activities of both small and large particles into a total particulate fraction in order to explain total $^{210}\text{Po}/^{210}\text{Pb}$ disequilibria in the surface waters, and utilizing the characteristics of the total particles (instead of just the large particles) in the estimation of the POC export fluxes (Tang et al., companion paper submitted to this volume).

Traditionally, large particles collected by in-situ filtration with pumps, most commonly defined as particles larger than 53 or 70 μm , were assumed to dominate the sinking flux (Dugdale and Goering, 1967; Bishop et al., 1977; Fowler and Knauer, 1986; Honjo et al., 1992; Walsh and Gardner, 1992) such that the composition ($\text{POC}/^{210}\text{Po}$) of the large particle size class was used to convert ^{210}Po fluxes into POC export (e.g. Friedrich and Rutgers van der Loeff, 2002; Cochran and Masqué, 2003; Murray et al., 2005; Stewart et al., 2010; Roca-Martí et al., 2016). Given that the true size spectrum of sinking particles for the timescale relevant to the

$^{210}\text{Po}/^{210}\text{Pb}$ method is unknown and the POC flux estimates are sensitive to the particulate POC/ ^{210}Po ratio, both small and large particles should be sampled for POC/ ^{210}Po due to the variability in the POC/ ^{210}Po ratio in different size classes (Hayes et al., in review).”

Conclusion:

48. p15, L415-420: again this was not clearly demonstrated. This conclusion should be very robust because it can have large implications in the future sampling strategy. Differently: does the sampling and analysis of two particulate size fractions is necessary in the future? So this has to be very robustly demonstrated. I agree with the fact that the high proportion of particulate nuclides is found in the small particle indicates that small particles are important in the sorption process. But I'm clearly not convinced from the data showed in the manuscript there is evidence to say that the small particles play an important role in the export of particles. If so, this should be strengthened. I may suggest to synthesis the most important findings based on the data only. There is nothing on the time elapsed since the last bloom for example.

We agree that conclusions should be based on the data only and, therefore, we will remove the text about the relationship between small phytoplankton and export. Conclusions will be changed to the following:

“In this study, we reported the vertical distribution of total and size-fractionated particulate ^{210}Po and ^{210}Pb activities in the North Atlantic during the GEOVIDE GA01 cruise. More than 90% of the radionuclide activity was found in the dissolved phase, while a small proportion was associated with particles in this transect. Total ^{210}Po activity was generally depleted relative to total ^{210}Pb activity in the upper 100 m due to the preferential adsorption of ^{210}Po activity by particles. Such deficiencies of ^{210}Po activities generally extended to the deep waters at most of the stations. In the Western European Basin, the excess of ^{210}Po activities at stations 1 and 13 in the North East Atlantic Deep Water was attributed to the release of ^{210}Po during dissolution of sinking biogenic particles.

There appear to be geographic differences in particulate $^{210}\text{Po}/^{210}\text{Pb}$ activity ratios measured during GEOVIDE and previous studies, with particularly low values in the high-latitude North Atlantic and Arctic. While this observation deserves more attention, we support previous suggestions that this is due to the terrestrial origin/riverine input of particles with a low $^{210}\text{Po}/^{210}\text{Pb}$ AR into the river-dominated shallow seas of the Arctic. The age of the particles and water masses as well as the importance of biogeochemical processes (e.g. respiration, remineralization) may also explain some of these observations, as there was a significant relationship between the total particulate activity ratio and AOU when both were measured in the North Atlantic (> 20 °N) and Arctic Oceans.

Over 80% of the particulate radionuclide activity was on small particles, indicating that the scavenging of both radionuclides was driven by small particles. Therefore, we suggest considering the activities of ^{210}Po and ^{210}Pb from both small and large particles in order to study the water column $^{210}\text{Po}/^{210}\text{Pb}$ disequilibria and quantify POC export along the GA01 transect. This has been addressed in a companion paper in this issue. We recommend that both small and large particles should be sampled for POC/ ^{210}Po estimates for the application of the $^{210}\text{Po}/^{210}\text{Pb}$ method in future studies of POC export.”

Fig 3:

49. I doubt the sentence "A closer look at only the zoom" is correct in the caption. Those words will be removed from the caption. The caption will be changed as: “The upper 250 m of the depth profiles of total ^{210}Po ($^{210}\text{Po}_t$, red circles) and ^{210}Pb activities ($^{210}\text{Pb}_t$, grey squares) along the GEOVIDE section. The horizontal orange and magenta lines denote the mixed layer depth (MLD) and the base of the euphotic zone ($Z_{1\%}$), respectively. The depth profiles are shown in the order of sampling and grouped by region (refer to Fig. 2 for the text abbreviations).”

50. Stn 60: 2 dot are missing for ^{210}Pb at approximately 50 m and 120 m depth. The range of horizontal axis (activity) for each plot will be changed from 0-20 to 0-25 dpm 100 L^{-1} and the two data points will be shown in the plot of stn. 60. Please see the plot below:

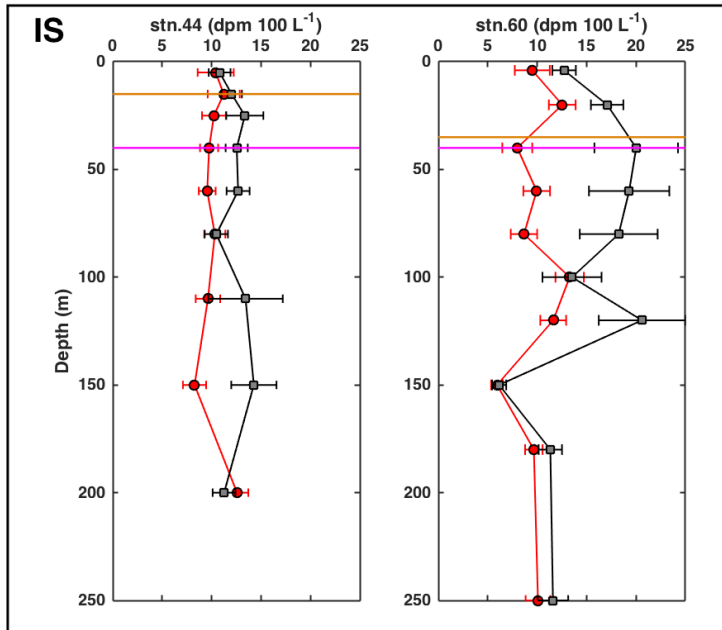


Figure 6:

51. negative AOU value need to be explained?

Negative AOU value is now explained in the text. Please see our response to specific comment 20.

52. with the uncertainty on Po/Pb AR there is (most of the time) not significant deviation from the 1 AR for the "other points". I suggest to integrate the "other points" within the regression keeping the only separation lower or above 25 $\mu\text{mol/kg}$ for OAU.

We agree. The original Figure 6 will be changed to the following:

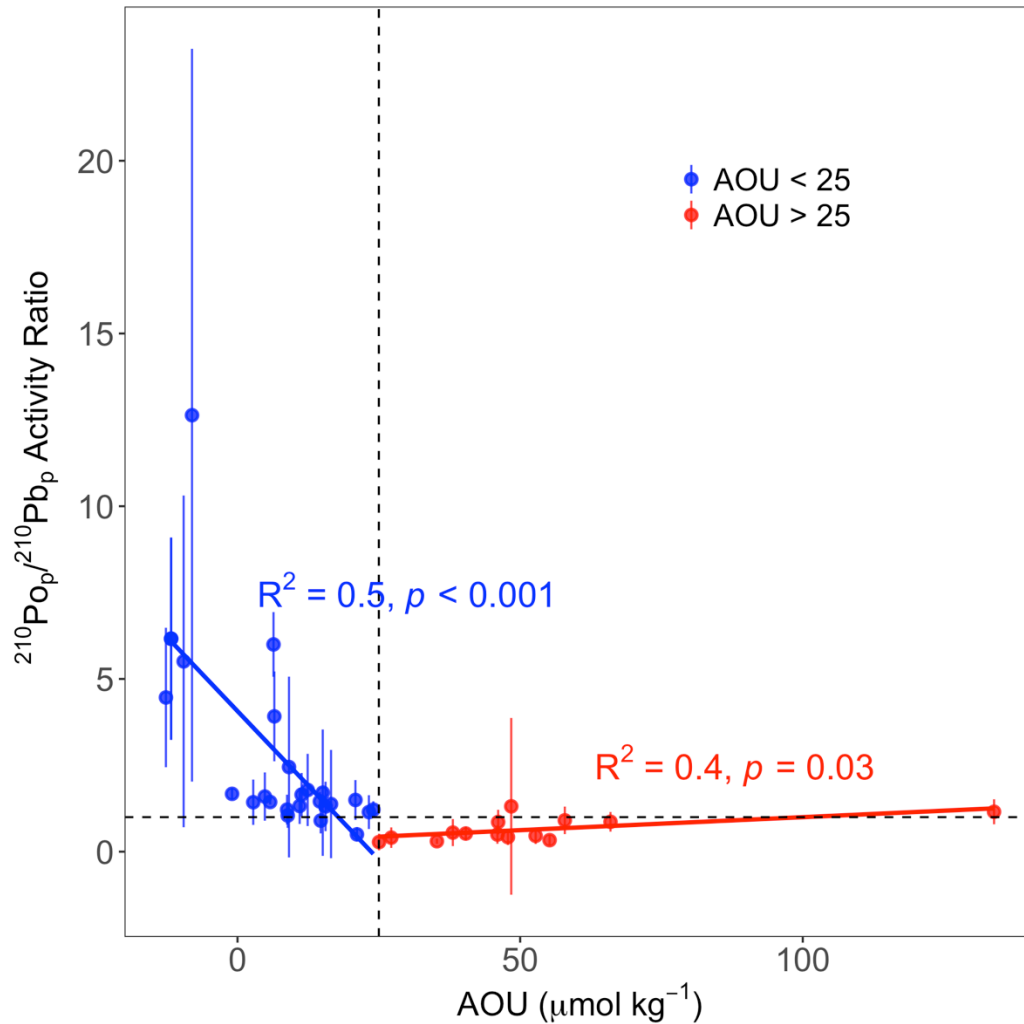


Fig. 9. The relationship between AOU ($\mu\text{mol kg}^{-1}$) and total particulate $^{210}\text{Po}/^{210}\text{Pb}$ activity ratio ($^{210}\text{Po}_p/^{210}\text{Pb}_p$) from the upper 200 m in the northern hemisphere ($> 22^\circ\text{N}$) investigated by a linear regression model (red and blue lines). The 40 stations include data from previous studies, ARK-XXII/2 ($77.38\text{--}87.83^\circ\text{N}$, $n = 15$) in the Arctic, BOFS ($48.89\text{--}49.87^\circ\text{N}$, $n = 7$), GA03 ($22.38\text{--}39.70^\circ\text{N}$, $n = 7$), and this study, GA01 ($40.33\text{--}59.80^\circ\text{N}$, $n = 11$) in the North Atlantic. The horizontal dashed line represents $^{210}\text{Po}_p/^{210}\text{Pb}_p$ AR = 1 and the vertical dashed line represents $\text{AOU} = 25 \mu\text{mol kg}^{-1}$. Blue circles denote $\text{AOU} < 25 \mu\text{mol kg}^{-1}$, while red circles denote $\text{AOU} > 25 \mu\text{mol kg}^{-1}$.

Figure 7:

53. the axis labels on the figure and in the caption are not the same. Please homogenize. We agree. The caption of Figure 10 (no longer 7 because of the addition of figures) will be changed as:

“Comparison of the partitioning coefficient (K_d) between the dissolved and small particulate phases ($K_d(\text{Po})_s$, $K_d(\text{Pb})_s$) vs. between the dissolved and total particulate phases ($K_d(\text{Po})_p$, $K_d(\text{Pb})_p$) for (a) ^{210}Po and (b) ^{210}Pb . The 1:1 line is indicated as the solid line in each plot.”

References:

- Amacher, J., Neuer, S. and Lomas, M.: DNA-based molecular fingerprinting of eukaryotic protists and cyanobacteria contributing to sinking particle flux at the Bermuda Atlantic time-series study, *Deep Sea Research Part II*, 93, 71-83, 2013.
- Bacon, M. P., Belostock, R. A., Tecotzky, M., Turekian, K. K. and Spencer, D. W.: Lead-210 and polonium-210 in ocean water profiles of the continental shelf and slope south of New England, *Continental Shelf Research*, 8, 841-853, 1988.
- Bacon, M. P., Brewer, P. G., Spencer, D. W., Murray, J. W. and Goddard, J.: Lead-210, polonium-210, manganese and iron in the Cariaco Trench, *Deep Sea Research Part A. Oceanographic Research Papers*, 27, 119-135, 1980.
- Bacon, M. P., Spencer, D. W. and Brewer, P. G.: $^{210}\text{Pb}/^{226}\text{Ra}$ and $^{210}\text{Po}/^{210}\text{Pb}$ disequilibria in seawater and suspended particulate matter, *Earth and Planetary Science Letters*, 32, 277-296, 1976.
- Baskaran, M.: Po-210 and Pb-210 as atmospheric tracers and global atmospheric Pb-210 fallout: A Review, *International Topical Meeting on Polonium and Radioactive Lead Isotopes*, 102, 500-513, 2011.
- Benetti, M., Reverdin, G., Lique, C., Yashayaev, I., Holliday, N. P., Tynan, E., Torres-Valdes, S., Lherminier, P., Tréguer, P. and Sarthou, G.: Composition of freshwater in the spring of 2014 on the southern Labrador shelf and slope, *Journal of Geophysical Research: Oceans*, 122, 1102-1121, 2017.
- Bishop, J. K. B., Edmond, J. M., Ketten, D. R., Bacon, M. P. and Silker, W. B.: The chemistry, biology, and vertical flux of particulate matter from the upper 400 m of the equatorial Atlantic Ocean, *Deep Sea Research*, 24, 511-548, 1977.

Boyer, T., Conkright, M. E. and Levitus, S.: Seasonal variability of dissolved oxygen, percent oxygen saturation, and apparent oxygen utilization in the Atlantic and Pacific Oceans, Deep Sea Research Part I: Oceanographic Research Papers, 46, 1593-1613, 1999.

Clegg, S. L. and Whitfield, M.: A generalised model for the scavenging of trace metals in the open ocean: I. Particle cycling, Deep Sea Research Part A. Oceanographic Research Papers, 37, 809-832, 1990.

Clegg, S. L. and Whitfield, M.: A generalised model for the scavenging of trace metals in the open ocean-II. Thorium scavenging, Deep Sea Research Part A. Oceanographic Research Papers, 38, 91-120, 1991.

Cochran, J. K. and Masqué, P.: Short-lived U/Th Series Radionuclides in the Ocean: Tracers for Scavenging Rates, Export Fluxes and Particle Dynamics, Reviews in Mineralogy and Geochemistry, 52, 461-492, 2003.

Cooper, L.: Factors affecting the distribution of silicate in the North Atlantic Ocean and the formation of North Atlantic deep water, Journal of the Marine Biological Association of the United Kingdom, 30, 511-526, 1952.

Coppola, L., Prieur, L., Taupier-Letage, I., Estournel, C., Testor, P., Lefevre, D., Belamari, S., LeReste, S. and Taillandier, V.: Observation of oxygen ventilation into deep waters through targeted deployment of multiple Argo-O₂ floats in the north-western Mediterranean Sea in 2013, Journal of Geophysical Research: Oceans, 122, 6325-6341, 2017.

Dugdale, R. C. and Goering, J. J.: uptake of new and regenerated forms of nitrogen in primary production, Limnology and Oceanography, 12, 196-206, 1967.

Duteil, O., Koeve, W., Oschlies, A., Bianchi, D., Galbraith, E., Kriest, I. and Matear, R.: A novel estimate of ocean oxygen utilisation points to a reduced rate of respiration in the ocean interior, Biogeosciences, 10, 7723-7738, 2013.

Fisher, N. S., Burns, K. A., Cherry, R. D. and Heyraud, M.: Accumulation and cellular distribution of ²⁴¹Am, ²¹⁰Po and ²¹⁰Pb in two marine algae, Marine Ecology Progress Series, 11, 233-237, 1983.

Fowler, S. W. and Knauer, G. A.: Role of large particles in the transport of elements and organic compounds through the oceanic water column, Progress in Oceanography, 16, 147-194, 1986.

Friedrich, J. and Rutgers van der Loeff, M. M.: A two-tracer (²¹⁰Po–²³⁴Th) approach to distinguish organic carbon and biogenic silica export flux in the Antarctic Circumpolar Current, Deep Sea Research Part I: Oceanographic Research Papers, 49, 101-120, 2002.

García-Ibáñez, M. I., Pardo, P. C., Carracedo, L. I., Mercier, H., Lherminier, P., Ríos, A. F. and Pérez, F. F.: Structure, transports and transformations of the water masses in the Atlantic Subpolar Gyre, *Progress in Oceanography*, 135, 18-36, 2015.

García-Ibáñez, M. I., Pérez, F. F., Lherminier, P., Zunino, P., Mercier, H. and Tréguer, P.: Water mass distributions and transports for the 2014 GEOVIDE cruise in the North Atlantic, *Biogeosciences*, 15, 2075-2090, 2018.

GEOTRACES Planning Group: GEOTRACES Science Plan, Baltimore, Maryland, 2006.

Gourain, A., Planquette, H., Cheize, M., Menzel-Barraqueta, J. L., Boutorh, J., Shelley, R. U., Pereira-Contreira, L., Lemaitre, N., Lacan, F., Lherminier, P. and Sarthou, G.: Particulate trace metals along the GEOVIDE section, *Biogeosciences*, 2018.

Hayes, C. T., Black, E. E., Andersen, R. A., Baskaran, M., Buesseler, K. O., Charette, M. A., Cheng, H., Cochran, J. K., Edwards, R. L., Fitzgerald, P., Lam, P. J., Lu, Y., Morris, S. O., Ohnemus, D. C., Pavia, F. J., Stewart, G. and Tang, Y.: Flux of particulate elements in the North Atlantic Ocean constrained by multiple radionuclides, *Global Biogeochemical Cycles*, in review.

Hong, G.-H., Park, S.-K., Baskaran, M., Kim, S.-H., Chung, C.-S. and Lee, S.-H.: Lead-210 and polonium-210 in the winter well-mixed turbid waters in the mouth of the Yellow Sea, *Continental Shelf Research*, 19, 1049-1064, 1999.

Honjo, S., Spencer, D. W. and Gardner, W. D.: A sediment trap intercomparison experiment in the Panama Basin, 1979, *Deep Sea Research Part A. Oceanographic Research Papers*, 39, 333-358, 1992.

Ito, T., Follows, M. J. and Boyle, E. A.: Is AOU a good measure of respiration in the oceans?, *Geophysical Research Letters*, 31, 1-4, 2004.

Keeling, R. F., Stephens, B. B., Najjar, R. G., Doney, S. C., Archer, D. and Heimann, M.: Seasonal variations in the atmospheric O₂/N₂ ratio in relation to the kinetics of air-sea gas exchange, *Global Biogeochemical Cycles*, 12, 141-163, 1998.

Lam, P. J., Ohnemus, D. C. and Auro, M. E.: Size-fractionated major particle composition and concentrations from the US GEOTRACES North Atlantic Zonal Transect, *Deep Sea Research Part II*, 116, 303-320, 2015.

Lomas, M. W. and Moran, S. B.: Evidence for aggregation and export of cyanobacteria and nano-eukaryotes from the Sargasso Sea euphotic zone, *Biogeosciences*, 8, 203-216, 2011.

Masqué, P., Sanchez-Cabeza, J. A., Bruach, J. M., Palacios, E. and Canals, M.: Balance and residence times of ²¹⁰Pb and ²¹⁰Po in surface waters of the northwestern Mediterranean Sea, *Continental Shelf Research*, 22, 2127-2146, 2002.

Mercier, H., Lherminier, P., Sarafanov, A., Gaillard, F., Daniault, N., Desbruyeres, D., Falina, A., Ferron, B., Gourcuff, C., Huck, T. and Thierry, V.: Variability of the meridional overturning circulation at the Greenland–Portugal OVIDE section from 1993 to 2010, *Progress In Oceanography*, 132, 250-261, 2015.

Moore, H. E., Poet, S. E., Martell, E. A. and Wilkening, M. H.: Origin of ^{222}Rn and its long-lived daughters in air over Hawaii, *Journal of Geophysical Research*, 79, 5019-5024, 1974.

Murray, J. W., Paul, B., Dunne, J. P. and Chapin, T.: ^{234}Th , ^{210}Pb , ^{210}Po and stable Pb in the central equatorial Pacific: Tracers for particle cycling, *Deep Sea Research Part I: Oceanographic Research Papers*, 52, 2109-2139, 2005.

Puigcorbé, V., Benitez-Nelson, C. R., Masqué, P., Verdeny, E., White, A. E., Popp, B. N., Prahl, F. G. and Lam, P. J.: Small phytoplankton drive high summertime carbon and nutrient export in the Gulf of California and Eastern Tropical North Pacific, *Global Biogeochemical Cycles*, 29, 1309-1332, 2015.

Richardson, T. L. and Jackson, G. A.: Small Phytoplankton and Carbon Export from the Surface Ocean, *Science*, 315, 838-840, 2007.

Rigaud, S., Puigcorbé, V., Camara-Mor, P., Casacuberta, N., Roca-Martí, M., Garcia-Orellana, J., Benitez-Nelson, C. R., Masqué, P. and Church, T.: A methods assessment and recommendations for improving calculations and reducing uncertainties in the determination of ^{210}Po and ^{210}Pb activities in seawater, *Limnology and Oceanography Methods*, 11, 561-571, 2013.

Rigaud, S., Stewart, G., Baskaran, M., Marsan, D. and Church, T.: ^{210}Po and ^{210}Pb distribution, dissolved-particulate exchange rates, and particulate export along the North Atlantic US GEOTRACES GA03 section, *Deep Sea Research Part II*, 116, 60-78, 2015.

Roca-Martí, M., Puigcorbé, V., Rutgers van der Loeff, M. M., Katlein, C., Fernández-Méndez, M., Peeken, I. and Masqué, P.: Carbon export fluxes and export efficiency in the central Arctic during the record sea-ice minimum in 2012: a joint $^{234}\text{Th}/^{238}\text{U}$ and $^{210}\text{Po}/^{210}\text{Pb}$ study, *Journal of Geophysical Research: Oceans*, 121, 5030-5049, 2016.

Sarthou, G., Lherminier, P., Achterberg, E. P., Alonso-Pérez, F., Bucciarelli, E., Boutorh, J., Bouvier, V., Boyle, E. A., Branellec, P., Carracedo, L. I., Casacuberta, N., Castrillejo, M., Cheize, M., Contreira, P. L., Cossa, D., Daniault, N., De Saint-Léger, E., Dehairs, F., Deng, F., Desprez de Gésincourt, F., Devesa, J., Foliot, L., Fonseca-Batista, D., Gallinari, M., García-Ibáñez, M. I., Gourain, A., Grossteffan, E., Hamon, M., Heimbürger, L. E., Henderson, G. M., Jeandel, C., Kermabon, C., Lacan, F., Le Bot, P., Le Goff, M., Le Roy, E., Lefèvre, A., Leizour, S., Lemaitre, N., Masqué, P., Ménage, O., Menzel Barraqueta, J. L., Mercier, H., Perault, F., Pérez, F. F., Planquette, H., Planchon, F., Roukaerts, A., Sanial, V., Sauzède, R., Shelley, R. U., Stewart, G.,

Sutton, J., Tang, Y., Tisnérat-Laborde, N., Tonnard, M., Tréguer, P., van Beek, P., Zurbrick, C. M. and Zunino, P.: Introduction to the French GEOTRACES North Atlantic Transect (GA01): GEOVIDE cruise, Biogeosciences, in review.

Shelley, R. U., Roca-Martí, M., Castrillejo, M., Sanial, V., Masqué, P., Landing, W. M., van Beek, P., Planquette, H. and Sarthou, G.: Quantification of trace element atmospheric deposition fluxes to the Atlantic Ocean (> 40°N; GEOVIDE, GEOTRACES GA01) during spring 2014, Deep Sea Research Part I: Oceanographic Research Papers, 119, 34-49, 2017.

Stanley, R. H. R., Doney, S. C., Jenkins, W. J. and Lott, D. E. I.: Apparent oxygen utilization rates calculated from tritium and helium-3 profiles at the Bermuda Atlantic Time-series Study site, Biogeosciences, 9, 1969-1983, 2012.

Stewart, G. M., Bradley Moran, S. and Lomas, M. W.: Seasonal POC fluxes at BATS estimated from ^{210}Po deficits, Deep Sea Research Part I: Oceanographic Research Papers, 57, 113-124, 2010.

Stewart, G. M., Fowler, S. W., Teyssié, J. L., Cotret, O., Cochran, J. K. and Fisher, N. S.: Contrasting transfer of polonium-210 and lead-210 across three trophic levels in marine plankton, Marine Ecology Progress Series, 290, 27-33, 2005.

Tang, Y., Lemaitre, N., Castrillejo, M., Roca-Martí, M., Masqué, P. and Stewart, G.: The export flux of particulate organic carbon derived from $^{210}\text{Po}/^{210}\text{Pb}$ disequilibria along the North Atlantic GEOTRACES GA01 (GEOVIDE) transect, Biogeosciences, submitted.

Tang, Y., Stewart, G., Lam, P. J., Rigaud, S. and Church, T.: The influence of particle concentration and composition on the fractionation of ^{210}Po and ^{210}Pb along the North Atlantic GEOTRACES transect GA03, Deep Sea Research Part I: Oceanographic Research Papers, 128, 42-54, 2017.

Turekian, K. K., Nozaki, Y. and Benninger, L. K.: Geochemistry of Atmospheric Radon and Radon Products, Annual Review of Earth and Planetary Sciences, 5, 227-255, 1977.

Walsh, I. D. and Gardner, W. D.: A comparison of aggregate profiles with sediment trap fluxes, Deep Sea Research Part A. Oceanographic Research Papers, 39, 1817-1834, 1992.

Wei, C. L., Yi, M. C., Lin, S. Y., Wen, L. S. and Lee, W. H.: Seasonal distributions and fluxes of ^{210}Pb and ^{210}Po in the northern South China Sea, Biogeosciences, 11, 6813-6826, 2014.

Zunino, P., Lherminier, P., Mercier, H., Daniault, N., Garcia-Ibanez, M. I. and Pérez, F. F.: The GEOVIDE cruise in May-June 2014 revealed an intense MOC over a cold and fresh subpolar North Atlantic, Biogeosciences, 2018.

1 **Distributions of total and size-fractionated particulate ^{210}Po and ^{210}Pb activities along the**
2 **North Atlantic GEOTRACES GA01 (GEOVIDE) cruise-transect: partitioning between the**
3 **particulate and dissolved phase**

4
5 Yi Tang^{1,2}, Maxi Castrillejo^{3,4}, Montserrat Roca-Martí³, Pere Masqué^{3,5}, Nolwenn Lemaitre⁶,
6 Gillian Stewart^{2,1}

7
8 ¹ ~~Department of~~ Earth and Environmental Sciences, the Graduate Center, City University of New York, New York,
9 USA

10 ² School of Earth and Environmental Sciences, Queens College, City University of New York, Flushing, USA

11 ³ Institut de Ciència i Tecnologia Ambientals & Departament de Física, Universitat Autònoma de Barcelona,
12 Bellaterra, 08193, Spain

13 ⁴ Laboratory of Ion Beam Physics, ETH-Zürich, Otto-Stern-Weg 5, Zürich, 8093, Switzerland

14 ⁵ School of Science and Centre for Marine Ecosystems Research, Edith Cowan University, Joondalup, Western
15 Australia, Australia

16 ⁶ Department of Earth Sciences, Institute of Geochemistry and Petrology, ETH-Zürich, Zürich, Switzerland

17 *Correspondence to:* Gillian Stewart (Gillian.Stewart@qc.cuny.edu)

18 **Abstract**

19 Vertical distributions of total and particulate ^{210}Po and ^{210}Pb activities in the water column
20 were measured at eleven stations in the North Atlantic during the GEOTRACES GA01 GEOVIDE
21 cruise in May - June 2014. Total ^{210}Po activity was on average 24% lower than ^{210}Pb activity in
22 the upper 100 m, and was closer to unity in the mesopelagic (100 – 1000 m). The partitioning
23 coefficients (K_d) along the transect suggest the preferential association of ^{210}Po relative to ^{210}Pb
24 onto particles. The prominent role of small particles in sorption was confirmed by the observation
25 that over 80% of the particulate radionuclide activity was on small particles. To account for the
26 observed surface water $^{210}\text{Po}/^{210}\text{Pb}$ disequilibria, particulate radionuclide activities and export of
27 both small (1-53 μm) and large ($> 53 \mu\text{m}$) particles must be considered. A comparison between
28 the GEOVIDE total particulate $^{210}\text{Po}/^{210}\text{Pb}$ activity ratios (AR) and the ratios in previous studies
29 revealed a distinct geographic distribution, with lower particulate AR in the high-latitude North
30 Atlantic (including this study) and Arctic in relation to all other samples. For the samples where
31 apparent oxygen utilization (AOU) was calculated at the same depth and time as the $^{210}\text{Po}/^{210}\text{Pb}$
32 AR (40 stations including this study), there was a two-phase correlation between the total
33 particulate AR and AOU likely reflecting the nature of the particles and demonstrating the
34 competing forces of remineralization and radionuclide decay from particles as they age.

35

36

37 1 Introduction

38 The major goal of the international GEOTRACES program is to characterize the distributions
39 of trace elements and isotopes (TEIs) in the ocean on a global scale, and to identify and quantify
40 processes that control these distributions (GEOTRACES Planning Group, 2006). The GEOVIDE
41 section was a contribution of the French GEOTRACES program to this global program in the
42 subpolar North Atlantic. The GEOVIDE GA01 cruise was carried out in 2014 in the North Atlantic
43 and consisted of two sections: a section along the OVIDE (Observatoire de la variabilité
44 interannuelle et décennale en Atlantique Nord) line between Lisbon (Portugal) and Cape Farewell
45 (southern tip of Greenland), and a Cape Farewell to St. John's (Canada) section across the
46 Labrador Sea (Fig. 1). Since 2002, the OVIDE section has been occupied biennially to collect
47 physical and biogeochemical data (Mercier et al., 2015). The knowledge of the currents, water
48 masses, and biogeochemical provinces gained from the previous OVIDE campaigns enabled the
49 optimal strategy for TEIs sampling and provided help for the interpretation of the distribution of
50 TEIs in the subpolar North Atlantic (García-Ibáñez et al., 2015). In addition to the OVIDE line,
51 the Labrador Sea section provided a unique opportunity to study TEIs distributions along the
52 boundary current of the western North Atlantic subpolar gyre (Sarhou et al., in review). ~~The major
53 goal of the international GEOTRACES program is to characterize the distributions of trace
54 elements and isotopes (TEIs) in the ocean on a global scale, and to identify and quantify processes
55 that control these distributions (GEOTRACES Planning Group, 2006). The GEOVIDE section
56 was a contribution of the French GEOTRACES program to this global survey in the North Atlantic.
57 The GEOVIDE GA01 cruise was carried out in 2014 in the North Atlantic at latitudes greater than
58 40 °N and consisted of two sections: the seventh repetition of the OVIDE section from Lisbon
59 (Portugal) to Cape Farewell (southeast tip of Greenland), and a Cape Farewell to St. John's
60 (Canada) section across the Labrador Sea (Fig. 1). The water mass properties and main current
61 transports have been well studied in the OVIDE section during six previous repeated hydrological
62 surveys (2002–2012) (García-Ibáñez et al., 2015). Conditions along the Cape Farewell–St. John's
63 section, however, were relatively unknown. The combination of the two sections constitutes a
64 mixture of complex water masses, circulation patterns, and oceanic boundaries, presenting a
65 special opportunity to analyze the rates of the processes that govern the distribution of TEIs.~~

66 Polonium-210 (^{210}Po , $T_{1/2} = 138.4$ d) and its radioactive grandparent Lead-210 (^{210}Pb , $T_{1/2} =$
67 22.3 y) are two non-conservative ^{238}U decay series products. The GEOTRACES program has

68 included both radionuclides in its TEIs list primarily due to ^{210}Po 's enhanced bioaccumulation and
69 the use of the $^{210}\text{Po}/^{210}\text{Pb}$ pair as a proxy for assessing particle export in the upper ocean. The
70 distribution of ^{210}Po and ^{210}Pb has been widely measured over the last several decades in the
71 Atlantic (e.g. Bacon et al., 1976; Sarin et al., 1999; Rigaud et al., 2015; Ceballos-Romero et al.,
72 2016), Pacific (e.g. Nozaki and Tsunogai, 1976; Murray et al., 2005; Verdeny et al., 2008), Indian
73 (e.g. Cochran et al., 1983; Sarin et al., 1994; Subha Anand et al., 2017), Arctic (e.g. Moore and
74 Smith, 1986; He et al., 2015; Roca-Martí et al., 2016) and Southern Oceans (e.g. Shimmield et al.,
75 1995; Friedrich and Rutgers van der Loeff, 2002). However, since the data reported by Bacon et
76 al. (1980b) at the Labrador Sea stations (47.8 – 53.7 °N), there are few studies of ^{210}Po and ^{210}Pb
77 activity in the North Atlantic at latitudes greater than 40 °N. The GEOVIDE cruise, which targeted
78 the North Atlantic from 40 °N to 60 °N, provided an opportunity to fill this data gap.

79 Besides ascertaining the distribution of the natural radionuclides under specific geographic
80 conditions, this project aimed to answer questions about their biogeochemical behaviors in various
81 marine environments. Owing to the significantly longer half-life of ^{210}Pb relative to ^{210}Po , the two
82 radionuclides are expected to be in secular equilibrium (total $^{210}\text{Po}/^{210}\text{Pb}$ activity ratio = 1) in the
83 ocean, assuming no net removal or addition of either radionuclide. A deficit of ^{210}Po activity
84 relative to ^{210}Pb activity ($^{210}\text{Po}/^{210}\text{Pb}$ activity ratio < 1), however, is commonly found in the upper
85 ocean (e.g. Bacon et al., 1976; Nozaki and Tsunogai, 1976; Cochran et al., 1983; Sarin et al., 1999).
86 This has been attributed to a higher particle reactivity of ^{210}Po (higher partitioning coefficient, K_d)
87 than ^{210}Pb in seawater. Particles, therefore, become enriched in ^{210}Po ($^{210}\text{Po}/^{210}\text{Pb}$ activity ratio >
88 1) and their sinking to deeper waters results in a ^{210}Po activity deficit relative to ^{210}Pb activity in
89 the upper water column where particles are formed.

90 In this work, we describe the distributions of total and size-fractionated particulate ^{210}Po and
91 ^{210}Pb activity along the GEOVIDE cruise in the North Atlantic. These data are a significant
92 contribution to the high-latitude North Atlantic ^{210}Po and ^{210}Pb activity data set. We present a
93 compilation of particulate $^{210}\text{Po}/^{210}\text{Pb}$ activity ratios (AR) from previous studies in the global ocean
94 and the results are discussed in regards to the aging of water and biochemical processes. We also
95 describe the relationship among small particles, adsorption, and scavenging of radionuclides.
96 These results lead to recommendations for the estimation of particulate organic carbon export flux
97 based on the $^{210}\text{Po}/^{210}\text{Pb}$ disequilibrium, a topic that is covered in a companion paper (Tang et al., ,
98 companion paper submitted to this volume). ~~In this work, we present the distributions of total and~~

99 ~~particulate ^{210}Po and ^{210}Pb activity at 11 stations along the GEOVIDE cruise. These data are a~~
100 ~~significant contribution to the high-latitude North Atlantic ^{210}Po and ^{210}Pb activity data set. In~~
101 ~~addition, we calculate the K_d of ^{210}Po and ^{210}Pb during scavenging, discuss why this value has a~~
102 ~~complicated interpretation, and is mostly likely driven by sorption to small particles. We also put~~
103 ~~our somewhat unusually low particulate $^{210}\text{Po}/^{210}\text{Pb}$ activity ratios (AR) into a global context and~~
104 ~~look for any possible cause of variation along the cruise path.~~

105

106 **2 Methods**

107 **2.1 Sample collection**

108 The French GEOTRACES cruise to the North Atlantic (GEOVIDE, Section GA01; May 15 –
109 June 30, 2014) was completed on the *N/O-R/V Pourquoi Pas?*. The research vessel departed from
110 Lisbon, Portugal, headed northwest to the Greenland shelf, crossed the Labrador Sea, and ended
111 in St John’s, Newfoundland, Canada (Fig. 1). A rosette equipped with conductivity-temperature-
112 depth sensors and 12 L Niskin bottles was used to collect 200 seawater samples (5 – 10 L each)
113 from 10 full water column “super” (10 multi-cast) stations (16 – 22 depths/station) and 1 “~~X~~large
114 ~~XLarge~~” (5-cast) station to 800 m (station 26, 9 depths) for the determination of total ^{210}Po and
115 ^{210}Pb activity. Upon recovery, seawater samples were transferred to 10 L acid-cleaned containers.
116 In addition, particulate radionuclide activities in two size classes (1-53 μm and $> 53 \mu\text{m}$) were
117 collected at 3 – 10 depths per station using large volume *in-situ* filtration systems (Challenger
118 Oceanic pumps and McLane pumps) equipped with 142 mm filter holders. Each filter head
119 contained a stacked 53 μm PETEX screen followed by a 1 μm pore size quartz fiber QMA filter.
120 The volume filtered was determined via flow meters mounted below each filter head, and the mean
121 volume pumped through each head was 881 L. Once recovered, clear polyethylene caps were
122 placed on the top of the pump heads and they were brought into a clean laboratory for sub-sampling.
123

124 **2.2 Total ^{210}Po and ^{210}Pb**

125 Total ^{210}Po and ^{210}Pb activities were determined from the seawater samples by the cobalt-
126 ammonium pyrrolidine dithiocarbamate (Co-APDC) technique (Fleer and Bacon, 1984). Samples
127 were acidified to a $\text{pH} < 2$ with concentrated HCl immediately after collection and spiked with
128 known amounts of ^{209}Po and stable lead as chemical yield tracers. After vigorous stirring and at
129 least 6–12 h of isotope equilibration, cobalt nitrate and APDC solutions were added to co-

130 precipitate Po and Pb. Samples were filtered through a 0.45 μm membrane filter and the filters
131 with the precipitate were placed transferred into a clean falcon tubes bottle, sealed with parafilm,
132 and stored in double-bags. As the delay between sample collection and first Po plating increases,
133 the uncertainty of the calculated ^{210}Po activity also increases. In addition, it is necessary to balance
134 counting periods with the number of samples as the uncertainty due to alpha spectrometry counting
135 decreases by increasing the counting time. To limit the delay between sampling and processing
136 and to ensure higher counting statistics by having more alpha spectrometers devoted to this project,
137 sample processing and analyses were split between Universitat Autònoma de Barcelona (UAB)
138 (samples from stations 1, 13, and 21) and Queens College (QC) (stations 26, 32, 38, 44, 60, 69,
139 and 77). ~~Further sample processing and analyses were split between the Laboratori de~~
140 ~~Radioactivitat Ambiental (LRA) at Universitat Autònoma de Barcelona (UAB) (samples from~~
141 ~~stations 1, 13, and 21) and the Stewart laboratory at Queens College (QC) (stations 26, 32, 38, 44,~~
142 ~~60, 69, and 77) to ensure higher counting statistics in the samples.~~ Both laboratories followed the
143 same procedure. Briefly, the filters were digested into a solution of concentrated HNO_3 and HCl ,
144 and after the solution was evaporated to dryness, the samples were recovered in 1M and 0.5 M
145 HCl solution at UAB and QC, respectively (a 0.5-2 M HCl solution is recommended, Rigaud et
146 al., 2013). ~~Briefly, the filters were digested in a mixture of concentrated HNO_3 and HCl ,~~
147 ~~evaporated to dryness, and eventually dissolved in 1M and 0.5 M HCl at UAB and QC,~~
148 ~~respectively.~~ A polished pure silver disc (Flynn, 1968) with one side covered by enamel paint was
149 placed into the weak acid solution and heated so that the polonium nuclides were spontaneously
150 plated onto only one side of the disc. The activities of both Po nuclides on the disc were measured
151 by alpha spectrometry. Any ^{210}Po and ^{209}Po remaining in the plating solution was removed using
152 AG 1-X8 anion exchange resin and the final solution was re-spiked with ^{209}Po and stored for more
153 than 6 months to allow ingrowth of ^{210}Po from the decay of ^{210}Pb .

154 The ^{210}Pb activity was then determined by re-plating the solutions using silver discs and
155 measuring the ingrown ^{210}Po . Two aliquots of the plating solutions for each sample were taken
156 before the first and second platings for the measurement of total Pb concentration by inductively
157 coupled plasma mass spectrometry (ICP-MS) to determine sample recovery during processing.
158 The average recoveries produced by the LRAUAB and Stewart groups QC were $83 \pm 11\%$ ($n =$
159 54) and $76 \pm 14\%$ ($n = 144$), respectively. The activities of ^{210}Po and ^{210}Pb at the time of collection
160 were determined by a series of corrections, including nuclide decay, ingrowth, chemical recoveries,

161 detector backgrounds, and blank contamination following the methods in Rigaud et al. (2013). The
162 activity uncertainties from UAB were on average 8% for both ^{210}Po and ^{210}Pb activity, while the
163 QC uncertainties were on average 13% for ^{210}Po activity and 16% for ^{210}Pb activity. The greater
164 uncertainties of ^{210}Po and ^{210}Pb activities in the samples processed at QC were due to the longer
165 delay between sampling and first plating (68 vs. 50 d) and higher uncertainties in the determination
166 of the recovery of lead. ~~Finally, the initial activities of ^{210}Po and ^{210}Pb at the time of collection
167 were determined by a series of corrections, including nuclide decay, ingrowth, chemical recoveries,
168 detector backgrounds, and blank contamination following the methods in Rigaud et al. (2013). The
169 activity uncertainties from LRA were on average 8% for both ^{210}Po and ^{210}Pb activity, while the
170 activity uncertainties from the Stewart group were on average 13% for ^{210}Po activity and 16% for
171 ^{210}Pb activity.~~

172

173 **2.3 Particulate ^{210}Po and ^{210}Pb**

174 After collection via in situ pumping, one quarter (equivalent to ~ 220 L) of the PETEX screen
175 containing > 53 μm or “large” particles was processed for radionuclide activity. Swimmers were
176 carefully removed from all samples. The QMA filters containing 1-53 μm or “small” particles
177 were sub-sampled (2 – 4 punches of 12 mm-diameter) achieving a mean effective volume of ~ 66
178 L. The screens and punches were stored in double-bags at -80 $^{\circ}\text{C}$ until the analyses onshore. The
179 particulate samples were split between the two laboratories in parallel to the seawater samples.
180 The filters were spiked with ^{209}Po tracer solution and stable lead, digested using a mixture of
181 concentrated HF, HNO_3 and HCl at UAB, but only HNO_3 and HCl at QC. After multiple rounds
182 of digestion and evaporation to near dryness, the samples were recovered in 0.5 M HCl solution.
183 Any remaining pieces of filter which were not completely digested were carefully removed, rinsed
184 with 0.5 M HCl solution several times, and then discarded. The analyses of the particulate
185 radionuclide activities were identical to those for the seawater samples described in section 2.2.

186

187 **2.4 Concentration of suspended particulate matter (SPM)**

188 The Helene Planquette group (University of Brest, co-authors in this issue) collected
189 subsamples from the same screens and filters that were sampled previously for radionuclides to
190 determine major phase composition (particulate organic matter (POM), lithogenic material,
191 calcium carbonate (CaCO_3), opal, $\text{Fe}(\text{OH})_3$, and MnO_2) (references therein Lam et al.,

192 ~~2015)utilized the material on the balance of the screens and filters after subsampling for~~
193 ~~radionuclides to determine major phase composition (particulate organic matter (POM), lithogenic~~
194 ~~material, calcium carbonate (CaCO₃), opal, Fe(OH)₃, and MnO₂) (references therein Lam et al.,~~
195 ~~2015). The complete details of sampling and analyses will be described in a separate manuscript~~
196 ~~(Lemaitre et al., in prep.), but the~~ mass concentration of ~~total~~ SPM was calculated as the sum of
197 the chemical dry weight of the major particulate phases.

198 The calculated SPM concentration was compared to the *in-situ* transmission data obtained from
199 the rosette CTD sensor (Fig. S1). The overall negative relationship was statistically significant (R^2
200 = 0.7, $n = 53$, $p < 0.0001$), suggesting that the SPM concentrations determined were reasonable
201 estimates of particle concentration in the water column. We used the SPM values to determine the
202 partitioning coefficient, K_d , for ²¹⁰Po and ²¹⁰Pb in section 4.4.

203

204 **2.5 Primary production**

205 ~~Daily primary production (PP) at each station was determined using the ¹³C labeling technique~~
206 ~~by the Dehairs group. The details of sampling and analysis for PP is presented in depth elsewhere~~
207 ~~(Fonseca-Batista et al., 2018). Briefly, seawater samples (3–6 depths/station) were collected from~~
208 ~~the surface to the depth of 0.2% photosynthetically active radiation (PAR). The seawater was then~~
209 ~~incubated on deck for 24 h under conditions of photometric depths. After incubation, seawater was~~
210 ~~filtered through GF/F filters (0.7 μm porosity), followed by ¹³C determination using elemental~~
211 ~~analysis isotope ratio mass spectrometry. Daily PP was derived from the depth-integrated ¹³C~~
212 ~~uptake rates.~~

213

214 **2.5 Satellite-based data**

215 The 8-day composites of surface chlorophyll-a concentration for each station were retrieved
216 from NASA's MODIS products (<https://oceancolor.gsfc.nasa.gov>) for the period from January to
217 July 2014. The time-series chlorophyll-a concentrations were used to show the development of a
218 phytoplankton bloom over time along the transect.

219

220 **2.6 Apparent oxygen utilization and h Historical values**

221 The historical data of the particulate ²¹⁰Po and ²¹⁰Pb activity, and the hydrological parameters
222 (pressure, temperature, salinity, and dissolved oxygen) were obtained from databases and

223 publications. The location, date, database address or publication name, and type of data (particulate
224 ^{210}Po and ^{210}Pb activity or hydrological parameters) from all other studies is listed in supplemental
225 Table S1.

~~226 We compared the GEOVIDE data (particulate radionuclide activity and apparent oxygen
227 utilization) to historical databases and publications. The apparent oxygen utilization (AOU, μmol
228 kg^{-1}), a measurement of respiration and water mass age (Stanley et al., 2012), can be derived from
229 hydrological parameters (pressure, temperature, salinity, and dissolved oxygen) using the built-in
230 function in Ocean Data View. The location, date, database address or publication name, and type
231 of data (particulate ^{210}Po and ^{210}Pb activity or hydrological parameters) from all other studies is
232 listed in the supplemental Table S1.~~

233

234 **2.7 Apparent oxygen utilization**

235 Apparent oxygen utilization ($\text{AOU} = \text{O}_2_{\text{saturated}} - \text{O}_2_{\text{measured}}$) is defined as the difference between
236 the saturated oxygen at a given temperature and salinity and the measured in-situ oxygen
237 concentration (Ito et al., 2004; Duteil et al., 2013). A positive AOU indicates either water mass
238 aging and outgassing of oxygen or biological activity, namely respiration (e.g. Keeling et al., 1998;
239 Boyer et al., 1999). Negative AOU, indicating that the water is oversaturated with dissolved
240 oxygen, can appear under the conditions of an intense bloom (e.g. Coppola et al., 2017).

241 The dissolved oxygen concentration was measured by Winkler titration and the saturated
242 oxygen concentration was calculated as a function of in-situ temperature and salinity, and one
243 atmosphere of total pressure based on the built-in function in Ocean Data View (<https://odv.awi.de>).

244

245 **2.8 Statistical analyses**

246 Statistical analyses were carried out in R Studio version 3 using Fitting Linear Models, and
247 Welch Two Sample t-tests. Linear regression analysis was used to investigate the relationship
248 between total particulate $^{210}\text{Po}/^{210}\text{Pb}$ AR and AOU. The Welch Two Sample t-test was applied to
249 assess whether the mean of the total particulate $^{210}\text{Po}/^{210}\text{Pb}$ AR was the same as the mean of the
250 small particulate $^{210}\text{Po}/^{210}\text{Pb}$ AR. It was also applied to investigate the means of the total ^{210}Pb
251 activity in the western and eastern sections along the transect.

252

253 **3 Results**

254 3.1 Total ^{210}Po and ^{210}Pb activities

255 Total ^{210}Po activities ($^{210}\text{Po}_t$) in all samples ranged from 2.2 to 16.4 dpm 100 L⁻¹ and the mean
256 $^{210}\text{Po}_t$ was 8.8 ± 2.4 dpm 100 L⁻¹ (n = 198, Fig. 2). $^{210}\text{Po}_t$ activities were generally low within the
257 mixed layer and euphotic zone (15 – 47 m), slightly increased or remained relatively constant in
258 the depth range between the mixed layer and 250 m, and then decreased with water depth at most
259 of the stations except station 26. Near the seafloor, stations 1, 13 and 44 had a slight increase of
260 $^{210}\text{Po}_t$ activity.

261 Total ^{210}Pb activities ($^{210}\text{Pb}_t$) were between 2.1 and 20.6 dpm 100L⁻¹ with a mean value of 10.0
262 ± 3.0 dpm 100 L⁻¹ (n = 198, Fig. 2). $^{210}\text{Pb}_t$ activities were low in the surface, slightly increased in
263 the subsurface and decreased with water depth. Stations 1, 13, 44, and 60 exhibited an increase
264 near the seafloor.

265 The mean $^{210}\text{Po}_t/^{210}\text{Pb}_t$ activity ratio (AR) of all samples was 0.92 ± 0.28 (n = 198, Fig. 2).
266 When considering different basins separately, there is a tendency of decreasing $^{210}\text{Po}_t/^{210}\text{Pb}_t$ AR
267 from the West European Basin (1.10 ± 0.35) westwards to the Iceland Basin (0.90 ± 0.19) and the
268 Irminger Sea and the Labrador Sea (0.80 ± 0.18 and 0.83 ± 0.21 , respectively).

269 For all regions, significant deficits of $^{210}\text{Po}_t$ (0.80 ± 0.20 , n = 40) were observed within the
270 mixed layer and euphotic zone (Fig. 3). Secular equilibrium was also observed at some shallow
271 depths (i.e. 80 m at station 44) and even in surface waters (i.e. 15 m at station 38). $^{210}\text{Po}_t$ excesses
272 relative to $^{210}\text{Pb}_t$, which were larger than $^{210}\text{Po}_t$ surface depletions at the same stations, were
273 observed below the surface at some depths at stations 1, 13, and 21 in the West European Basin
274 (Fig. 2). At depths below the surface to ~ 1500 m in the Iceland Basin, the Irminger Sea, and the
275 Labrador Sea, the water samples still indicated a ^{210}Po deficiency (AR: 0.84 ± 0.17 , n = 27). Secular
276 equilibrium was generally reached near the bottom depths in all basins except at stations 13 and
277 60 where the water samples were either enriched in $^{210}\text{Po}_t$ ($^{210}\text{Po}_t/^{210}\text{Pb}_t$ AR = 1.58 ± 0.16) or
278 depleted in $^{210}\text{Po}_t$ ($^{210}\text{Po}_t/^{210}\text{Pb}_t$ AR = 0.50 ± 0.12), respectively.

279 ~~Total ^{210}Po activities ($^{210}\text{Po}_t$) in all samples ranged from 2.2 to 16.4 dpm 100 L⁻¹ and the mean~~
280 ~~$^{210}\text{Po}_t$ for all samples was 8.8 ± 2.4 dpm 100 L⁻¹ (n = 198, Fig. 2). The corresponding total ^{210}Pb~~
281 ~~activities ($^{210}\text{Pb}_t$) were between 2.1 and 20.6 dpm 100L⁻¹ with a mean value of 10.0 ± 3.0 dpm 100~~
282 ~~L⁻¹ (n = 198).~~

283 ~~The mean $^{210}\text{Po}_t/^{210}\text{Pb}_t$ activity ratio (AR) of all samples was 0.92 ± 0.28 (Fig. 2, n = 198).~~
284 ~~When considering different basins separately, there is a tendency of decreasing $^{210}\text{Po}_t/^{210}\text{Pb}_t$ AR~~

285 from the Western European Basin (1.10 ± 0.35) westwards to the Iceland Basin (0.90 ± 0.19) and
286 the Irminger Sea and the Labrador Sea (0.80 ± 0.18 and 0.83 ± 0.21 , respectively). For all regions,
287 within the mixed layer and euphotic zone (15–47 m), significant deficits of $^{210}\text{Po}_t$ (0.80 ± 0.20 , n
288 $= 40$) were observed (Fig. 3). $^{210}\text{Po}_t$ had enrichments below the surface at some depths at stations
289 1, 13, and 21 (Fig. 2) where the sub-surface $^{210}\text{Po}_t$ excesses were much larger than the surface
290 depletion. In the depth below the surface to ~1500 m in the Iceland Basin, the Irminger Sea, and
291 the Labrador Sea, the water samples still indicated a ^{210}Po deficiency (0.84 ± 0.17 , $n = 27$). Secular
292 equilibrium was generally reached near the bottom depths in all basins except at stations 13 and
293 60 where the water samples were enriched ($^{210}\text{Po}_t/^{210}\text{Pb}_t$ AR = 1.58 ± 0.16) and depleted
294 ($^{210}\text{Po}_t/^{210}\text{Pb}_t$ AR = 0.50 ± 0.12) in $^{210}\text{Po}_s$, respectively. Secular equilibrium was also observed at
295 some shallow depths (i.e. 80 m at station 44) and even in surface waters (i.e. 15 m at station 38).

296

297 3.2 Particulate ^{210}Po and ^{210}Pb activities

298 Small particulate ^{210}Po ($^{210}\text{Po}_s$) activities varied in a wide range from 0.08 to 4.82 dpm 100L⁻¹
299 (mean: 0.76 ± 0.63 dpm 100L⁻¹, $n = 81$), about 83% of the values in the small particles were lower
300 than 1.0 dpm 100L⁻¹ with higher $^{210}\text{Po}_s$ values generally observed in the surface samples (Fig. 4,
301 Table S2). The range of small particulate ^{210}Pb ($^{210}\text{Pb}_s$) activities was 0.07 to 2.89 dpm 100L⁻¹
302 (mean: 0.56 ± 0.46 dpm 100L⁻¹, $n = 81$). The vertical profiles of $^{210}\text{Pb}_s$ were generally similar to
303 those of $^{210}\text{Po}_s$, with relatively high activity in the surface, lower activity in the subsurface and
304 increasing activity with depth (Fig. 4). This has been seen in the North Atlantic along the
305 GEOTRACES GA03 transect (Rigaud et al., 2015). The mean $^{210}\text{Po}_s/^{210}\text{Pb}_s$ activity ratio (AR) was
306 1.43 ± 0.96 in the surface waters ($n = 14$, ≤ 47 m), and 1.57 ± 0.90 with all samples included ($n =$
307 81 , 8 – 3440 m). While most surface observations had an AR of $^{210}\text{Po}_s/^{210}\text{Pb}_s$ higher than unity, 5
308 surface samples at stations 69 and 77 showed an enrichment of ^{210}Pb activity over ^{210}Po
309 ($^{210}\text{Po}_s/^{210}\text{Pb}_s$ AR: 0.62 ± 0.18).

310 Large particulate ^{210}Po ($^{210}\text{Po}_l$) activities ranged from 0.01 to 0.83 dpm 100L⁻¹ with a mean of
311 0.10 ± 0.12 dpm 100L⁻¹ ($n = 59$, Fig. 5, Table S2). The range of ^{210}Pb activity in the large particles
312 ($^{210}\text{Pb}_l$) was from 0.02 to 0.67 dpm 100L⁻¹ (mean: 0.12 ± 0.14 dpm 100L⁻¹, $n = 59$). The highest
313 $^{210}\text{Po}_l$ and $^{210}\text{Pb}_l$ values were found at 30 m at station 26. The mean $^{210}\text{Po}_l/^{210}\text{Pb}_l$ activity ratio (AR)
314 was 1.09 ± 1.54 in the surface waters ($n = 14$, ≤ 47 m), and 1.06 ± 0.86 when all data were
315 considered ($n = 59$, 8-800 m). There were 17% of the samples with a depletion of ^{210}Po activity

316 relative to ^{210}Pb activity in large particles (mean AR: 0.49 ± 0.23), particularly in surface waters
317 from the western section. We address this issue further in sections 4.2 and 4.3.

318 The percentages of total ^{210}Po activity in the small and large particles ranged from 0.9 to 46.7%
319 (mean: $8.0 \pm 6.7\%$) and from 0.1 to 8.9% (mean: $1.2 \pm 1.5\%$), respectively. The percentage of total
320 ^{210}Pb activity ranged from 0.7 to 21.4% (mean: $4.9 \pm 3.8\%$) and from 0.2 to 5.9% (mean: $1.1 \pm$
321 1.2%) in the small and large particulate phase, respectively. These values revealed that both
322 radionuclides were predominantly present in the dissolved phase along this transect, as is
323 commonly found in the ocean. The particulate percentages reported here are similar to the values
324 reported from the F.S. “Meteor” cruise 32 in the North Atlantic (Bacon et al., 1976) and along the
325 North Atlantic GA03 transect (Rigaud et al., 2015).

326 We then combined radionuclide activity on the small and large particles from the same depth
327 as the total particulate activity. There were 56 samples in total (surface to 800 m) and 41 of them
328 were from the upper 200 m. Most of the total particulate ^{210}Po ($^{210}\text{Po}_p$) and ^{210}Pb ($^{210}\text{Pb}_p$) activity
329 was on the small particles, with 86% of $^{210}\text{Po}_p$ and 80% of $^{210}\text{Pb}_p$ on the small size fraction (data
330 not shown). The total particulate ^{210}Po and ^{210}Pb AR ($^{210}\text{Po}_p/^{210}\text{Pb}_p$) had the same mean as that of
331 the small particulate ^{210}Po and ^{210}Pb AR ($^{210}\text{Po}_s/^{210}\text{Pb}_s$) (Welch Two Sample t-test, $n = 56$, $p = 0.1$),
332 indicating that the values of the $^{210}\text{Po}_p/^{210}\text{Pb}_p$ activity ratios were driven by the small particles.
333 While the majority of particulate matter was enriched in ^{210}Po ($^{210}\text{Po}_p/^{210}\text{Pb}_p$ AR > 1), there were
334 13 out of 56 total samples from various depths that were depleted in ^{210}Po relative to ^{210}Pb . While
335 ~~the majority of particulate matter was enriched in ^{210}Po ($^{210}\text{Po}_p/^{210}\text{Pb}_p$ AR > 1), there were some~~
336 ~~surface samples that were depleted in ^{210}Po relative to ^{210}Pb .~~ The $^{210}\text{Po}_p/^{210}\text{Pb}_p$ activity ratios from
337 this study are compared to the results from previous studies in various oceanic regimes in section
338 4.2.

339

340 4 Discussion

341 4.1 Total ^{210}Po and ^{210}Pb activities

342 The overall profiles of $^{210}\text{Po}_t$ and $^{210}\text{Pb}_t$ activities were different among basins (Fig. 2). The
343 deficiencies of $^{210}\text{Po}_t$ activities with respect to $^{210}\text{Pb}_t$ activities in the surface samples from the
344 Iceland Basin, the Irminger Sea, and the Labrador Sea were generally greater than those from the
345 Western European Basin. Such disequilibria generally extended to the deep waters (1700 – 2950
346 m). In contrast, $^{210}\text{Po}_t$ activities in the Western European Basin were generally enriched relative to

347 $^{210}\text{Pb}_t$ activities from below the surface to the bottom of the profile. In the Western European Basin,
348 the sub-surface $^{210}\text{Po}_t$ activity excess was much larger than the surface depletion, suggesting that
349 some external source would be needed to maintain this excess ^{210}Po activity within the water
350 column. One possible source of these sub-surface ^{210}Po activity excesses below 2000 m at stations
351 1 and 13 could be the North-East Atlantic Deep Water, lower (NEADWL) which was the dominant
352 water mass in the Iberian Basin from 2000 m to the bottom, and had a concentration of silicate up
353 to $48 \mu\text{mol kg}^{-1}$ (García-Ibáñez et al., 2015). High activity of ^{210}Po in deep samples could be due
354 to the dissolution of diatoms or herbivore feces (Cooper, 1952). As these particles sink and dissolve,
355 ^{210}Po activity may have been preferentially released to the dissolved phase compared to ^{210}Pb
356 activity (Bacon et al., 1976), leading to ^{210}Po excess observed in the deep waters at stations 1 and
357 13. For the sub-surface ^{210}Po activity excesses at station 1 between 400 and 1000 m where lateral
358 inputs of particulate Fe from the margin was observed (Gourain et al., 2018), the likely process is
359 diffusion of ^{210}Po from those particles originated from the margin and such excess could be
360 transported westwards to station 13 by lateral advection. An alternative source of ^{210}Po activity
361 excess between 50 and 250 m at stations 1 and 13 (Fig. 3) could be the eastern boundary upwelling
362 along the coast of the Iberian Peninsula (García-Ibáñez et al., 2015). Even though no strong
363 upwelling events were revealed from temperature and density profiles during the cruise, northerly
364 winds favoring upwelling were recorded 2 – 3 months before the sampling (Shelley et al., 2017).
365 The deep water may have excess ^{210}Po activity due to the remineralization of sinking particles.
366 The upwelling of this water mass prior to the sampling date could maintain such sub-surface excess
367 ^{210}Po activity. Similar findings have been reported in the Cariaco Trench for the upper 300 m of
368 the water column by Bacon et al. (1980a). ~~One possible source of these sub-surface ^{210}Po activity
369 excesses could be the eastern boundary upwelling along the coast of the Iberian Peninsula (García-
370 Ibáñez et al., 2015). Even though no strong upwelling events were revealed from temperature and
371 density profiles during the cruise, northerly winds favoring upwelling were recorded 2–3 months
372 before the sampling (Shelley et al., 2017). The deep water may have excess ^{210}Po activity due to
373 the remineralization of sinking particles. The upwelling of this water mass prior to the sampling
374 date could maintain excess ^{210}Po activity in the water column if the previous export of ^{210}Po activity
375 was large enough. Similar findings have been reported in the Cariaco Trench by Bacon et al.
376 (1980a).~~

377 As atmospheric deposition is the main source of ^{210}Pb to the water column (e.g. Masqué et al.,
378 2002), we divided the GA01 transect into a western section (stn. 44 – 77) and an eastern section
379 (stn. 1 – 38) based on atmospheric deposition boxes described in Shelley et al., (2017). Total
380 atmospheric deposition fluxes of a suite of aerosol-sourced trace metals (TEs) were ~~all~~ reported to
381 be higher in the east than the west for 18 out of 19 TEs (Shelley et al., 2017). However, a two
382 sample t-test revealed a greater mean of $^{210}\text{Pb}_t$ activity in surface waters in the western than in the
383 eastern section ($p < 0.02$, mean: 12.1 vs. 10.4 dpm 100 L⁻¹), despite the fact that ^{210}Pb is usually
384 associated with aerosols. Even though the direct input of atmospheric ^{210}Pb may be larger in the
385 east (assuming it behaves like the other trace metals, but without aerosol ^{210}Pb data we cannot
386 confirm this), alternative inputs of ^{210}Pb from freshwater (e.g., sea ice processes and meteoric
387 water) could be a greater source of ^{210}Pb activity to the west. The freshwater sources over the
388 Greenland shelf and slope have been identified by Benetti et al. (2017), and were believed to be
389 an important source of Fe (Tonnard et al., in review) and Al (Menzel-Barraqueta et al., in review)
390 off of Greenland during this cruise. This ~~unexpected~~ result highlights the need in the future to
391 measure ^{210}Pb activity simultaneously in the atmospheric and local freshwater sources in order to
392 account for all source terms.

393

394 **4.2 Total particulate $^{210}\text{Po}/^{210}\text{Pb}$ AR**

395 A proposed explanation for the depletion of ^{210}Po activity relative to ^{210}Pb activity (AR <1) in
396 some particles is effective recycling, commonly characterized by a subsurface excess of dissolved
397 ^{210}Po activity released from enriched particles leaving the surface. Bacon et al. (1976) suggested
398 that the efficiency of this recycling could reach up to 50%, while there is no significant concurrent
399 release of ^{210}Pb activity in the water column. Laboratory studies have found the release rate of
400 ^{210}Po in marine particulate matter to be significant; for example, 41% of the ^{210}Po activity in
401 euphausiid fecal pellets was released over 5 days as presented in Heyraud et al. (1976). An
402 alternative explanation for the depletion of ^{210}Po activity in particles is their lithogenic origin.
403 $^{210}\text{Po}/^{210}\text{Pb}$ AR in lithogenic particles was reported to be similar to or less than unity (Nozaki et
404 al., 1998; Tateda et al., 2003). In addition, the AR < 1 observed at station 1 (120, 250, and 550 m)
405 could be associated with lithogenic particles from the Iberian Margin where 100% of the
406 particulate Fe (PFe) had a lithogenic origin while the lithogenic contribution to PFe at other
407 stations was smaller (Gourain et al., 2018) ~~The AR < 1 observed at station 1 (120, 250, and 550 m)~~

408 ~~could be associated with lithogenic particles from the Iberian Margin where the lithogenic~~
409 ~~contribution to particulate and dissolved Fe and dissolved Al were reported to be significant~~
410 ~~(Gourain et al., 2018; Menzel-Barraqueta et al., in review).~~

411 The time-series chlorophyll-a concentrations (8-day composite,
412 <https://oceancolor.gsfc.nasa.gov>) from January to July 2014 at each station revealed bloom
413 conditions about 4 months prior to the sampling time (Fig. 4 Fig. 6). We estimated the days since
414 the last bloom began prior to the sampling date for each station (Table 1) and put these data into
415 the context of the low $^{210}\text{Po}_p/^{210}\text{Pb}_p$ AR (< 1) in the total particles $> 1 \mu\text{m}$ (Fig. 7). Eight stations
416 had total particulate samples with $^{210}\text{Po}_p/^{210}\text{Pb}_p$ AR lower than unity from either shallow or deep
417 waters. Specifically, when the time since the last bloom began was relatively short (24 – 47 d) the
418 samples with $^{210}\text{Po}_p/^{210}\text{Pb}_p$ AR < 1 were observed in the shallow waters (10 – 60 m). In contrast,
419 as longer time (50 – 74 d) passed since the last bloom, the depths at which samples had
420 $^{210}\text{Po}_p/^{210}\text{Pb}_p$ AR < 1 were found to be much deeper (120 – 500 m). The results indicated that post-
421 bloom particles could be recycled for weeks in shallow depths and take weeks to months to sink
422 to deeper waters.

423 The averages of $^{210}\text{Po}_p/^{210}\text{Pb}_p$ AR within the upper 200 m water column were put into a global
424 context with previously reported results (Fig. 5 Fig. 8). Total particulate $^{210}\text{Po}/^{210}\text{Pb}$ AR in the
425 open ocean in previous studies (e.g., Equatorial/western Pacific, Bellingshausen Sea, BATS,
426 Labrador Sea) were generally greater than unity. In contrast to the open ocean, the data show a
427 distinct trend of depletion of relative ^{210}Po activity in marine particles from the shallow seas of the
428 high latitude northern hemisphere. The lowest total particulate $^{210}\text{Po}/^{210}\text{Pb}$ AR values (Table 2, 0.4
429 – 0.5) were found in the ~~central Arctic and~~ Chukchi shelf (He et al., 2015) and other seas from the
430 Eurasian sector (Barents, Kara and Laptev Seas) but also in central Arctic (Friedrich, 2011).
431 Previous studies have observed depletion of relative ^{210}Po activity in nearshore particles in the
432 Yellow Sea (Hong et al., 1999), in the turbid waters off of western Taiwan (Wei et al., 2012), on
433 the shelf of Woods Hole, MA (Rigaud et al., 2015), and now in the margin station off St. John's,
434 Canada (this study). The previous authors attributed the relative depletion of particulate ^{210}Po
435 activity in the nearshore waters to the terrestrial origin/riverine input of particles with a low
436 $^{210}\text{Po}/^{210}\text{Pb}$ AR. This may partially explain low activity ratios in the samples from the shelf of the
437 Arctic Ocean as well, since it receives $\sim 10\%$ of global river runoff and is the most riverine-
438 influenced of all of the world's oceans (Opsahl et al., 1999; Carmack et al., 2006). The Arctic

439 Basin, similarly, had ~~wide-spread~~ widespread deficits of particulate ^{210}Po activity in the upper
440 water column during the sea-ice minimum in 2007 (Roca-Marti et al., in review). Besides shelf
441 particles, ~~The~~ the authors suggested that other particle types could also play a role in lowering the
442 particulate AR, including sea-ice sediments, remineralized material, fecal pellets, and
443 picoplankton aggregates.

444

445 **4.3 Relationship between total particulate $^{210}\text{Po}/^{210}\text{Pb}$ AR and AOU**

446 AOU is a time-integrated measure of the amount of oxygen removed during the
447 biogeochemical processes (e.g. respiration, remineralization, oxidation) in the ocean interior.
448 Therefore, AOU is a product of apparent oxygen utilization rate (AOUR) and the age of water
449 mass (e.g. Stanley et al., 2012), i.e. high AOU could be due to either intense biogeochemical
450 processes that have occurred in a short period of time (young water mass) or weaker processes
451 over a longer period of time (old water mass). Consequently, the rate of these biogeochemical
452 processes and time (water mass age) would have different/similar impacts on the $^{210}\text{Po}_p/^{210}\text{Pb}_p$ AR
453 value depending on the initial AR in the particles and the natural of the particles. ~~Apparent oxygen
454 utilization ($\text{AOU} = \text{O}_2\text{-saturation} - \text{O}_2\text{-measured}$), the amount of oxygen that has been consumed by
455 remineralization of exported organic matter in the water column, can be used to indicate the
456 intensity of particle recycling (Ito et al., 2004; Duteil et al., 2013). While AOU is generated both
457 by water mass ageing and concomitant biological oxygen consumption (e.g. Ito et al., 2004;
458 Sonnerup et al., 2015), the two components of AOU would be predicted to have opposite impacts
459 on the $^{210}\text{Po}_p/^{210}\text{Pb}_p$ AR value. For example, the $^{210}\text{Po}_p/^{210}\text{Pb}_p$ AR would tend to increase with time
460 if the initial AR is < 1 because particulate ^{210}Po activity would increase from the decay of ^{210}Pb
461 and trend towards secular equilibrium ($^{210}\text{Po}_p/^{210}\text{Pb}_p$ AR = 1), and to decrease with time if the
462 initial AR is > 1 as the original excess of particulate ^{210}Po activity would disappear after 7 half-
463 lives of ^{210}Po . ~~old particles would tend to have a higher $^{210}\text{Po}_p/^{210}\text{Pb}_p$ activity ratio (closer to 1)
464 because particulate ^{210}Po activity would increase from the decay of ^{210}Pb within mineral lattices
465 and trend towards secular equilibrium ($^{210}\text{Po}_p/^{210}\text{Pb}_p$ AR = 1).~~ In contrast, oxygen consumption
466 due to bacterial remineralization would preferentially release ^{210}Po activity from particles into the
467 dissolved pool (e.g. Stewart et al., 2008), leading to a lower $^{210}\text{Po}_p/^{210}\text{Pb}_p$ AR in those particles.~~

468 The combination of average $^{210}\text{Po}_p/^{210}\text{Pb}_p$ AR and their corresponding average AOU in the
469 upper 200 m at 40 stations from 4 independent studies, including ARK-XXII/2 (77.38 – 87.83 °N,

470 n = 15) in the Arctic, BOFS (48.89 – 49.87 °N, n = 7), GA03 (22.38 – 39.70 °N, n = 7), and GA01
471 (this study, 40.33 – 59.80 °N, n = 11) in the North Atlantic (see map in Fig. 5 Fig. 8) suggests two
472 distinct linear trends (Fig. 6 Fig. 9). When AOU was lower than 25 $\mu\text{mol kg}^{-1}$, the $^{210}\text{Po}_p/^{210}\text{Pb}_p$
473 AR was found to be greater than unity, together with a linear negative relationship (n = 27, $R^2 =$
474 0.5 , $p < 0.001$) towards the AOU at 25 $\mu\text{mol kg}^{-1}$. In contrast, AOU values greater than 25 μmol
475 kg^{-1} were coincident with a $^{210}\text{Po}_p/^{210}\text{Pb}_p$ AR < 1, and there was a linear positive relationship (n =
476 12, $R^2 = 0.4$, $p = 0.03$) towards the highest AOU values measured. The two contradictory linear
477 trends likely reflect the nature of the particles. For example, the observation of $^{210}\text{Po}_p/^{210}\text{Pb}_p$ AR >
478 1 with AOU < 25 $\mu\text{mol kg}^{-1}$ may suggest relatively fresh/organic particles in the young water mass.
479 When AOU increases either due to water mass aging or higher AOUR, the $^{210}\text{Po}_p/^{210}\text{Pb}_p$ AR
480 decreases with a slope of -0.17 ± 0.04 . On the other hand, refractory/lithogenic particles may be
481 suggested by the observation of $^{210}\text{Po}_p/^{210}\text{Pb}_p$ AR < 1 with AOU > 25 $\mu\text{mol kg}^{-1}$. For those particles,
482 increasing in AOU either due to water mass aging or higher AOUR would change the $^{210}\text{Po}_p/^{210}\text{Pb}_p$
483 AR to a much lesser degree than that for organic particles with a slope of 0.008 ± 0.003 . ~~The two~~
484 ~~contradictory linear trends likely reflect the opposite impacts of the two components (water mass~~
485 ~~aging and remineralization) of AOU on $^{210}\text{Po}_p/^{210}\text{Pb}_p$ AR. This suggests that the variation in the~~
486 ~~$^{210}\text{Po}_p/^{210}\text{Pb}_p$ AR was mainly driven by remineralization processes under the condition of AOU <~~
487 ~~25 $\mu\text{mol kg}^{-1}$, lowering the total particulate activity ratio; whereas the decay of ^{210}Pb into ^{210}Po~~
488 ~~towards secular equilibrium may dominate when AOU was > 25 $\mu\text{mol kg}^{-1}$, leading to an increase~~
489 ~~in $^{210}\text{Po}_p/^{210}\text{Pb}_p$ AR.~~ This explanation, however, appears to only hold for the high latitude Northern
490 Hemisphere where $^{210}\text{Po}_p/^{210}\text{Pb}_p$ activity ratios were generally lower than those in the other oceanic
491 settings (Fig. 5 Fig. 8). In the high latitude Southern Hemisphere near Antarctic (e.g., ANT-X/6),
492 for example, there is no apparent relationship between $^{210}\text{Po}_p/^{210}\text{Pb}_p$ activity ratios and AOU. This
493 relationship (or lack thereof) deserves more study in the future.

494

495 ~~4.4 Small particles, sorption, and calculating POC export~~ Relationship among small particles, 496 adsorption, and scavenging

497 The partitioning coefficient, K_d (L kg^{-1}), has been used to describe the particle adsorption
498 behavior of radionuclides. It is defined as the ratio of the adsorbed radionuclide activity (A_p , dpm
499 100L^{-1}) to the dissolved radionuclide activity (A_d , dpm 100L^{-1}), normalized by the suspended
500 particulate matter concentration (SPM , $\mu\text{g L}^{-1}$):

501
$$K_d = \frac{A_p}{A_d} \times \frac{1}{SPM} 10^9 \quad (1)$$

502 Owing to the different biological and chemical behaviors of ^{210}Po and ^{210}Pb , the interpretation
503 of measured K_d for ^{210}Po ($K_d(\text{Po})$) may not be as clear as that for ^{210}Pb ($K_d(\text{Pb})$). As claimed
504 previously in Tang et al., (2017), $K_d(\text{Po})$ is complicated because it appears to reflect both the
505 surface adsorption and potential bioaccumulation.

506 In this study, the size-fractionated data of both radionuclide activity and SPM allowed us to
507 calculate the partitioning coefficients for both radionuclides on small and total particles. The
508 dissolved radionuclide activity was calculated as the difference between total and particulate
509 activity. The coefficients for the small particulate and the total particulate phases were normalized
510 by the SPM in the small and total particulate phases, respectively. We present only the coefficients
511 for the small particulate phases ($K_d(\text{Po})_s$, $K_d(\text{Pb})_s$) and the total particulate phases ($K_d(\text{Po})_p$,
512 $K_d(\text{Pb})_p$) because most of the particulate activity (> 80%) was associated with the small particles
513 along the GEOVIDE transect, and most conceptualized scavenging models consider either the
514 two-box model (dissolved – total particulate phases, i.e. $K_d(\text{Po})_p$) or the three-box model (dissolved
515 – small – large, i.e. $K_d(\text{Po})_s$) (Clegg and Whitfield, 1990; 1991; Rigaud et al., 2015) and thus
516 activity is concentrated from the dissolved phase to the total or small particles.

517 The average values of $K_d(\text{Po})$ was 1.6 times of those of $K_d(\text{Pb})$ in both small and total
518 particulate phases, suggesting a higher affinity with particles for ^{210}Po with respect to ^{210}Pb , which
519 is commonly observed in the global ocean (Bacon et al., 1988; Hong et al., 1999; Masqué et al.,
520 2002; Wei et al., 2014; Tang et al., 2017). The K_d values for the small particulate phase were
521 slightly higher than those for the total particulate phase but overall these values were very similar
522 for both radionuclides (Fig. 10), suggesting that adsorption/scavenging of radionuclides was driven
523 by small particles along the transect. In addition, there are increasing studies which argue that
524 small particles can form aggregates that sink, and their contribution to carbon export could be
525 larger than previously thought (e.g. Richardson and Jackson, 2007; Lomas and Moran, 2011;
526 Amacher et al., 2013; Puigcorbé et al., 2015). We, therefore, recommend combining the activities
527 of both small and large particles into a total particulate fraction in order to explain total $^{210}\text{Po}/^{210}\text{Pb}$
528 disequilibria in the surface waters, and utilizing the characteristics of the total particles (instead of
529 just the large particles) in the estimation of the POC export fluxes (Tang et al., companion paper
530 submitted to this volume).

531 Traditionally, large particles collected by in-situ filtration with pumps, most commonly defined
532 as particles larger than 53 or 70 μm , were assumed to dominate the sinking flux (Dugdale and
533 Goering, 1967; Bishop et al., 1977; Fowler and Knauer, 1986; Honjo et al., 1992; Walsh and
534 Gardner, 1992) such that the composition (POC/ ^{210}Po) of the large particle size class was used to
535 convert ^{210}Po fluxes into POC export (e.g. Friedrich and Rutgers van der Loeff, 2002; Cochran
536 and Masqué, 2003; Murray et al., 2005; Stewart et al., 2010; Roca-Martí et al., 2016). Given that
537 the true size spectrum of sinking particles for the timescale relevant to the $^{210}\text{Po}/^{210}\text{Pb}$ method is
538 unknown and the POC flux estimates are sensitive to the particulate POC/ ^{210}Po ratio, both small
539 and large particles should be sampled for POC/ ^{210}Po due to the variability in the POC/ ^{210}Po ratio
540 in different size classes (Hayes et al., in review).

~~541 The assumption that the largest particles dominate export in the ocean (e.g. Bishop et al., 1977;
542 Fowler and Knauer, 1986; Michaels and Silver, 1988; Honjo et al., 1992; Walsh and Gardner,
543 1992) has been challenged by increasing studies which argue that small particles can form
544 aggregates that sink, and their contribution to carbon export could be larger than previously
545 thought (e.g. Richardson and Jackson, 2007; Lomas and Moran, 2011; Amacher et al., 2013;
546 Puigcorb  et al., 2015).~~

~~547 We investigated the role of small phytoplankton to carbon export along the GA01 transect via
548 investigation of pigments and *in-situ* primary production. The fraction of pigment-based size
549 classes suggested a significant contribution of small particles (nano-phytoplankton: 2–20 μm
550 60%, pico-phytoplankton: < 2 μm , 13%) to primary production in the eastern section while larger
551 particles (micro-phytoplankton: > 20 μm , 60%) may have dominated production in the western
552 section of the GA01 transect (Tonnard et al., in prep.). The rate of primary production in the eastern
553 section (mean: $99 \pm 50 \text{ mmol C m}^{-2} \text{ d}^{-1}$), however, was similar to that in the west (mean: 93 ± 58
554 $\text{mmol C m}^{-2} \text{ d}^{-1}$) (data not shown). While we do not have direct evidence of small particles sinking,
555 we are making an assumption that our study sites behave as the above cited papers have seen
556 elsewhere. Therefore, a possible link between small particles and production, and possibly export
557 (proportional to their role in production according to Richardson and Jackson, 2007), may exist
558 along the transect.~~

~~559 The partitioning coefficient, $K_d (\text{L kg}^{-1})$, has been used to describe the particle adsorption behavior
560 of radionuclides. It is defined as the ratio of the adsorbed radionuclide activity ($\text{dpm } 100\text{L}^{-1}$) to~~

561 the dissolved radionuclide activity (A_d , dpm $100L^{-1}$), normalized by the suspended particulate matter
562 concentration (SPM , $\mu g L^{-1}$):

$$563 K_d = \frac{A_p}{A_d} \times \frac{1}{SPM} 10^9 \quad (1)$$

564 —Owing to the different biological and chemical behaviors of ^{210}Po and ^{210}Pb , the interpretation
565 of measured K_d for ^{210}Po ($K_d(Po)$) may not be as clear as that for ^{210}Pb ($K_d(Pb)$) (i.e. $K_d(Po)$ also
566 takes the fraction of absorbed ^{210}Po into account, Tang et al., 2017). As such, it would be more
567 appropriate to think of both $K_d(Po)$ and $K_d(Pb)$ as the intensity parameter for the radionuclide
568 association with particles.

569 In this study, the size-fractionated data of radionuclide activity and SPM allowed us to
570 calculate the partitioning coefficients for both radionuclides on small and large particles. We
571 present only the coefficients for the small particulate phases ($K_d(Po)_s$, $K_d(Pb)_s$) and the total
572 particulate phases ($K_d(Po)_p$, $K_d(Pb)_p$) because most of the particulate activity ($> 80\%$) was
573 associated with the small particles along the GEOVIDE transect, and most conceptualized
574 scavenging models consider either the two-box model (dissolved — total particulate phases, i.e.
575 $K_d(Po)_p$) or the three-box model (dissolved — small — large, i.e. $K_d(Po)_s$) (Clegg and Whitfield,
576 1990; 1991; Rigaud et al., 2015) and thus activity is concentrated from the dissolved phase to the
577 total or small particles. The K_d values for the small particulate phase were slightly higher than
578 those for the total particulate phase but overall these values were very similar for both
579 radionuclides (Fig. 7). Combining the fact that adsorption/scavenging was in fact driven by small
580 particles with the contribution of small phytoplankton to production, the importance of small
581 particles to radionuclide export is suggested. We recommend combining the activities of both
582 small and large particles into a total particulate fraction in order to explain total $^{210}Po/^{210}Pb$
583 disequilibria in the surface waters, and utilizing the characteristics of the total particles (instead of
584 just the large particles) in the estimation of the POC export fluxes (Tang et al., in prep.).

585

586 5 Conclusions

587 In this study, we reported the vertical distribution of total and size-fractionated particulate ^{210}Po
588 and ^{210}Pb activities in the North Atlantic during the GEOVIDE GA01 cruise. More than 90% of
589 the radionuclide activity was found in the dissolved phase, while a small proportion was associated
590 with particles in this transect. Total ^{210}Po activity was generally depleted relative to total ^{210}Pb
591 activity in the upper 100 m due to the preferential adsorption of ^{210}Po activity by particles. Such

592 deficiencies of ^{210}Po activities generally extended to the deep waters at most of the stations. In the
593 West European Basin, the excess of ^{210}Po activities at stations 1 and 13 in the North East Atlantic
594 Deep Water was attributed to the release of ^{210}Po during dissolution of sinking biogenic particles.

595 There appear to be geographic differences in particulate $^{210}\text{Po}/^{210}\text{Pb}$ activity ratios measured
596 during GEOVIDE and previous studies, with particularly low values in the high-latitude North
597 Atlantic and Arctic. While this observation deserves more attention, we support previous
598 suggestions that this is due to the terrestrial origin/riverine input of particles with a low $^{210}\text{Po}/^{210}\text{Pb}$
599 AR into the river-dominated shallow seas of the Arctic. The age of the particles and water masses
600 as well as the importance of biogeochemical processes (e.g. respiration, remineralization) may also
601 explain some of these observations, as there was a significant relationship between the total
602 particulate activity ratio and AOU when both were measured in the North Atlantic ($> 20^\circ\text{N}$) and
603 Arctic Oceans.

604 Over 80% of the particulate radionuclide activity was on small particles, indicating that the
605 scavenging of both radionuclides was driven by small particles. Therefore, we suggest considering
606 the activities of ^{210}Po and ^{210}Pb from both small and large particles in order to study the water
607 column $^{210}\text{Po}/^{210}\text{Pb}$ disequilibria and quantify POC export along the GA01 transect. This has been
608 addressed in a companion paper in this issue. We recommend that both small and large particles
609 should be sampled for POC/ ^{210}Po estimates for the application of the $^{210}\text{Po}/^{210}\text{Pb}$ method in future
610 studies of POC export.

611 ~~In this study, we reported the vertical distribution of total and size-fractionated particulate ^{210}Po
612 and ^{210}Pb activities in the North Atlantic during the GEOVIDE GA01 cruise. More than 90% of
613 the radionuclide activity was found in the dissolved phase, while a small proportion was associated
614 with particles in this transect. Total ^{210}Po activity was generally depleted relative to total ^{210}Pb
615 activity in the upper 100 m due to the assumed preferential adsorption and uptake of ^{210}Po activity
616 by particles.~~

617 ~~Over 80% of the particulate radionuclide activity was on small particles, and it appeared that
618 the adsorption/scavenging of both radionuclides was driven by small particles. Considering this
619 and the contributions of small phytoplankton to primary production (and possibly export), we
620 suggest combining the activities of both ^{210}Po and ^{210}Pb from both small and large particles into a
621 total particulate fraction ($> 1\ \mu\text{m}$) in order to explain the water column $^{210}\text{Po}/^{210}\text{Pb}$ disequilibria
622 and calculate POC export.~~

623 ~~There appear to be geographic differences in particulate $^{210}\text{Po}/^{210}\text{Pb}$ activity ratios measured~~
624 ~~during GEOVIDE and previous studies, with particularly low values in the high-latitude North~~
625 ~~Atlantic and Arctic. While this observation deserves more attention, we support previous~~
626 ~~suggestions that this is due to the terrestrial origin/riverine input of particles with a low $^{210}\text{Po}/^{210}\text{Pb}$~~
627 ~~AR into the river dominated shallow basins of the Arctic. Considering the age of the particles and~~
628 ~~water masses as well as the importance of remineralization may also explain some of these~~
629 ~~observations, as there was a significant relationship between the total particulate activity ratio and~~
630 ~~AOU when both were measured in the high latitude North Atlantic and Arctic Oceans.~~

631
632

633 **Acknowledgements**

634

635 Thank you to the chief scientists (G. Sarthou and P. Lherminier) of the GEOVIDE cruise, and the
636 captain (G. Ferrand), and crew of the ~~N/O~~ *R/V Pourquoi Pas?* for their support of this work. Many
637 thanks to P. Branellec, F. Desprez de Gésincourt, M. Hamon, C. Kermabon, P. Le Bot, S. Leizour,
638 O. Ménage, F. Pérault, and E. de Saint-Léger for their technical support during the GEOVIDE
639 expedition, and to C. Schmechtig for the GEOVIDE database management. P. Lam is also
640 acknowledged for providing two modified McLane ISP. Special thanks go to the member of the
641 pump group including F. Planchon, V. Sanial, and C. Jeandel. The author would like to thank C.
642 Mariez, S. Roig, F. Planchon, and H. Planquette who helped in providing particle composition data
643 ~~and A. Roukaerts, D. Fonseca-Batista, F. Deman, and F. Dehairs for primary production data.~~ We
644 also would like to acknowledge the funding agencies: the French National Research Agency
645 (ANR-13-BS06-0014, ANR-12-PDOC-0025-01), the French National Center for Scientific
646 Research (CNRS-LEFE-CYBER), the LabexMER (anr-10-LABX-19), and Ifremer. **Funding was**
647 **provided to P. Masque by the Generalitat de Catalunya (Grant 2017 SGR-1588). This work**
648 **contributes to the ICTA ‘Unit of Excellence’ (MinECo, MDM2015-0552).** G. Stewart and Y. Tang
649 were supported by NSF award #OCE 1237108. M. Castrillejo and M. Roca-Martí were funded by
650 an FPU PhD studentship (AP-2012-2901 and AP2010-2510, respectively) from the Ministerio de
651 Educación, Cultura y Deporte of Spain. M. Castrillejo was also supported by the ETH Zurich
652 Postdoctoral Fellowship Program (17-2 FEL-30), co-funded by the Marie Curie Actions for People
653 COFUND Program. Additional thanks go to G. Hemming (**Queens College**) and T. Rasbury (**Stony**

654 Brook University) for laboratory assistance with the ICP-MS analyses. We also thank two
655 anonymous reviewers for their constructive comments to improve the manuscript.

656 **References:**

657 Amacher, J., Neuer, S. and Lomas, M.: DNA-based molecular fingerprinting of eukaryotic protists
658 and cyanobacteria contributing to sinking particle flux at the Bermuda Atlantic time-series study,
659 Deep Sea Research Part II, 93, 71-83, 2013.

660
661 Bacon, M. P.: ^{210}Pb and ^{210}Po results from F.S. "Meteor" cruise 32 in the North
662 Atlantic, PANGAEA, 1977.

663
664 Bacon, M. P., Belostock, R. A., Tecotzky, M., Turekian, K. K. and Spencer, D. W.: Lead-210 and
665 polonium-210 in ocean water profiles of the continental shelf and slope south of New England,
666 Continental Shelf Research, 8, 841-853, 1988.

667
668 Bacon, M. P., Brewer, P. G., Spencer, D. W., Murray, J. W. and Goddard, J.: Lead-210, polonium-
669 210, manganese and iron in the Cariaco Trench, Deep Sea Research Part A. Oceanographic
670 Research Papers, 27, 119-135, 1980a.

671
672 Bacon, M. P., Spencer, D. W. and Brewer, P. G.: $^{210}\text{Pb}/^{226}\text{Ra}$ and $^{210}\text{Po}/^{210}\text{Pb}$ disequilibria in
673 seawater and suspended particulate matter, Earth and Planetary Science Letters, 32, 277-296, 1976.

674
675
676 Bacon, M. P., Spencer, D. W. and Brewer, P. G.: Lead-210 and Polonium-210 as Marine
677 Geochemical Tracers: Review and Discussion of Results from the Labrador Sea, Natural radiation
678 environment III, T. F. Gesell and W. M. Lowder, 1, 473-501, 1980b.

679
680 Benetti, M., Reverdin, G., Lique, C., Yashayaev, I., Holliday, N. P., Tynan, E., Torres-Valdes, S.,
681 Lherminier, P., Tréguer, P. and Sarthou, G.: Composition of freshwater in the spring of 2014 on
682 the southern Labrador shelf and slope, Journal of Geophysical Research: Oceans, 122, 1102-1121,
683 2017.

684
685 Bishop, J. K. B., Edmond, J. M., Ketten, D. R., Bacon, M. P. and Silker, W. B.: The chemistry,
686 biology, and vertical flux of particulate matter from the upper 400 m of the equatorial Atlantic
687 Ocean, Deep Sea Research, 24, 511-548, 1977.

688
689 BODC, Lowry, R. K., Machin, P. and Cramer, R. N.: Compilation of the results of EU-project
690 BOFS, PANGAEA, 2016.

691
692 Boyer, T., Conkright, M. E. and Levitus, S.: Seasonal variability of dissolved oxygen, percent
693 oxygen saturation, and apparent oxygen utilization in the Atlantic and Pacific Oceans, Deep Sea
694 Research Part I: Oceanographic Research Papers, 46, 1593-1613, 1999.

695
696 Carmack, E., Barber, D., Christensen, J., Macdonald, R., Rudels, B. and Sakshaug, E.: Climate
697 variability and physical forcing of the food webs and the carbon budget on panarctic shelves,
698 Progress in Oceanography, 71, 145-181, 2006.

699
700 Ceballos-Romero, E., Le Moigne, F. A. C., Henson, S., Marsay, C. M., Sanders, R. J., García-
701 Tenorio, R. and Villa-Alfageme, M.: Influence of bloom dynamics on Particle Export Efficiency

702 in the North Atlantic: a comparative study of radioanalytical techniques and sediment traps,
703 Marine Chemistry, 186, 198-210, 2016.

704

705 Clegg, S. L. and Whitfield, M.: A generalised model for the scavenging of trace metals in the open
706 ocean: I. Particle cycling, Deep Sea Research Part A. Oceanographic Research Papers, 37, 809-
707 832, 1990.

708

709 Clegg, S. L. and Whitfield, M.: A generalised model for the scavenging of trace metals in the open
710 ocean-II. Thorium scavenging, Deep Sea Research Part A. Oceanographic Research Papers, 38,
711 91-120, 1991.

712

713 Cochran, J. K., Bacon, M. P., Krishnaswami, S. and Turekian, K. K.: ^{210}Po and ^{210}Pb
714 distributions in the central and eastern Indian Ocean, Earth and Planetary Science Letters, 65, 433-
715 452, 1983.

716

717 Cochran, J. K. and Masqué, P.: Short-lived U/Th Series Radionuclides in the Ocean: Tracers for
718 Scavenging Rates, Export Fluxes and Particle Dynamics, Reviews in Mineralogy and
719 Geochemistry, 52, 461-492, 2003.

720

721 Cooper, L.: Factors affecting the distribution of silicate in the North Atlantic Ocean and the
722 formation of North Atlantic deep water, Journal of the Marine Biological Association of the United
723 Kingdom, 30, 511-526, 1952.

724

725 Coppola, L., Prieur, L., Taupier-Letage, I., Estournel, C., Testor, P., Lefevre, D., Belamari, S.,
726 LeReste, S. and Taillandier, V.: Observation of oxygen ventilation into deep waters through
727 targeted deployment of multiple Argo-O₂ floats in the north-western Mediterranean Sea in 2013,
728 Journal of Geophysical Research: Oceans, 122, 6325-6341, 2017.

729

730 Dugdale, R. C. and Goering, J. J.: uptake of new and regenerated forms of nitrogen in primary
731 production, Limnology and Oceanography, 12, 196-206, 1967.

732

733 Duteil, O., Koeve, W., Oschlies, A., Bianchi, D., Galbraith, E., Kriest, I. and Matar, R.: A novel
734 estimate of ocean oxygen utilisation points to a reduced rate of respiration in the ocean interior,
735 Biogeosciences, 10, 7723-7738, 2013.

736

737 Fleer, A. P. and Bacon, M. P.: Determination of ^{210}Pb and ^{210}Po in seawater and marine
738 particulate matter, Nuclear Instruments and Methods in Physics Research, 223, 243-249, 1984.

739

740 Flynn, W. W.: The determination of low levels of polonium-210 in environmental materials,
741 Analytica Chimica Acta, 43, 221-227, 1968.

742

743 Fonseca-Batista, D., Li, X., Riou, V., Michotey, V., Fripiat, F., Deman, F., Guasco, S., Brion, N.,
744 Lemaitre, N., Planchon, F., Tonnard, M., Planquette, H., Gallinari, M., Sarthou, G., Elskens, M.,
745 Chou, L. and Dehairs, F.: Evidence of high N₂ fixation rates in productive waters of the temperate
746 Northeast Atlantic, Biogeosciences, 2018.

747

748 Fowler, S. W. and Knauer, G. A.: Role of large particles in the transport of elements and organic
749 compounds through the oceanic water column, *Progress in Oceanography*, 16, 147-194, 1986.
750

751 Friedrich, J.: Polonium-210 and Lead-210 activities measured on 17 water bottle profiles and 50
752 surface water samples during POLARSTERN cruise ARK-XXII/2, PANGAEA, 2011.
753

754 Friedrich, J., Robert, M. and Stimac, I.: Polonium-210 and Lead-210 activities measured on 9
755 water bottle profiles during POLARSTERN cruise ANT-XXIV/3, PANGAEA, 2011.
756

757 Friedrich, J. and Rutgers van der Loeff, M. M.: A two-tracer (^{210}Po – ^{234}Th) approach to
758 distinguish organic carbon and biogenic silica export flux in the Antarctic Circumpolar Current,
759 *Deep Sea Research Part I: Oceanographic Research Papers*, 49, 101-120, 2002.
760

761 García-Ibáñez, M. I., Pardo, P. C., Carracedo, L. I., Mercier, H., Lherminier, P., Ríos, A. F. and
762 Pérez, F. F.: Structure, transports and transformations of the water masses in the Atlantic Subpolar
763 Gyre, *Progress in Oceanography*, 135, 18-36, 2015.
764

765 GEOTRACES Planning Group: GEOTRACES Science Plan, Baltimore, Maryland, 2006.
766

767 Gourain, A., Planquette, H., Cheize, M., Menzel-Barraqueta, J. L., Boutorh, J., Shelley, R. U.,
768 Pereira-Contreira, L., Lemaitre, N., Lacan, F., Lherminier, P. and Sarthou, G.: Particulate trace
769 metals along the GEOVIDE section, *Biogeosciences*, 2018.
770

771 Hayes, C. T., Black, E. E., Andersen, R. A., Baskaran, M., Buesseler, K. O., Charette, M. A.,
772 Cheng, H., Cochran, J. K., Edwards, R. L., Fitzgerald, P., Lam, P. J., Lu, Y., Morris, S. O.,
773 Ohnemus, D. C., Pavia, F. J., Stewart, G. and Tang, Y.: Flux of particulate elements in the North
774 Atlantic Ocean constrained by multiple radionuclides, *Global Biogeochemical Cycles*, in review.
775

776 He, J., Yu, W., Lin, W., Men, W. and Chen, L.: Particulate organic carbon export fluxes on
777 Chukchi Shelf, western Arctic Ocean, derived from $^{210}\text{Po}/^{210}\text{Pb}$ disequilibrium, *Chinese Journal*
778 *of Oceanology and Limnology*, 33, 741-747, 2015.
779

780 Heyraud, M., Fowler, S. W., Beasley, T. M. and Cherry, R. D.: Polonium-210 in euphausiids: A
781 detailed study, *Marine Biology*, 34, 127-136, 1976.
782

783 Hong, G.-H., Park, S.-K., Baskaran, M., Kim, S.-H., Chung, C.-S. and Lee, S.-H.: Lead-210 and
784 polonium-210 in the winter well-mixed turbid waters in the mouth of the Yellow Sea, *Continental*
785 *Shelf Research*, 19, 1049-1064, 1999.
786

787 Honjo, S., Spencer, D. W. and Gardner, W. D.: A sediment trap intercomparison experiment in the
788 Panama Basin, 1979, *Deep Sea Research Part A. Oceanographic Research Papers*, 39, 333-358,
789 1992.
790

791 Hu, W., Chen, M., Yang, W., Zhang, R., Qiu, Y. and Zheng, M.: Enhanced particle scavenging in
792 deep water of the Aleutian Basin revealed by ^{210}Po - ^{210}Pb disequilibria, *Journal of Geophysical*
793 *Research: Oceans*, 119, 3235-3248, 2014.

794
795 Ito, T., Follows, M. J. and Boyle, E. A.: Is AOU a good measure of respiration in the oceans?,
796 Geophysical Research Letters, 31, 1-4, 2004.
797
798 Keeling, R. F., Stephens, B. B., Najjar, R. G., Doney, S. C., Archer, D. and Heimann, M.: Seasonal
799 variations in the atmospheric O₂/N₂ ratio in relation to the kinetics of air-sea gas exchange, Global
800 Biogeochemical Cycles, 12, 141-163, 1998.
801
802 Kim, G. and Church, T. M.: Seasonal biogeochemical fluxes of ²³⁴Th and ²¹⁰Po in the Upper
803 Sargasso Sea: Influence from atmospheric iron deposition, Global Biogeochemical Cycles, 15, 651-
804 661, 2001.
805
806 Lam, P. J., Ohnemus, D. C. and Auro, M. E.: Size-fractionated major particle composition and
807 concentrations from the US GEOTRACES North Atlantic Zonal Transect, Deep Sea Research Part
808 II, 116, 303-320, 2015.
809
810 Lemaître, N., Planquette, H., Planchon, F., Roig, S., Sarthon, G. and Dehairs, F.: High variability
811 of export fluxes along the North Atlantic GEOTRACES section GA01: Importance of minerals as
812 ballast of particulate organic carbon export, in prep.
813
814 Lomas, M. W. and Moran, S. B.: Evidence for aggregation and export of cyanobacteria and nano-
815 eukaryotes from the Sargasso Sea euphotic zone, Biogeosciences, 8, 203-216, 2011.
816
817 Masqué, P., Sanchez-Cabeza, J. A., Bruach, J. M., Palacios, E. and Canals, M.: Balance and
818 residence times of ²¹⁰Pb and ²¹⁰Po in surface waters of the northwestern Mediterranean Sea,
819 Continental Shelf Research, 22, 2127-2146, 2002.
820
821 Menzel-Barraqueta, J.-L., Schlosser, C., Planquette, H., Gourain, A., Cheize, M., Boutorh, J.,
822 Shelley, R., Contreira, L. P., Gledhill, M., Hopwood, M. J., Lherminier, P., Sarthou, G. and
823 Achterberg, E. P.: Aluminium in the North Atlantic Ocean and the Labrador Sea (GEOTRACES
824 GA01 section): roles of continental inputs and biogenic particle removal, Biogeosciences, in
825 review.
826
827 Mercier, H., Lherminier, P., Sarafanov, A., Gaillard, F., Daniault, N., Desbruyeres, D., Falina, A.,
828 Ferron, B., Gourcuff, C., Huck, T. and Thierry, V.: Variability of the meridional overturning
829 circulation at the Greenland–Portugal OVIDE section from 1993 to 2010, Progress In
830 Oceanography, 132, 250-261, 2015.
831
832 Michaels, A. F. and Silver, M. W.: Primary production, sinking fluxes and the microbial food web,
833 Deep Sea Research Part A. Oceanographic Research Papers, 35, 473-490, 1988.
834
835 Moore, R. M. and Smith, J. N.: Disequilibria between ²²⁶Ra, ²¹⁰Pb and ²¹⁰Po in the Arctic Ocean
836 and the implications for chemical modification of the Pacific water inflow, Earth and Planetary
837 Science Letters, 77, 285-292, 1986.
838

839 Murray, J. W., Paul, B., Dunne, J. P. and Chapin, T.: ^{234}Th , ^{210}Pb , ^{210}Po and stable Pb in the
840 central equatorial Pacific: Tracers for particle cycling, *Deep Sea Research Part I: Oceanographic*
841 *Research Papers*, 52, 2109-2139, 2005.
842
843 Nozaki, Y., Dobashi, F., Kato, Y. and Yamamoto, Y.: Distribution of Ra isotopes and the ^{210}Pb
844 and ^{210}Po balance in surface seawaters of the mid Northern Hemisphere, *Deep Sea Research Part*
845 *I: Oceanographic Research Papers*, 45, 1263-1284, 1998.
846
847 Nozaki, Y. and Tsunogai, S.: ^{226}Ra , ^{210}Pb and ^{210}Po disequilibria in the Western North Pacific,
848 *Earth and Planetary Science Letters*, 32, 313-321, 1976.
849
850 Opsahl, S., Benner, R. and Amon, R. M. W.: Major flux of terrigenous dissolved organic matter
851 through the Arctic Ocean, *Limnology and Oceanography*, 44, 2017-2023, 1999.
852
853 Peck, G. and Smith, J. D.: Uranium decay series radionuclides in the Western Equatorial Pacific
854 Ocean and their use in estimating POC fluxes, J.-M. Fernandez and R. Fichez, Paris, 459-469,
855 2002.
856
857 Puigcorb , V., Benitez-Nelson, C. R., Masqu , P., Verdeny, E., White, A. E., Popp, B. N., Prahl,
858 F. G. and Lam, P. J.: Small phytoplankton drive high summertime carbon and nutrient export in
859 the Gulf of California and Eastern Tropical North Pacific, *Global Biogeochemical Cycles*, 29,
860 1309-1332, 2015.
861
862 Richardson, T. L. and Jackson, G. A.: Small Phytoplankton and Carbon Export from the Surface
863 Ocean, *Science*, 315, 838-840, 2007.
864
865 Rigaud, S., Puigcorb , V., Camara-Mor, P., Casacuberta, N., Roca-Mart , M., Garcia-Orellana, J.,
866 Benitez-Nelson, C. R., Masqu , P. and Church, T.: A methods assessment and recommendations
867 for improving calculations and reducing uncertainties in the determination of ^{210}Po and ^{210}Pb
868 activities in seawater, *Limnology and Oceanography Methods*, 11, 561-571, 2013.
869
870 Rigaud, S., Stewart, G., Baskaran, M., Marsan, D. and Church, T.: ^{210}Po and ^{210}Pb distribution,
871 dissolved-particulate exchange rates, and particulate export along the North Atlantic US
872 GEOTRACES GA03 section, *Deep Sea Research Part II*, 116, 60-78, 2015.
873
874 Roca-Mart , M., Puigcorbe, V., Friedrich, J., Rutgers van der Loeff, M. M., Rabe, B., Korhonen,
875 M., Canara-Mor, P., Garcia-Orellana, J. and Masqu , P.: Distribution of ^{210}Pb and ^{210}Po in the
876 Arctic water column during 2007 sea-ice minimum: particle export in the ice-covered basins, *Deep*
877 *Sea Research I*, in review.
878
879 Roca-Mart , M., Puigcorb , V., Rutgers van der Loeff, M. M., Katlein, C., Fern ndez-M ndez, M.,
880 Peeken, I. and Masqu , P.: Carbon export fluxes and export efficiency in the central Arctic during
881 the record sea-ice minimum in 2012: a joint $^{234}\text{Th}/^{238}\text{U}$ and $^{210}\text{Po}/^{210}\text{Pb}$ study, *Journal of*
882 *Geophysical Research: Oceans*, 121, 5030-5049, 2016.
883

884 Sarin, M. M., Kim, G. and Church, T. M.: 210Po and 210Pb in the South-equatorial Atlantic:
885 Deep Sea Research Part II, 46, 907-917, 1999.

886

887 Sarin, M. M., Krishnaswami, S., Ramesh, R. and Somayajulu, B. L. K.: 238U decay series nuclides
888 in the northeastern Arabian Sea: Scavenging rates and cycling processes, Continental Shelf
889 Research, 14, 251-265, 1994.

890

891 Sarthou, G., Lherminier, P., Achterberg, E. P., Alonso - Pérez, F., Bucciarelli, E., Boutorh, J.,
892 Bouvier, V., Boyle, E. A., Branellec, P., Carracedo, L. I., Casacuberta, N., Castrillejo, M., Cheize,
893 M., Contreira, P. L., Cossa, D., Daniault, N., De Saint - Léger, E., Dehairs, F., Deng, F., Desprez
894 de Gésincourt, F., Devesa, J., Foliot, L., Fonseca - Batista, D., Gallinari, M., García - Ibáñez, M.
895 I., Gourain, A., Grossteffan, E., Hamon, M., Heimbürger, L. E., Henderson, G. M., Jeandel, C.,
896 Kermabon, C., Lacan, F., Le Bot, P., Le Goff, M., Le Roy, E., Lefèbvre, A., Leizour, S., Lemaitre,
897 N., Masqué, P., Ménage, O., Menzel Barraqueta, J. L., Mercier, H., Perault, F., Pérez, F. F.,
898 Planquette, H., Planchon, F., Roukaerts, A., Sanial, V., Sauzède, R., Shelley, R. U., Stewart, G.,
899 Sutton, J., Tang, Y., Tisnérat - Laborde, N., Tonnard, M., Tréguer, P., van Beek, P., Zurbrick, C.
900 M. and Zunino, P.: Introduction to the French GEOTRACES North Atlantic Transect (GA01):
901 GEOVIDE cruise, Biogeosciences, in review.

902

903 Shelley, R. U., Roca-Martí, M., Castrillejo, M., Sanial, V., Masqué, P., Landing, W. M., van Beek,
904 P., Planquette, H. and Sarthou, G.: Quantification of trace element atmospheric deposition fluxes
905 to the Atlantic Ocean (> 40°N; GEOVIDE, GEOTRACES GA01) during spring 2014, Deep Sea
906 Research Part I: Oceanographic Research Papers, 119, 34-49, 2017.

907

908 Shimmiel, G. B., Ritchie, G. D. and Fileman, T. W.: The impact of marginal ice zone processes
909 on the distribution of 210Pb, 210Po and 234Th and implications for new production in the
910 Bellingshausen Sea, Antarctica, Deep Sea Research Part II, 42, 1313-1335, 1995.

911

912 Smetacek, V., de Baar, H. J. W., Bathmann, U., Lochte, K. and Rutgers van der Loeff, M. M.:
913 Export production by 234Th, including 210Po and 210Pb measured on water bottle samples during
914 POLARSTERN cruise ANT-X/6, PANGAEA, 1997.

915

916 Sonnerup, R. E., Mecking, S., Bullister, J. L. and Warner, M. J.: Transit time distributions and
917 oxygen utilization rates from chlorofluorocarbons and sulfur hexafluoride in the Southeast Pacific
918 Ocean, Journal of Geophysical Research: Oceans, 120, 3761-3776, 2015.

919

920 Stanley, R. H. R., Doney, S. C., Jenkins, W. J. and Lott, D. E. I.: Apparent oxygen utilization rates
921 calculated from tritium and helium-3 profiles at the Bermuda Atlantic Time-series Study site,
922 Biogeosciences, 9, 1969-1983, 2012.

923

924 Stewart, G., Cochran, J. K., Miquel, J. C., Masqué, P., Szlosek, J., Rodriguez y Baena, A. M.,
925 Fowler, S. W., Gasser, B. and Hirschberg, D. J.: Comparing POC export from 234Th/238U and
926 210Po/210Pb disequilibria with estimates from sediment traps in the northwest Mediterranean,
927 Deep Sea Research Part I: Oceanographic Research Papers, 54, 1549-1570, 2007.

928

929 Stewart, G. M., Bradley Moran, S. and Lomas, M. W.: Seasonal POC fluxes at BATS estimated
930 from ^{210}Po deficits, Deep Sea Research Part I: Oceanographic Research Papers, 57, 113-124,
931 2010.

932

933 Stewart, G. M., Fowler, S. W. and Fisher, N. S.: Chapter 8 The Bioaccumulation of U- and Th-
934 Series Radionuclides in Marine Organisms, Radioactivity in the Environment. Elsevier, Volume
935 13, 269-305, 2008.

936

937 Subha Anand, S., Rengarajan, R., Shenoy, D., Gauns, M. and Naqvi, S. W. A.: POC export fluxes
938 in the Arabian Sea and the Bay of Bengal: A simultaneous $^{234}\text{Th}/^{238}\text{U}$ and $^{210}\text{Po}/^{210}\text{Pb}$ study,
939 Marine Chemistry, 2017.

940

941 Tang, Y., Lemaitre, N., Castrillejo, M., Roca-Marti, M., Masqué, P. and Stewart, G.: The export
942 flux of particulate organic carbon derived from $^{210}\text{Po}/^{210}\text{Pb}$ disequilibria along the North Atlantic
943 GEOTRACES GA01 (GEOVIDE) transect, Biogeosciences,

944

945 Tang, Y., Stewart, G., Lam, P. J., Rigaud, S. and Church, T.: The influence of particle
946 concentration and composition on the fractionation of ^{210}Po and ^{210}Pb along the North Atlantic
947 GEOTRACES transect GA03, Deep Sea Research Part I: Oceanographic Research Papers, 128,
948 42-54, 2017.

949

950 Tateda, Y., Carvalho, F. P., Fowler, S. W. and Miquel, J.-C.: Fractionation of ^{210}Po and ^{210}Pb in
951 coastal waters of the NW Mediterranean continental margin, Continental Shelf Research, 23, 295-
952 316, 2003.

953

954 Tonnard, M., Donval, A., Lampert, L., Claustre, H., Ras, J., Dimier, C., Sarthou, G., Planquette,
955 H., van der Merwe, P., Boutorh, J., Cheize, M., Menzel, J.-L., Pereira Contraira, L., Shelley, R.,
956 Bowie, A. R., Treguer, P., Gallinari, M., Duprez de Gesincourt, F., Germain, Y. and Leherminier,
957 P.: Phytoplankton assemblages along the GEOVIDE section (GEOTRACES section GA01) using
958 CHEMTAX, in prep.

959

960 Tonnard, M., Planquette, H., Bowie, A. R., van der Merwe, P., Gallinari, M., de Gesincourt, F. D.,
961 Germain, Y., Gourain, A., Benetti, M., Reverdin, G., Treguer, P., Boutorh, J., Cheize, M.,
962 Barraqueta, J.-L. M., Pereira-Contreira, L., Shelley, R., Lherminier, P. and Sarthou, G.: Dissolved
963 iron in the North Atlantic Ocean and Labrador Sea along the GEOVIDE section (GEOTRACES
964 section GA01), Biogeosciences, in review.

965

966 Towler, P.: Radionuclides measured on water bottle samples during FRANKLIN cruise FR05/92,
967 PANGAEA, 2003.

968

969 Towler, P.: Radionuclides measured on water bottle samples during FRANKLIN cruise FR08/93,
970 PANGAEA, 2013.

971

972 Verdeny, E., Masqué, P., Maiti, K., Garcia-Orellana, J., Bruach, J. M., Mahaffey, C. and Benitez-
973 Nelson, C. R.: Particle export within cyclonic Hawaiian lee eddies derived from ^{210}Pb – ^{210}Po

974 disequilibrium, Deep Sea Research Part II: Topical Studies in Oceanography, 55, 1461-1472, 2008.
975
976
977 Walsh, I. D. and Gardner, W. D.: A comparison of aggregate profiles with sediment trap fluxes,
978 Deep Sea Research Part A. Oceanographic Research Papers, 39, 1817-1834, 1992.
979
980 Wei, C., Lin, S., Wen, L. and Sheu, D. D. D.: Geochemical behavior of ^{210}Pb and ^{210}Po in the
981 nearshore waters off western Taiwan, Marine Pollution Bulletin, 64, 214-220, 2012.
982
983 Wei, C. L., Yi, M. C., Lin, S. Y., Wen, L. S. and Lee, W. H.: Seasonal distributions and fluxes of
984 ^{210}Pb and ^{210}Po in the northern South China Sea, Biogeosciences, 11, 6813-6826, 2014.
985
986

987

988

989

990 Table 1. Biological characteristics of the water column determined by chlorophyll-a
 991 concentration (8-day composite) from Fig-4 Fig. 6, including the date when the last bloom
 992 began, the difference in chlorophyll-a concentration between the sampling time and last
 993 bloom peak, and the days since the last bloom. Activity ratios of $^{210}\text{Po}_p/^{210}\text{Pb}_p < 1$ and their
 994 corresponding depths are also shown. *NA* indicates that all samples from the corresponding
 995 depth range had $^{210}\text{Po}_p/^{210}\text{Pb}_p$ equal to or greater than 1 (no sample with $^{210}\text{Po}_p/^{210}\text{Pb}_p < 1$).

Station	Sampling date	The date last bloom began	Last bloom peak-current state	Days since last bloom	$^{210}\text{Po}_p/^{210}\text{Pb}_p < 1$	
					0-100 m	> 100 m
1	5/19/14	3/6/14	Large	74	<i>NA</i>	Yes (120, 250, 500 m)
13	5/24/14	4/7/14	Small	47	Yes (60 m)	<i>NA</i>
21	5/31/14	4/7/14	Large	54	<i>NA</i>	Yes (120 m)
26	6/4/14	4/15/14	Large	50	<i>NA</i>	Yes (400 m)
32	6/7/14	5/9/14	Small	29	<i>NA</i>	<i>NA</i>
38	6/10/14	5/17/14	Small	24	Yes (60 m)	<i>NA</i>
44	6/13/14	5/9/14	Small	35	<i>NA</i>	<i>NA</i>
60	6/18/14	5/17/14	Large	32	<i>NA</i>	<i>NA</i>
64	6/19/14	5/17/14	Small	33	Yes (30 m)	<i>NA</i>
69	6/22/14	5/25/14	Small	28	Yes (20, 30 m)	<i>NA</i>
77	6/26/14	5/25/14	Small	32	Yes (10, 20, 50 m)	<i>NA</i>

996

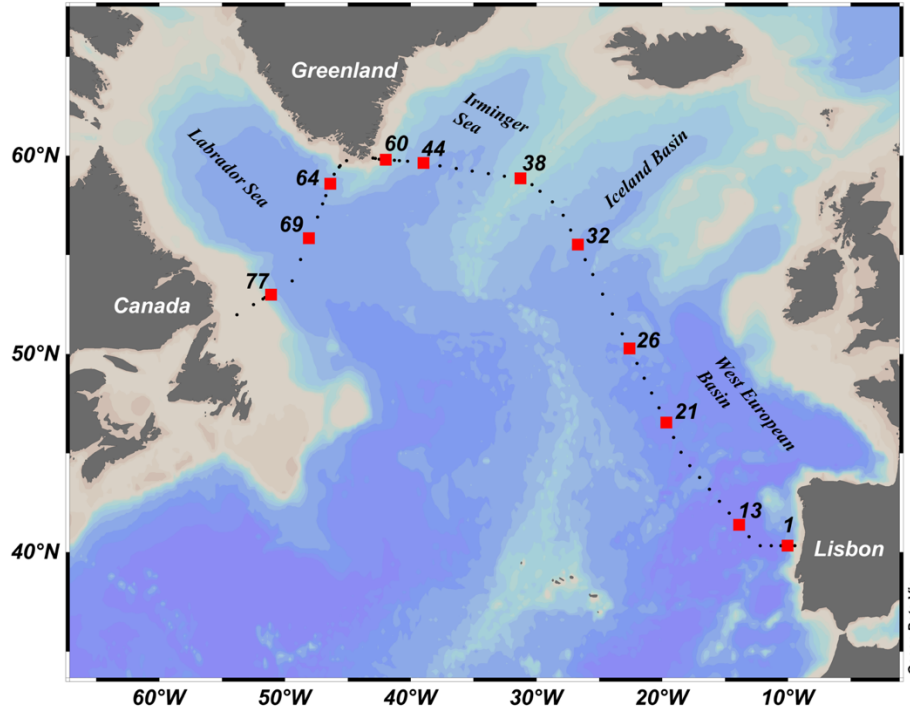
997 Table 2. ~~Globeat~~The compilation of total particulate $^{210}\text{Po}/^{210}\text{Pb}$ activity ratios ($^{210}\text{Po}_p/^{210}\text{Pb}_p$) averaged in the upper 200 m, including
 998 this study.

Region	Sampling Method	Date	Size (μm)	Depth (m)	$^{210}\text{Po}_p/^{210}\text{Pb}_p$	Reference
Arctic	CESAR	Apr – May 83	> 0.45	2-200	1.2 ± 0.7	(Moore and Smith, 1986)
	Arctic (ARK-XXII/2)	Jul-Sep 07	> 1	10-200	0.50 ± 0.20	(Friedrich, 2011)
	Chukchi Shelf	Jul-Sep 10	> 0.45	0-90	0.37 ± 0.10	(He et al., 2015)
Atlantic	F.S. Meteor	Nov-Dec 73	> 0.4	0-200	3.1 ± 1.4	(Bacon, 1977)
	Cariaco Trench	Dec 73	> 0.4	0-200	1.4 ± 0.6	(Bacon et al., 1980a)
	Labrador (R/V Knorr)	Jun 75	> 0.4	0-100	3.9 ± 1.5	(Bacon et al., 1980b)
	South of New England	Jul 80	> 0.45	4-200	1.8 ± 0.8	(Bacon et al., 1988)
	N. Atlantic (BOFS)	May-Jun 89, 90	> 0.45	0-150	6.0 ± 4.5	(BODC et al., 2016)
	South-equa. Atlantic	May-Jun 96	> 0.7	10-200	1.3 ± 1.1	(Sarin et al., 1999)
N. Atlantic (GA03)	BATS	Oct 96	> 0.45	0-200	3.7 ± 3.2	(Kim and Church, 2001)
	N. Atlantic (GA03)	Oct-Nov 10, Nov-Dec 11	> 0.8	30-200	1.5 ± 0.5	(Rigaud et al., 2015)
	N. Atlantic (GA01)	<i>In-situ</i> pump	May-Jun 14	8-200	1.4 ± 0.3	This study
Pacific	North Pacific	Nov 73	> 0.4	10-150	8.5 ± 5.7	(Bacon et al., 1976)
	W. Pacific (FR05/92)	Jul 92	> 0.45	0-200	1.3 ± 1.0	(Towler, 2003)
	Equa. Pacific	Go-Flo bottle	Aug-Sept 92	0-200	5.1 ± 1.2	(Murray et al., 2005)
Pacific	W. Pacific (FR08/93)	Nov 93	> 0.45	0-200	16 ± 4	(Towler, 2013)
	W. Pacific (FR07/97)	Aug 97	> 0.45	0-200	7.2 ± 1.5	(Peck and Smith, 2002)
	Aleutian Basin	Niskin bottle	Jul-Aug 08	0-200	1.9 ± 3.0	(Hu et al., 2014)
Antarctic	E. Pacific (GP16)	<i>In-situ</i> pump	> 1	15-200	2.4 ± 0.6	unpublished
	S. Ocean (ANT-X/6)	Niskin bottle	> 0.45	20-200	3.0 ± 1.4	(Smetacek et al., 1997)
	Bellingshausen Sea	Go-Flo bottle	> 0.45	0-100	14 ± 11	(Shimmield et al., 1995)

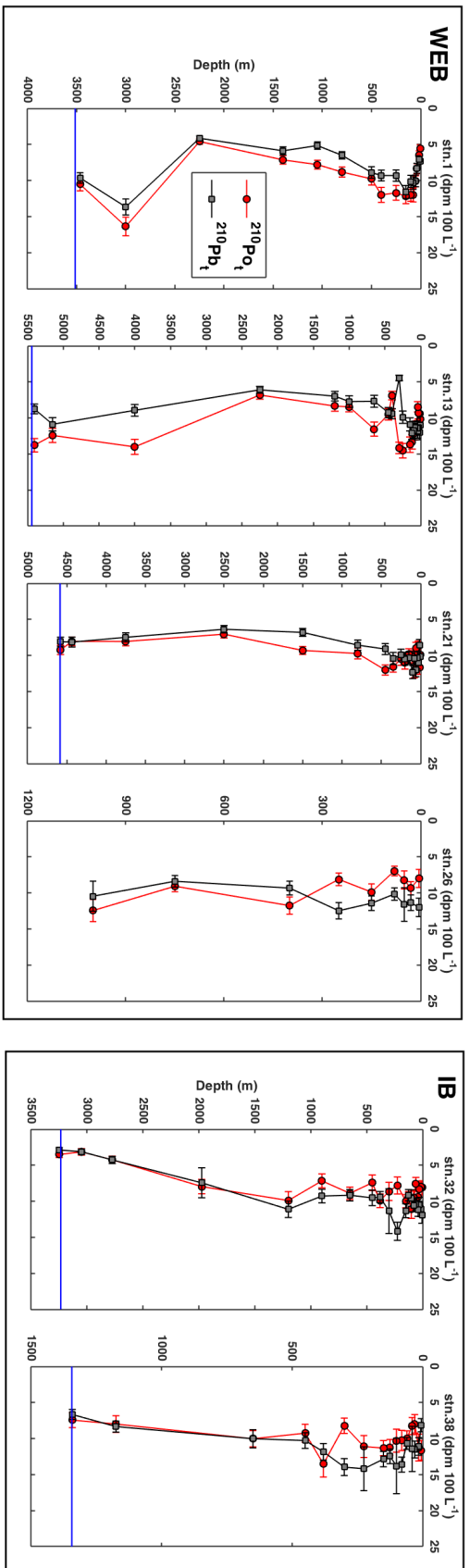
S. Ocean (ANT-XXIV/3)		Niskin bottle	Feb - Apr 08	> 0.45	25-200	1.3 ± 0.9	(Friedrich et al., 2011)
Margin Sea	S. China Sea	Go-Flo bottle	Jan-Oct 07, May 08	> 0.45	0-200	1.7 ± 1.1	(Wei et al., 2014)
	W. Taiwan	Go-Flo bottle	Apr 07	> 0.45	8-25	0.85 ± 0.12	(Wei et al., 2012)
	Yellow Sea	Niskin bottle	Feb 93	> 0.7	0-100	0.88 ± 0.08	(Hong et al., 1999)
	Mediterranean Sea	Sediment trap	Mar-Jun 03		200	4.5 ± 1.0	(Stewart et al., 2007)

999

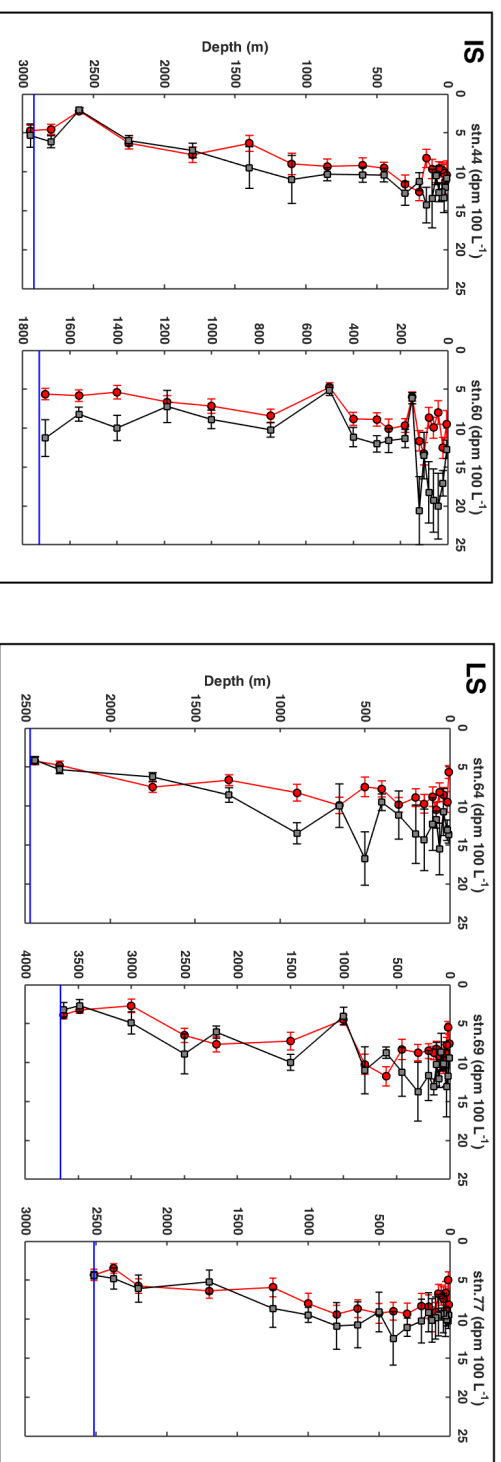
1000



1001
 1002 Fig. 1. Map of the GEOVIDE cruise track (black dots) and the 11 stations sampled for ^{210}Po and
 1003 ^{210}Pb activity (red squares). Each sampling location is labeled with a station number. The
 1004 sampling stations are divided into 4 regions (from east to west): West European Basin (stations
 1005 1, 13, 21, 26), Iceland Basin (stations 32, 38), Irminger Sea (stations 44, 60), and Labrador Sea
 1006 (stations 64, 69, 77).



1007



1008

1009

Fig. 2. The depth profiles of total ^{210}Po ($^{210}\text{Po}_t$, red circles) and ^{210}Pb activities ($^{210}\text{Pb}_t$, grey squares) along GEOVIDE section. The

1010

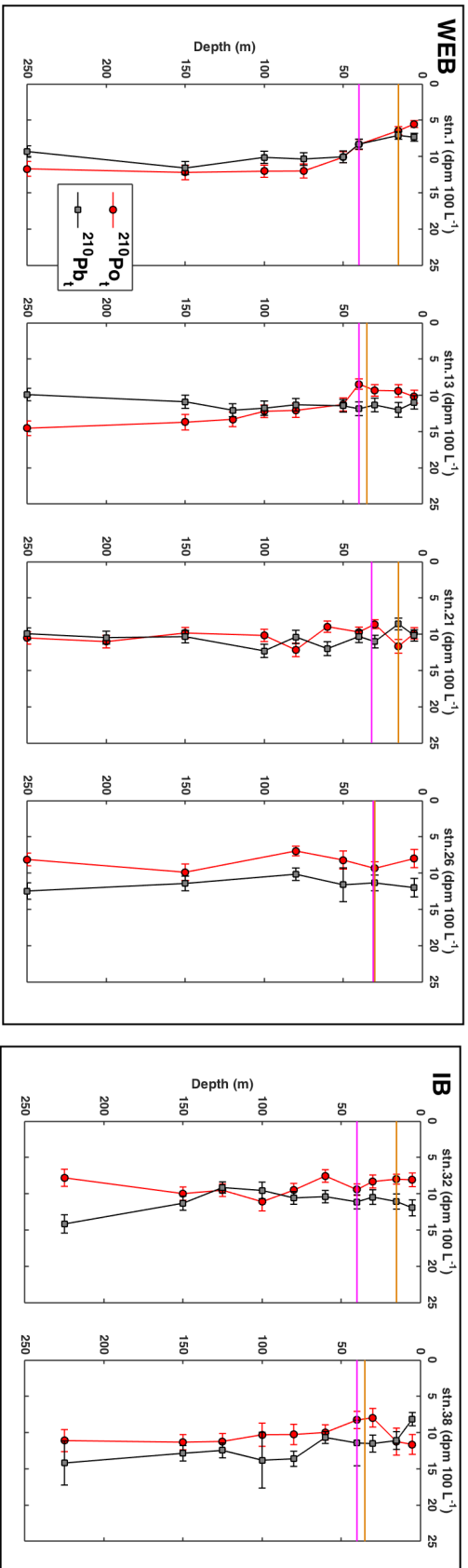
horizontal blue line is the bottom depth, which coincided with the deepest water sample except for station 26 which was sampled only

1011

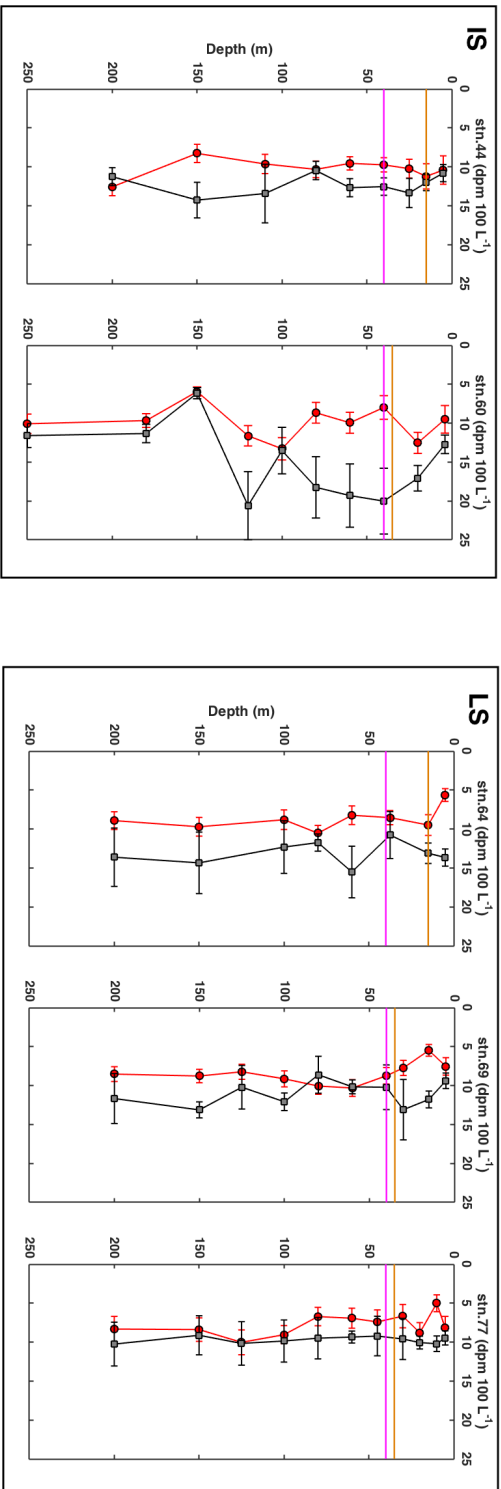
down to 1000 m. Note that the depth scale for each plot may be different. The profiles are shown in the order of sampling date with

1012 the region indicated on the top left of each box: West ~~ern~~ European Basin (WEB), Iceland Basin (IB), Irminger Sea (IS), Labrador Sea
1013 (LS).

1014



1015

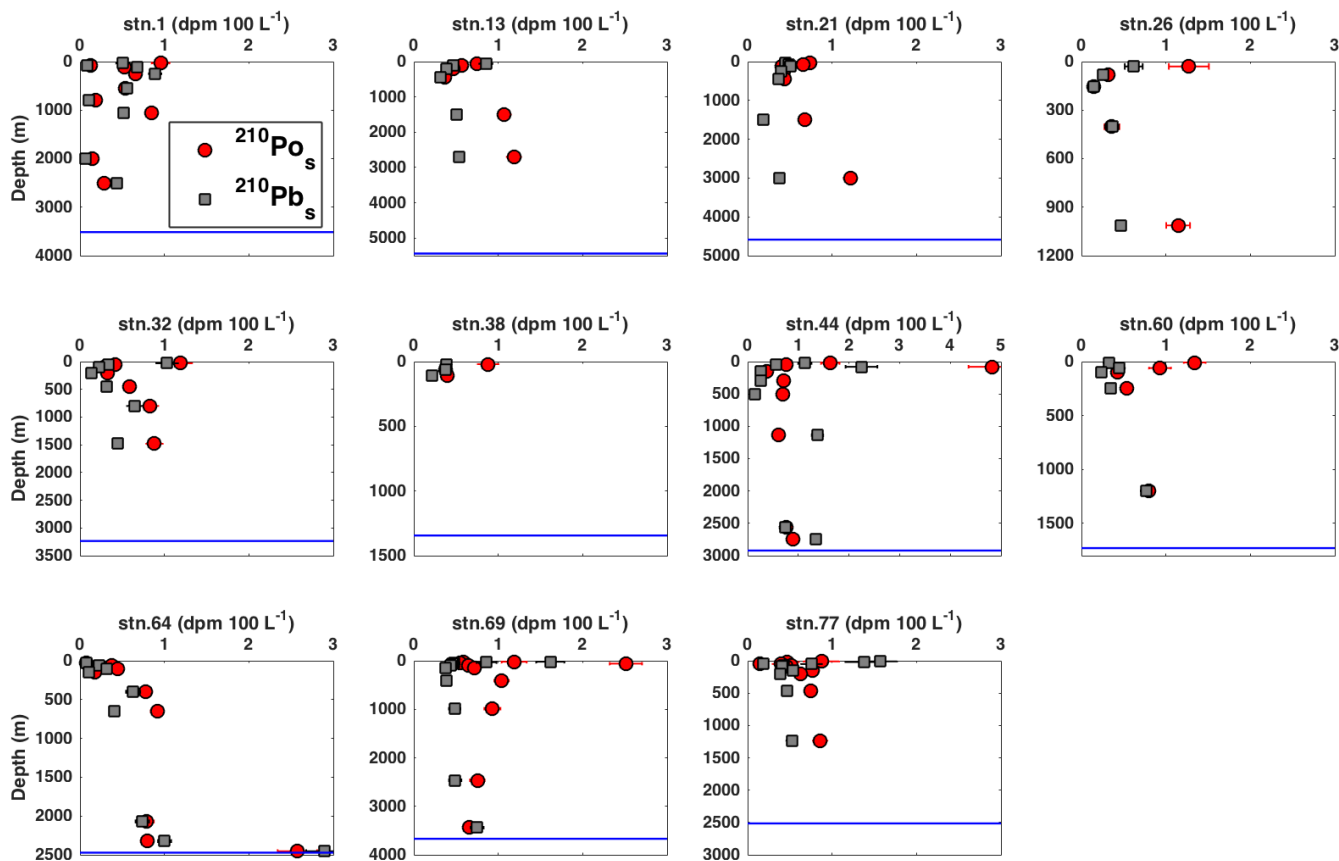


1016

1017 Fig. 3. **A closer look at only the zoom for the** The upper 250 m of the depth profiles of total ^{210}Po ($^{210}\text{Po}_t$, red circles) and ^{210}Pb

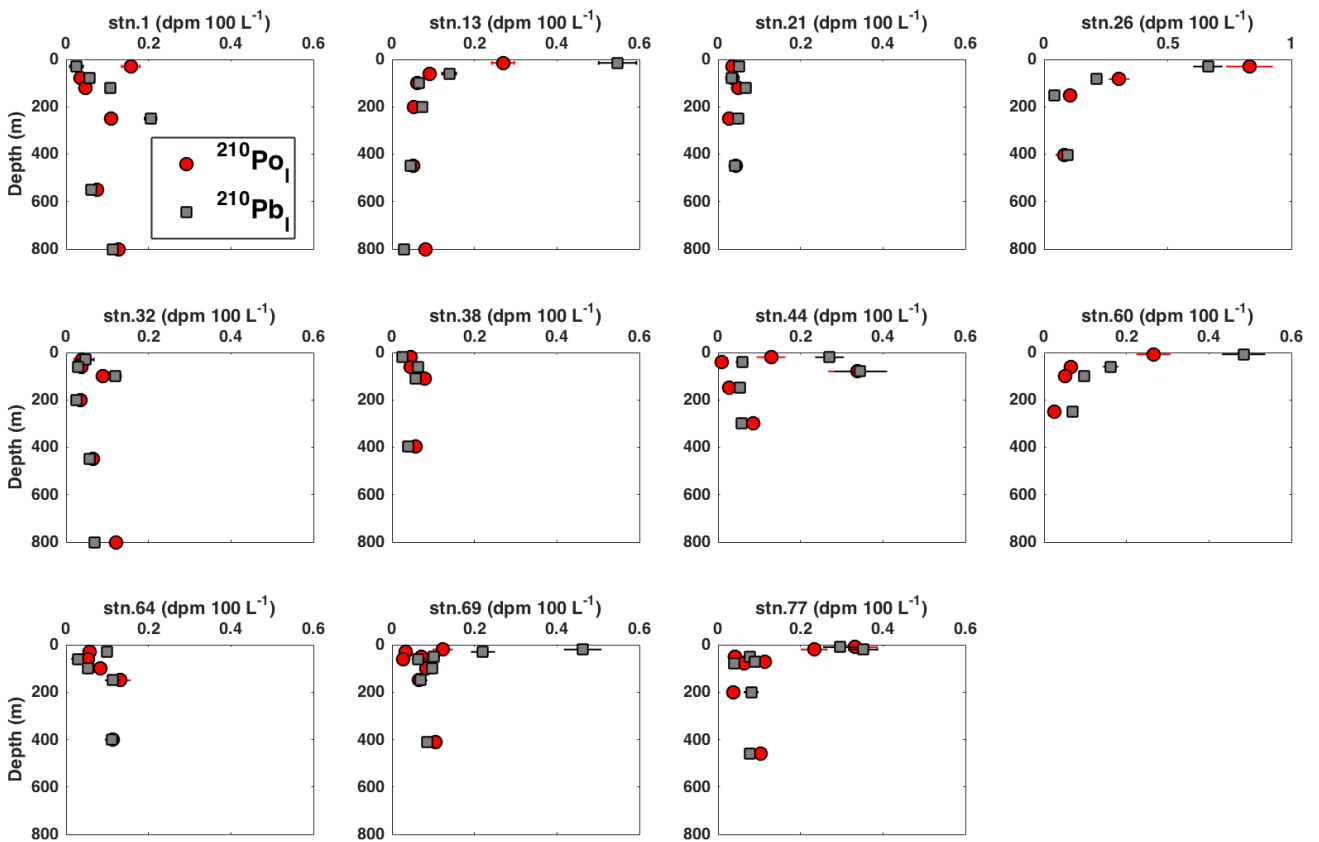
1018 activities ($^{210}\text{Pb}_t$, grey squares) along the GEOVIDE section. The horizontal orange and magenta lines denote the mixed layer depth

1019 (MLD) and the base of the euphotic zone ($Z_{1\%}$), respectively. The depth profiles are shown in the order of sampling and grouped by
1020 region (refer to Fig. 2 for the text abbreviations).



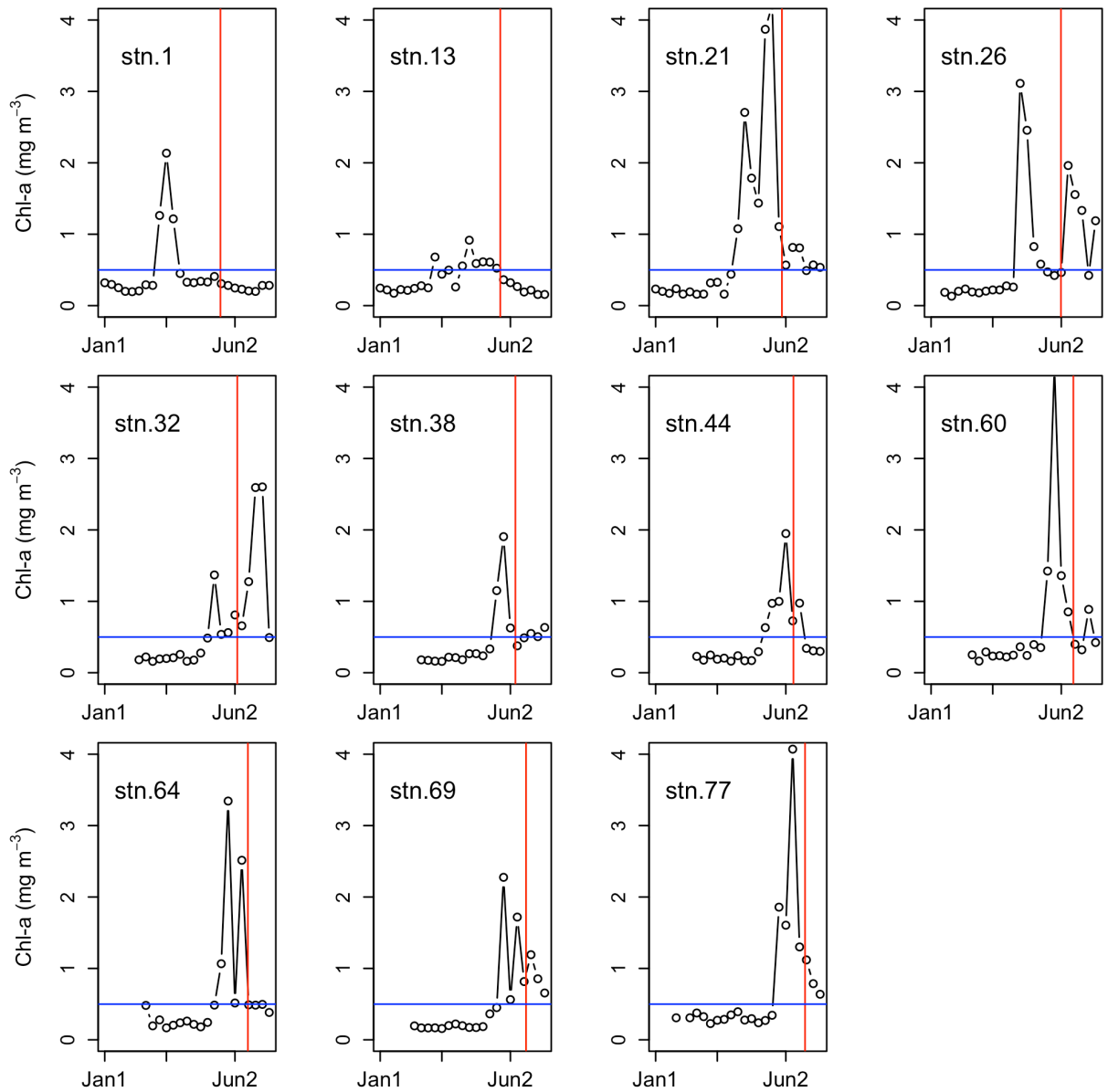
1021

1022 Fig. 4. Vertical profiles of the particulate ^{210}Po and ^{210}Pb activity in the small size fraction (1-53
 1023 μm , $^{210}\text{Po}_s$, $^{210}\text{Pb}_s$). Note that the depth scale may differ among plots, and the activity scale at
 1024 Station 44 differs from the scale on all other plots. The horizontal blue line represents the bottom
 1025 depth at that station.



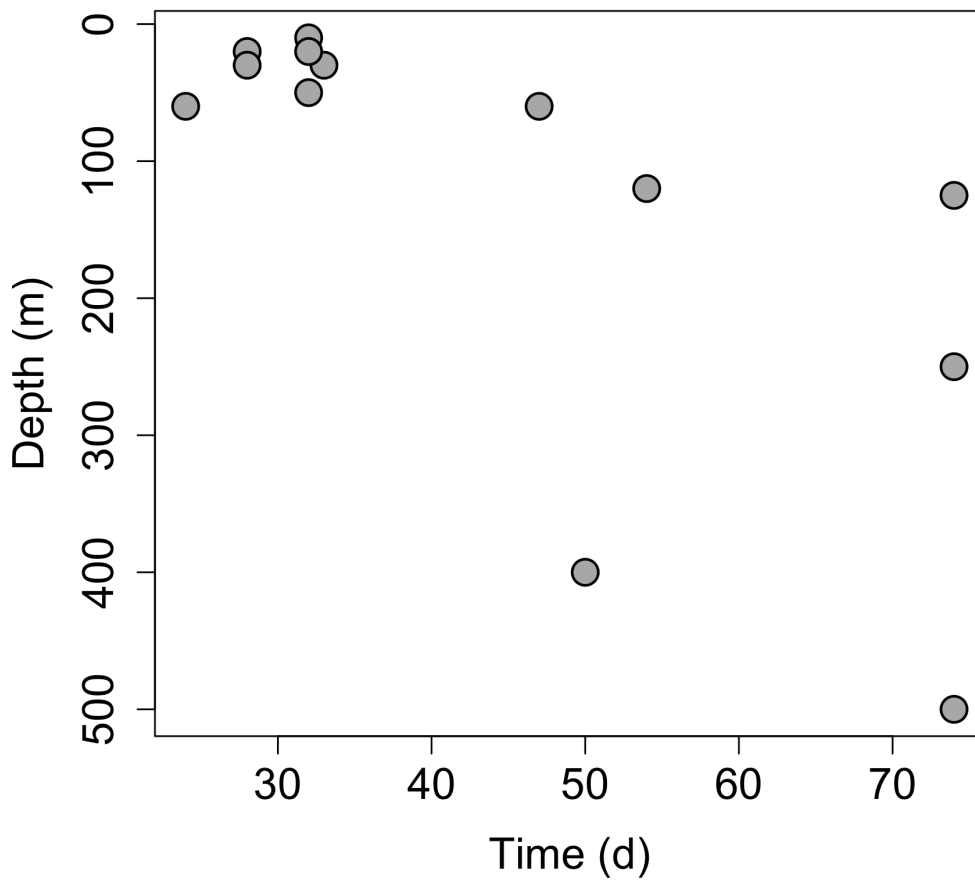
1026

1027 Fig. 5. The vertical profiles of the particulate ^{210}Po and ^{210}Pb activity in the large size fraction (>
 1028 $53 \mu\text{m}$, $^{210}\text{Po}_i$, $^{210}\text{Pb}_i$) in the top 800 m. Note that the activity scale at Station 26 differs from the
 1029 scale on all other plots.



1030
 1031
 1032
 1033
 1034
 1035
 1036

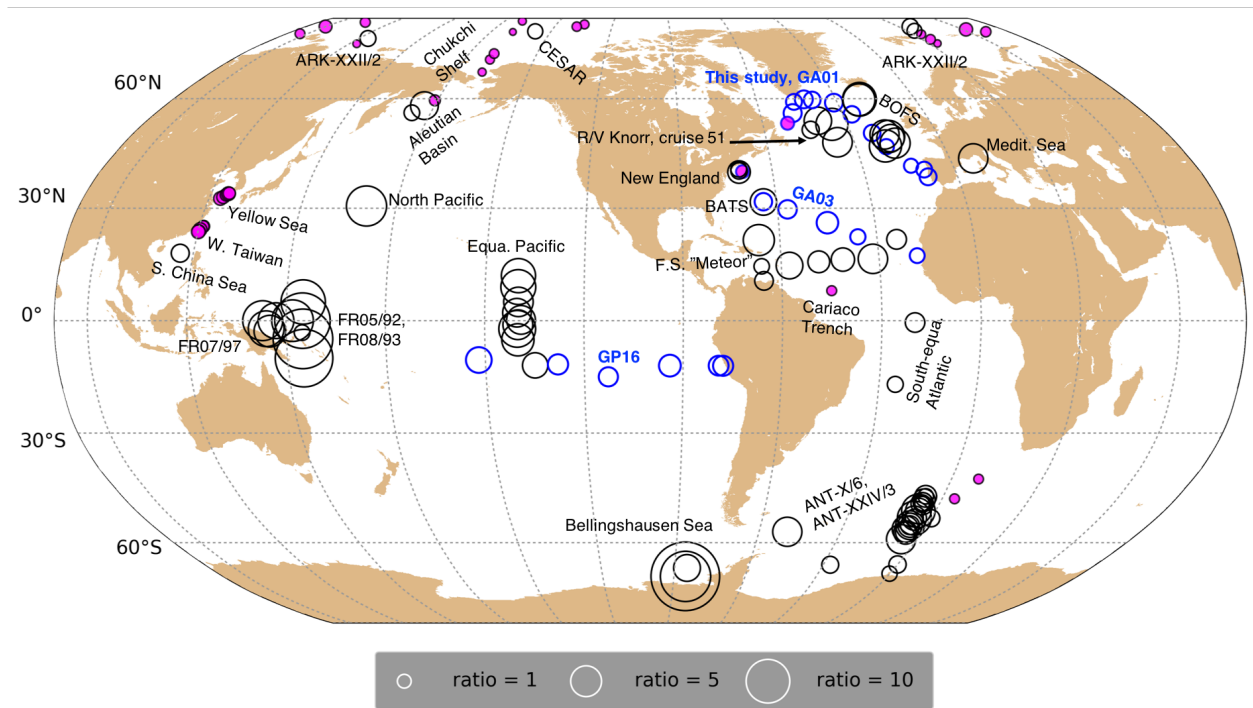
Fig. 4 Fig. 6. Time-series (January 1 – July 12, 2014) chlorophyll-a concentrations (8-day averages) from Aqua MODIS (<https://oceancolor.gsfc.nasa.gov>) at each station along the GA01 transect. The vertical red line denotes the sampling date at each station. The horizontal blue line denotes chlorophyll-a concentration of 0.5 mg m^{-3} . The time when chlorophyll-a concentration first exceeded 0.5 mg m^{-3} after the end of the last bloom defines the date **when** the next bloom began.



1037

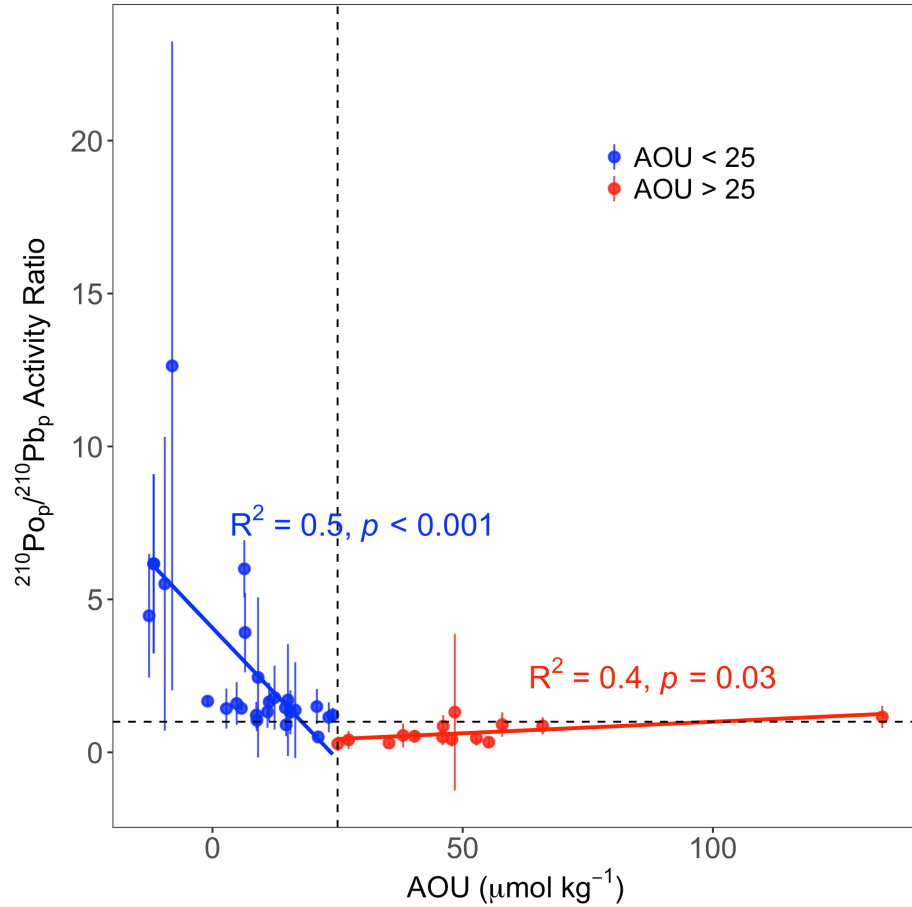
1038

1039 Fig.7. Depths at which the total particulate ($> 1 \mu\text{m}$) $^{210}\text{Po}/^{210}\text{Pb}$ activity ratio was lower than
 1040 unity vs. the time since the last bloom (data is presented in Table 1).



1041
 1042
 1043
 1044
 1045
 1046
 1047
 1048

Fig. 8. Comparison of particulate $^{210}\text{Po}/^{210}\text{Pb}$ activity ratios in the upper 200 m from this study and 20 previous studies (references in Table 2). Information about the study site, sampling date, method, and particle size of each study are shown in Table 2. The black circles represent data from previous studies while the **red blue** circles are the results from samples analyzed in the Stewart lab from three recent GEOTRACES transects (GA03, GP16, and this study, GA01 GEOVIDE). The filled **blue-magenta** and open circles indicate activity ratios lower and higher than 1, respectively.



1049

1050

1051

1052

1053

1054

1055

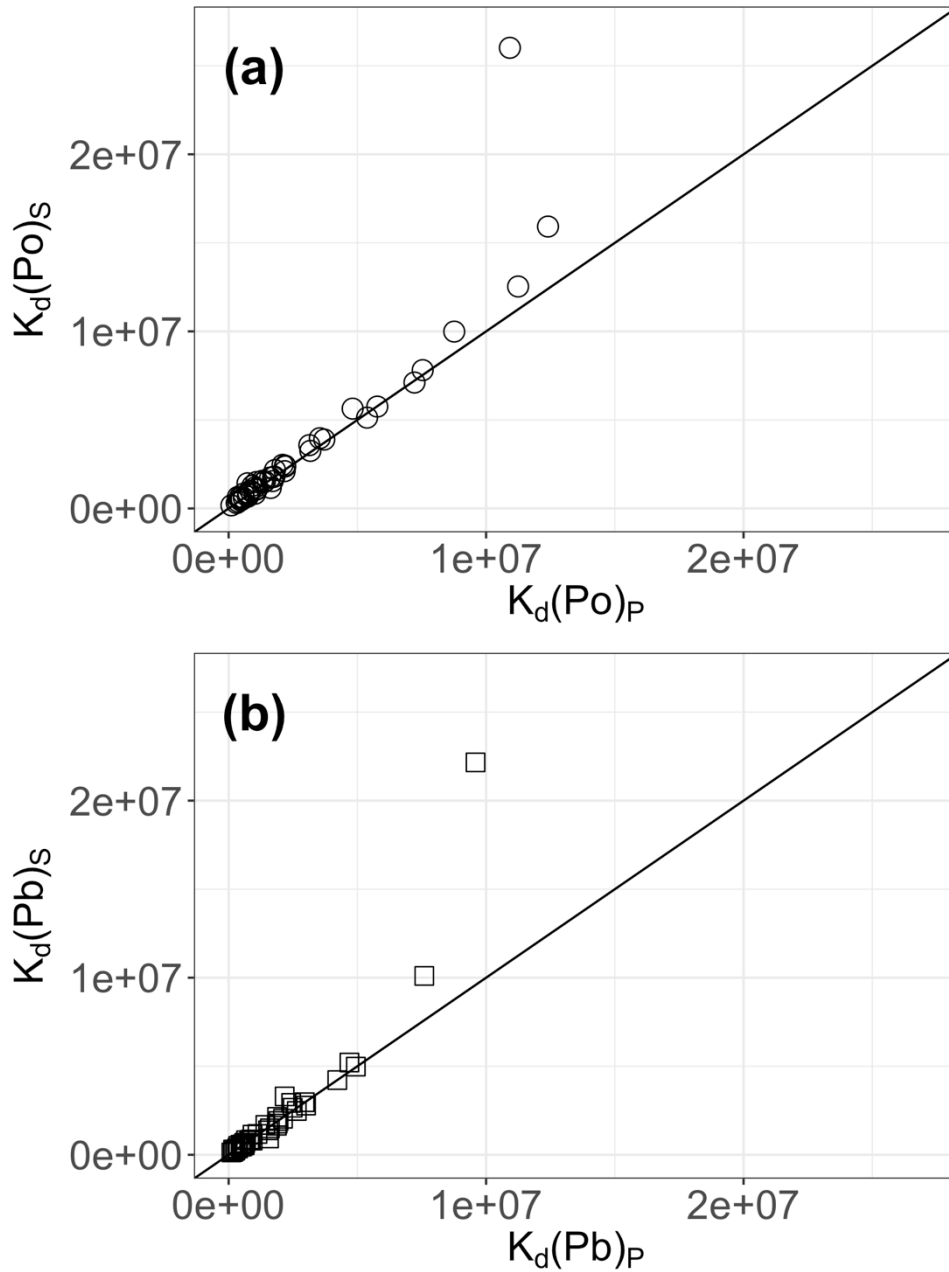
1056

1057

1058

1059

Fig. 6 Fig. 9. The relationship between AOU ($\mu\text{mol kg}^{-1}$) and total particulate $^{210}\text{Po}/^{210}\text{Pb}$ activity ratio ($^{210}\text{Po}_p/^{210}\text{Pb}_p$) from the upper 200 m in the northern hemisphere ($> 22^\circ\text{N}$) investigated by a linear regression model (red and blue lines). The 40 stations include data from previous studies, ARK-XXII/2 ($77.38\text{-}87.83^\circ\text{N}$, $n = 15$) in the Arctic, BOFS ($48.89\text{-}49.87^\circ\text{N}$, $n = 7$), GA03 ($22.38\text{-}39.70^\circ\text{N}$, $n = 7$), and this study, GA01 ($40.33\text{-}59.80^\circ\text{N}$, $n = 11$) in the North Atlantic. The horizontal dashed line represents $^{210}\text{Po}_p/^{210}\text{Pb}_p$ AR = 1 and the vertical dashed line represents AOU = $25 \mu\text{mol kg}^{-1}$. **Red** Blue circles denote **the average $^{210}\text{Po}_p/^{210}\text{Pb}_p > 1$ and** AOU $< 25 \mu\text{mol kg}^{-1}$, while **blue red** circles **denote the average $^{210}\text{Po}_p/^{210}\text{Pb}_p < 1$ and** AOU $> 25 \mu\text{mol kg}^{-1}$. **Data that are in** neither category are denoted by the black circles.



1060

1061

1062

1063

1064

Fig. 7 Fig. 10. Comparison of the partitioning coefficient (K_d) between the dissolved and small particulate phases ($K_{d,s}$ - $K_d(\text{Po})_s$, $K_d(\text{Pb})_s$) vs. between the dissolved and total particulate phases ($K_{d,p}$ $K_d(\text{Po})_p$, $K_d(\text{Pb})_p$) for (a) ^{210}Po and (b) ^{210}Pb . The 1:1 line is indicated as the solid line in each plot.